Passive sampling to understand and predict sources of wastewater and agricultural contamination in rural watersheds

by

Allison Vucenovic

A thesis
presented to the University of Waterloo
in fulfillment of the
thesis requirement for the degree of
Master of Science
in
Earth and Environmental Sciences

Waterloo, Ontario, Canada, 2023

© Allison Vucenovic 2023

Author's Declaration

This thesis consists of material all of which I authored or co-authored: see Statement of Contributions included in the thesis. This is a true copy of the thesis, including any required final revisions, as accepted by my examiners.

I understand that my thesis may be made electronically available to the public.

Statement of Contributions

Chapter 2 and parts of the Appendices will be submitted as a journal article. The majority of the work, including sample collection, sample analysis, figure preparation, writing, and editing were completed by me. This article will be co-authored by myself as well as my supervisors Dr. Carol Ptacek and Dr. Janis Thomas who provided helpful edits and comments to improve the quality of the article.

Abstract

Passive sampling techniques have emerged as valuable tools in environmental monitoring, offering distinct advantages over traditional discrete sampling methods. Discrete sampling techniques are only representative of the time of sampling, often over or underestimating concentrations of constituents in flowing surface waters. Passive samplers contain a collecting medium which accumulates and concentrates constituents to a higher level of detection, and reduces variability associated with discrete sampling. To identify and differentiate non-point sources in rural catchments, this study used passive samplers, including the diffusive gradient in thin-films (DGT) and polar organic chemical integrative sampler (POCIS), along with discrete sampling to detect a range of anthropogenic and agricultural tracers and nutrients.

Passive samplers were deployed for select compounds including nutrients (PO_4-P, NO_3-N, NH_4-N), anthropogenic tracers (caffeine, carbamazepine, gemfibrozil, ibuprofen, naproxen, sulfamethoxazole, acesulfame potassium, sucralose), and agricultural tracers (glyphosate, aminomethylphosphonic acid (AMPA)). Among the passive samplers deployed, the Metsorb®-DGT, selective for phosphate-bearing compounds, was evaluated for competition impacts between PO_4-P and glyphosate. Competition between analytes can occur for sorbents selective for a range of compounds with similar properties. A new sampler using a weak anion exchange (WAX) resin was developed for the uptake of artificial sweeteners acesulfame potassium (ACE-K) and sucralose (SUC).

Passive samplers were deployed at three distinct locations (*Hamlet*, *Agricultural*, and *Mixed-land Sites*), for 3 to 14 days, while discrete samples were collected every 3 days over 2 weeks in Fall of 2021 and Spring of 2022. The effect of potentially competing ions between phosphate-bearing compounds was evaluated by deploying triplicate Metsorb®-DGT sampler in

a solution of high PO_4-P and low glyphosate and AMPA. Strata-DGT samplers were developed as a potential sampler for the uptake of ACE-K and SUC and deployed in the Spring 2022 sampling event. The goals of this thesis were to (1) use DGT and POCIS to delineate anthropogenic contamination from agricultural activities to surface waters in rural communities, and to compare their effectiveness to discrete samples and (2) further develop and evaluate DGT samplers.

DGT and POCIS had comparable concentrations with 64% of compounds not statistically different ($\rho > 0.05$) from discrete samples. Diffusive boundary layer (DBL) corrections were applied to Spring 2022 DGT samples, increasing the mean absolute error between DGT concentrations (C_{DGT}) and discrete concentrations (C_{ACTIVE}) by 32% for all compounds. Phosphate was elevated at the *Hamlet Site* (74 ± 8.2 µg L^{-1}) in discrete samples compared to the *Agriculture Site* during the Fall 2021 sampling season. The *Hamlet Site* land use was 40% urban and 60% agriculture, while the *Agriculture* and *Mixed-land Sites* were 94% and 88% agricultural land use, respectively. Tracers consistently showed elevated concentrations of ACE-K (412 ± 202 µg L^{-1}) and SUC ($17{,}089 \pm 5370$ µg L^{-1}) in discrete samples across both sampling seasons as well as all other anthropogenic tracers at the *Hamlet Site*, while glyphosate and AMPA were elevated at the *Agriculture Site* (0.86 ± 1.66 µg L^{-1} and 1.41 ± 0.85 µg L^{-1}, respectively). Principal component analysis (PCA) and correlation coefficients indicated a positive relationship between phosphate and anthropogenic tracers at the *Hamlet Site*. Biological markers (Human-specific *Bacteroides*), specific to human fecal contamination, were also elevated at the *Hamlet Site* compared to the other sites. The results of this study clearly show septic system contamination in a headwater stream and suggest impacts of septic systems to these surface water bodies may be an underappreciated nonpoint source of nutrients.

There was no apparent competition on the Metsorb®-DGT sampler at initial concentrations of 104 µg L^{-1} of PO_4-P, 0.372 µg L^{-1} of glyphosate, and 2.14 µg L^{-1} of AMPA as uptake was mostly linear after 6 days of deployment. Strata X-AW resin was not a suitable binding medium for artificial sweeteners, resulting in concentrations only 39% of discrete samples for ACE-K at the *Hamlet Site*.

Overall, an array of passive samplers was helpful to distinguish nonpoint sources of septic system from agricultural contamination in rural head-water streams. Passive samplers generally showed comparable results to discrete samples, with the exception of ACE-K, and reduced the variability and additional sampling and analysis associated with discrete sample collection.

Acknowledgements

I would first like to thank my supervisor Dr. Carol Ptacek and committee member Dr. Janis Thomas for your support, mentorship, guidance, and valuable insight implementing this project over the last three years. I would also like to thank my second committee member Dr. Andrea Brookfield for your interest, recommendations, and support in my research project.

A huge thank you to YingYing Liu, Sara Fellin, and Yizhi Yuan for all your support and help running samples, training on analytical instruments, and answering my endless questions. Thank you to Dr. Melanie Raby and Dr. Paul Helm from the Ontario Ministry of the Environment, Conservation and Parks (MECP) for helpful technical discussions that strengthened this project. I would also like to thank Joy Hu for running ICP-OES analyses and Matthew Erdelsky, Luke Schofield, Olivia Clay, Sasha Morozova, Emily Dodsworth, Lisa Kester, and Nikki Bell for assistance in the field and laboratory.

Funding for this project was provided through a Canada-Ontario Agreement (COA) on Great Lakes Water Quality and Ecosystem Health grant (Project #1603) from Ontario Ministry of Environment, Conservation, and Parks (MECP) to the University of Waterloo (UW). Funding support was also provided by the Natural Sciences and Engineering Research Council of Canada Discovery Grant Program awarded to C. Ptacek.

Table of Contents

Author's Declaration ii
Statement of Contributions iii
Abstract iv
Acknowledgements vii
List of Figures x
List of Tables xii
List of Abbreviations xiv
Chapter 1: Introduction 1
1.1 Passive samplers 1
1.1.1 POCIS 2
1.1.2 DGT 3
1.2 Nutrients in the environment 4
1.2.1 Septic systems as anthropogenic nonpoint source of nutrients 6
1.2.2 Agricultural activities as nonpoint sources of nutrients 8
1.3 Tracers for determining sources of contamination 8
1.4 Development and evaluation of passive samplers 10
1.5 Research objectives 12
1.6 Thesis organization 13
Chapter 2: Array of passive surface-water samplers to assist in distinguishing nonpoint anthropogenic contamination from agricultural sources 14
2.1 Summary 14
2.2 Introduction 15
2.3 Methods 19
2.3.1 DGT and POCIS specifications 19
2.3.2 Field site characterization and study design 21
2.3.3 Sample analysis 25
2.3.4 Competing compounds evaluation 28
2.3.5 Statistical analysis and data visualization 29
2.4 Results 30
2.4.1 General water quality parameters 30

2.4.2 Seasonal discrete vs. passive sampler results of nutrient and tracer concentrations 30
2.4.3 Relationships among nutrients and tracers from discrete and passive samples 39
2.4.4 Competition study between phosphate-bearing compounds 42
2.5 Discussion 43
2.5.1 Comparison of passive to discrete samples 43
2.5.2 DGT vs POCIS 47
2.5.3 Competition study between phosphate-bearing compounds 48
2.5.4 Tracking nutrient input with tracers 49
2.6 Conclusions 52
Chapter 3: Conclusions and future recommendations 54
References 56
Appendix A: Development and evaluation of DGT samplers 66
Appendix B: Chemicals, passive sampler specifications 68
Appendix C: Analytical methods 70
Appendix D: Quality assurance/quality control (QA/QC) 73
Appendix E: Impacts to DGT sampling rates 76
Appendix F: Figures and tables 80

List of Figures

Figure 2-1. Locations of sampling sites (black dots), watershed boundaries, and regional land use for *Hamlet Site*, *Agriculture Site*, and *Mixed-land Site*. Watershed boundaries were delineated using the Ontario Watershed Information Tool (OWIT). Inset includes the location of the study area (red star) within the Grand River Watershed, Ontario, Canada..... 24

Figure 2-2. Line graphs showing concentrations of PO_4-P, NO_3-N, and NH_4-N for discrete samples collected every 3 days at each site during the 14-day Fall 2021 and Spring 2022 deployments. Bar graphs show the mean and standard deviation of concentrations for duplicate or triplicate DGT passive samplers deployed for 6 days, and discrete samples on days 0, 3, and 6. Values along the x-axis for line graphs indicate compounds were below detection limits. Dashed vertical lines represent the time comparison from discrete samples on the line graphs to that of the bar graphs. Letter 'S' represents significant differences between discrete and passive samplers. 33

Figure 2-3. Mass of analytes (ng) recovered from POCIS versus DGT per mg of HLB. Samplers were deployed in triplicate and include compounds from both the Fall 2021 and Spring 2022 sampling events. Data points occurring only along the x- or y-axis indicate analytes were only found on POCIS or DGT samplers, respectively. The dotted line represents where DGT = POCIS in terms of mass of analyte recovered per mg of HLB……..336

Figure 2-4. Line graphs showing concentrations of human-specific tracers CAF, CBZ, GEM, IBU, NAP, SMX, ACE-K, and SUC for discrete samples collected every 3 days at each site location during the 14-day Fall 2021 and Spring 2022 deployments. Bar graphs represent the mean and ± standard deviation of concentrations obtained from triplicate DGT and POCIS deployed for 14 days, and the mean concentration for discrete samples collected every 3 days for 14 days. Dashed vertical lines represent the time comparison from discrete samples on the line graphs to that of the DGT samplers on the bar graphs. Samples below the MDL on the line graphs are reported as half the MDL value. Letters represent statistical differences between discrete and passive samples (s) and between DGT and POCIS (D). * = Not detected……337

Figure 2-5. Line graphs represent concentrations of agricultural-specific tracers (glyphosate, AMPA) for discrete samples taken every 3 days at each site location during the 14-day Fall 2021 and Spring 2022 deployments. Bar graphs represent the mean and ±

standard deviation of duplicate or triplicate DGT passive samplers deployed for 6 days, and discrete samples taken on days 0, 3, and 6. Dashed vertical lines represent the time comparison from discrete samples on the line graphs to that of the bar graphs. Samples below the MDL on the line graphs are reported as half the MDL value. * = Not detected. 33

Figure 2-6. Nutrients, anthropogenic-, and agricultural-tracer site correlation visualized by PCA in two dimensions for (A) discrete samples and (B) DGT passive samplers. 41

Figure 2-7. Effect of competing compounds on Metsorb® sorbent visualized by (A) mean mass of compound accumulated on triplicate DGT-Metsorb® samplers and (B) ratio of C_{DGT}/C_{SOLN}. Experimental conditions: initial PO_4-P = 1040 µg L^{-1}; glyphosate = 0.372 µg L^{-1}; AMPA = 2.14 µg L^{-1}. 42

Figure F-1. Bar graphs showing mean and standard deviation of concentrations for duplicate or triplicate DGT passive samplers deployed for 3- or 14-days, and discrete samples on days 0 and 3, or days 0, 3, 6, 9, 12, 14. Letter 'S' represent significant differences between discrete and passive samplers. 80

Figure F-2. Bar graphs showing mean and standard deviation of concentrations for duplicate or triplicate DGT passive samplers during Spring 2022 with and without DBL corrections. Samplers were deployed for 6- or 14-days, and discrete samples on days 0, 3, and 6 or days 0, 3, 6, 9, 12, 14. Letter 'S' represent significant differences between discrete and passive samplers. 81

Figure F-3. Hydrograph for Irvine River near Salem (02GA005) from the Government of Canada (Water Office, data accessed: May 1st, 2023) from Oct. 1st 2021 – Oct. 20th 2021. Fall 2021 sampling event occured between Oct. 5th 2021 – Oct. 19th 2021. 82

Figure F-4. Hydrograph for Irvine River near Salem (02GA005) from the Government of Canada (Water Office, data accessed: May 1st, 2023) from May 27th 2022 – June 15th 2022. Spring 2022 sampling event occurred between May 31st 2022 – June 14th 2022..... 83

Figure F-5. (A) Wire cage used to protect passive samplers during deployment (B) Biofouling on DGT samplers after 6-days of deployment (C) Biofouling on POCIS after 2-weeks of deployment. 84

List of Tables

Table 2-1. Properties and diffusion coefficients/sampling rates of compounds. 20

Table 2-2. Land use characteristics for each sampling site. 23

Table F-1. Mean measurements/concentrations for discrete samples collected on Day 0 and every 3rd day for 2-weeks (n = 6), unless noted below, at each sampling location during both seasonal studies. 855

Table F-2. Mean measurements/concentrations for discrete samples collected on Days 0 and 14 (n=2) during Fall 2021 and Spring 2022. All compounds analyzed by MECP……...… 86

Table F-3. Spearman rank order results showing correlation coefficients (ρ) obtained for all sampling locations during the Fall 2021 sampling event between nutrient and tracer concentrations. Strong positive correlations (>0.80) are highlighted in green, moderate positive correlations (0.50 – 0.80) are highlighted in yellow, and strong negative correlations (<-0.72) are highlighted in red. Dashed line indicate that no test was conducted as the measurement was below MDL..……87

Table F-4. Spearman rank order results showing correlation coefficients (ρ) obtained for all sampling locations during the Spring 2022 sampling event between nutrient and tracer concentrations. Strong positive correlations (>0.80) are highlighted in green, moderate positive correlations (0.50 – 0.80) are highlighted in yellow, and strong negative correlations (<-0.72) are highlighted in red. Dashed line indicate that no test was conducted as the measurement was below MDL. 888

Table F-5. Loadings table associated with the discrete and DGT PCA plots. Values missing were eliminated using VIF. 89

Table F-6. Results of statistical analysis using a Kruskal-Wallis test to compare measured concentrations by discrete, DGT, and POCIS samples as well as between sites for both sampling events. For comparison of less than three groups a Mann Whitney U test was performed. Significant differences are highlighted in green and defined as $P < 0.05$ (95% confidence). Dashed lines indicate analyte was not sampled using that method. Compounds measuring below their respective MDLs were assigned a censored value of half the MDL. Discrete samples n = 3/6; DGT n = 2/3; POCIS n = 3..... 90

Table F-7. Results of statistical analysis using a Kruskal-Wallis test to compare measured concentrations by discrete, DGT, and POCIS samples between study sites for both sampling events. For comparison of less than three groups a Mann Whitney U test was performed. Statistical differences are highlighted in green and defined as $P < 0.05$ (95% confidence). Blank boxes indicate analyte was not sampled using that method. Compounds measuring below their respective MDLs were assigned a censored value of half the MDL. For the *Hamlet/Agriculture/Mixed-land Sites* n = 2/3/6. 91

List of Abbreviations

ACE-K	acesulfame potassium
AMPA	aminomethylphosphonic acid
C_{ACTIVE}	concentration of discrete samples
CAF	caffeine
CBZ	carbamazepine
C_{DGT}	concentration of DGT samples
C_{POCIS}	concentration of POCIS samples
DBL	diffusive boundary layer
DGT	diffusive gradient in thin-films
DIC	dissolved inorganic carbon
DOC	dissolved organic carbon
E. coli	*Escherichia coli*
FIB	fecal indicator bacteria
GEM	gemfibrozil
HAB	harmful algal blooms
IBU	ibuprofen
KW	Kruskal-Wallis
NAP	naproxen
PES	polyethersulfone
POCIS	polar organic chemical integrative sampler
SMX	sulfamethoxazole
SPE	solid phase extraction
SPMD	semipermeable membrane device
SUC	sucralose
TWA	time-weighted average
WWTP	wastewater treatment plant

Chapter 1: Introduction

1.1 Passive samplers

Passive samplers have been successfully used for environmental monitoring of contaminants in surface water and groundwater (Alvarez et al., 2004; Fang et al., 2019; Huckins et al., 1993; Kingston et al., 2000; Metcalfe et al., 2014; Renaud et al., 2022; Zhang & Davison, 1995). Passive samplers are an alternative to discrete samples for monitoring surface water contaminants. From discrete samples, measured concentrations of compounds represent the water quality at the time of sampling (Supowit et al., 2016). Large temporal changes in contaminant concentrations are common in surface water systems due to changes in precipitation events and major input events from point and nonpoint sources. Capture of these variations in concentrations may require collection of a large number of samples; conversely, infrequent sampling may lead to vastly overestimating or underestimating concentrations. Many dissolved constituents are present at trace concentrations; consequently, large volumes of water may be required to concentrate target analytes for detection on available analytical instrumentation. Passive samplers can enable detection of contaminants at ultra trace levels that might not be practically achieved with discrete samples.

Passive samplers use a collecting medium to concentrate target compounds that usually consist of an exchange resin or sorbent encapsulated in a device to accumulate target contaminants from the environment over time. Passive samplers rely on advective transport or molecular diffusion to promote contact of the target contaminant with the medium in a predictable manner (Alvarez, 2013; Alvarez et al., 2007). Passive samplers offer an *in situ* sampling technique that does not require multiple discrete sampling trips to determine

representative concentrations of surface water contaminants. Passive samplers also require smaller sample volumes for analysis as compounds are concentrated over the exposure time for higher levels of detection, providing a time-weighted average (TWA) concentration.

1.1.1 POCIS

The polar organic chemical integrative sampler (POCIS) has been used to monitor hydrophilic compounds with a partition coefficient (K_p) < 3 (Alvarez et al., 2004). The device is comprised of two metal rings filled with a solid-phase sorbent selective to target a compound of interest and microporous polyethersulfone (PES) membranes on either side. POCIS targets monitoring of polar organic compounds in aquatic environments. The most common sorbent used in POCIS is Oasis HLB®, a hydrophilic-lipophilic-balance reversed-phase sorbent. This sorbent is commonly used for uptake of pharmaceutical compounds as many have multiple functional groups, resulting in a strong tendency to bind to carbonaceous components of the sorbent (Alvarez, 2013). Several studies have evaluated the effectiveness of POCIS as an *in situ* sampler for polar organic compounds (Bernard et al., 2019; Criquet et al., 2017; Metcalfe et al., 2014; Vrana et al., 2021) and showed that calculated concentrations from POCIS devices are in good agreement with those obtained for discrete samples. POCIS measured concentrations (C_{POCIS}) are determined using the following equation (1-1) (Alvarez et al., 2004):

$$C_{POCIS} = \frac{M}{R_s t} \qquad (1\text{-}1)$$

where M is the mass of compound accumulated on the binding layer (ng), R_s is the sampling rate (L day^{-1}) (Table 2-1), and t is the deployment time (s).

1.1.2 DGT

The diffusive gradient in thin-films (DGT) passive sampler was first proposed by Davison et al. (1994) and was used for monitoring concentrations of Zn and other metals in seawater. The device is comprised of a gel binding layer, specific to the analyte of interest, overlain by a diffusive layer made from either agarose or polyacrylamide. Both layers are overlain by a porous membrane. Any labile species can be measured using this sampler if there is an acceptable binding resin (Vrana et al., 2005).

DGT samplers have been further developed for uptake of a range of compounds including pesticides (Fauvelle et al., 2015), pharmaceuticals (Chen et al., 2013) bisphenol (Zheng et al., 2015), and nutrients (Panther et al., 2010). The first DGT devices to accumulate PO_4-P in surface waters utilized a ferrihydrite binding phase (Zhang et al., 1998). Although the resin showed promising results for determination of PO_4-P, results were inconsistent as the resin was custom synthesized, likely contributing to the observed inconsistencies. A titanium dioxide (TiO_2) binding phase was first proposed for measurement of inorganic As and Se (Bennett et al., 2010), and later used for measurement of soluble reactive phosphorus (SRP) in marine and fresh waters (Panther et al., 2010). This sorbent, by the name Metsorb®, is commercially available and mitigates most inconsistencies associated with one-off synthesized resins.

The following equation (1-2) describes the relationship of mass accumulated by DGT binding layers and TWA water concentration (C_{DGT}); full theories on DGT uptake mechanics are described elsewhere (Davison & Zhang, 2016):

$$C_{DGT} = \frac{M\Delta g}{DAt} \qquad (1\text{-}2)$$

Where M is the mass accumulated on the binding layer (ng), Δg is the thickness of the diffusive layer (cm), D is the diffusion coefficient ($cm^2\ s^{-1}$), A is the effective or physical area through which the compound diffuses (cm^2), and t is the deployment time (s). The thickness of the diffusive boundary layer (DBL) was taken into consideration when estimating concentrations from DGT samplers during Spring 2022 sampling event. The DBL is the thickness of the layer near the surface of an object in flowing water. The DBL thickness will become thinner in faster flowing water but is never 0. The most effective way to estimate the DBL in a flowing solution is to deploy DGTs with varying diffusive membrane thicknesses (Davison & Zhang, 2016). The diffusive layer thicknesses are plotted against the reciprocal of the analyte accumulated on the binding layer to determine the DBL. When the DBL is taken into consideration, the effective area (A_E, 3.8 cm^2) is used instead of the physical area (A_P, 3.14 cm^2) in equation 1-2, and is modified to equation 1-3:

$$C_{DGT} = \frac{M}{A_E t}\left(\frac{\delta^{DL}+\delta^{DBL}}{D}\right) \qquad (1\text{-}3)$$

where δ^{DL} is the thickness of the diffusive layer (cm) and δ^{DBL} is the thickness of the DBL (cm).

1.2 Nutrients in the environment

Due to the environmental impacts of algal/cyanobacterial blooms and effects on the quality of drinking water, the Canada-United States Great Lakes Water Quality Agreement (GLWQA) was passed in 1972 to reduce phosphorus (P) outputs in surface waters. This act restricted amounts of P allowed in household products such as detergent and output from wastewater treatment plants (WWTPs). Following brief water quality improvements, eutrophication in the Great Lakes has re-emerged, particularly in Lake Erie (Mohamed et al., 2019). To address eutrophication and the resurgence of harmful algal/cyanobacterial blooms (HABs), the Canadian and US governments

agreed to a binational P reduction target of 40% of the spring season loads of total and dissolved P in priority tributaries (Government of Canada, 2016). Eutrophication of water bodies occurs globally, for example in the Anhui and Hubei regions (China) (Xia et al., 2020) and New South Wales (Australia) (Mitrovic et al., 2008).

Phosphate is the most bioavailable form of P, meaning it is the most readily used form by aquatic organisms. Different forms of P including inorganic and organic forms, both particulate, and dissolved, enter the aquatic environment in several ways. A considerable amount of particulate and dissolved P enters surface water bodies following runoff from the surrounding landscape, with most P uptake occurring in small agricultural watersheds after these events (Ross et al., 2022). P concentrations can vary greatly over different flow conditions, particularly in small streams, with transient high levels recently shown to be taken up and stored by periphyton (Pearce et al., 2023; Ross et al., 2022).

While P is considered a limiting nutrient in freshwater aquatic environments for the growth of algae, cyanobacteria and plants, excessive inputs of nitrogen (N) also contribute to eutrophication conditions. Naturally occurring species of N in the environment include; nitrate (NO_3^-), ammonium (NH_4^+), ammonia (NH_3^0), nitrite (NO_2^-), nitrous oxide (N_2O), organic N, and N gas ($N_{2,g}$). Most plants use NO_3^- and NH_3^0 for protein synthesis, making N a key nutrient for plant growth (Lusk et al., 2017). The nitrogen cycle is a biogeochemical cycle by which N is converted into different forms. The most common forms of N found in surface waters are NH_4^+ and NO_3^-. When dissolved in water, it can take on the ionized form of NH_4^+ (pK_a value of 8.86), or NH_3^0, depending on pH (Li et al., 2020).

Input of nutrients in the environment can occur from point and nonpoint sources. Point sources typically have a large input from a confined area and are easily identifiable, such as

WWTPs and large livestock facilities. Nonpoint sources include input from broad spatial areas including agricultural fields and livestock grazing areas, septic systems, and urban stormwater (Lin et al., 2019). Phosphate has been shown to adsorb to oxide phases, notably Fe (e.g., ferrihydrite), Mn (e.g., pyrolusite), and Al (e.g., gibbsite) oxides or (oxy)hydroxide amorphous or crystalline solids where it enters the aquatic environment from runoff following precipitation events. NO_3^- is highly soluble in water and does not adsorb onto particulate matter or form inorganic compounds and is mainly transformed through biological processes. P and N have been shown to be limiting nutrients for primary production of aquatic plant growth (Lapointe et al., 2017; Matlock et al., 1998; Schindler, 1977; Tyre et al., 2023).

1.2.1 Septic systems as anthropogenic nonpoint source of nutrients

Septic systems are onsite wastewater treatment units mainly used in rural and semi-urban areas where there are no municipal WWTPs. It is estimated that 14% of Canadian households (Statistics Canada, 2011) and 20% of US households (USEPA, 2023) use septic systems. Septic tanks hold wastewater and allow solid matter to accumulate on the bottom of the tank and act as an anaerobic digester. The effluent then flows into the drain field to induce infiltration to the unsaturated zone (USEPA, 2023). The effluent is gravity fed through perforated pipes to allow the wastewater to flow into the subsurface, ~30 to 90 cm deep. The wastewater is treated through aerobic and partially oxidizing conditions while infiltrating through the unsaturated zone, until recharge to the water table (Conn et al., 2006, 2010). Lateral transport of the effluent can lead to discharge into nearby surface waters (Oldfield et al., 2020). Detailed studies have indicated that even small rural populations that use septic systems can contribute significant nutrient pollution to headwater catchments (Digaletos et al., 2023; Jarvie et al., 2010; Withers et al., 2011).

A substantial amount of septic derived P can be attenuated through mineral precipitation phases after the effluent leaves the drain field (Zanini et al., 1998). While the mobility of P in the subsurface is controlled by many environmental factors (wastewater loading rate, depth of water table, etc.), the pH of the unsaturated zone under a septic system is a key factor in determining the attenuation of P, and therefore, the amount that reaches the water table (Oldfield et al., 2020). Immobilization of a substantial amount of septic derived P may occur at low pH conditions, under which precipitation of secondary phosphate minerals is favored. The amount of P released from septic tanks into tributaries is determined by the flow paths of the effluent, as well as the retention and attenuation of P. PO_4-P concentrations have been observed to be as elevated as 1.5 mg L^{-1} in groundwater downgradient from the septic tank (Ptacek, 1998), while another study showed soluble P concentrations discharging directly into a stream at concentrations of <1-14 mg L^{-1} (Withers et al., 2011). Septic systems account for around 5 ± 2% of total P loads to Lake Erie from Canada (Oldfield et al., 2020). This estimate includes the assumption that a fraction of septic systems fail with no attenuation of P occurring.

Large quantities of N are also released into the environment from septic systems. Typically, less than 5% of total N is removed from wastewater in septic systems (WERF, 2008). Volatilization of NH_3 or sedimentation of organic matter account for the small amount of N that is removed in the tank (Lusk et al., 2017). Due to anaerobic conditions inside septic tanks the main removal mechanism is denitrification. Organic N in a typical septic system is mineralised to NH_4 through ammonification, while other transformations of N are unlikely due to aerobic conditions needed for such processes (Lusk et al., 2017). Concentrations as high as 80 mg L^{-1} of (NO_3+NO_2)-N and greater than 15 mg L^{-1} for NH_4-N have been measured 20 m downgradient

from the source of input (Ptacek, 1998). Another study observed a septic tank discharging directly into a stream with comparable concentrations of N (8-63 mg L^{-1}) (Withers et al., 2011).

1.2.2 Agricultural activities as nonpoint sources of nutrients

Agriculture is considered a large contributor of nonpoint source nutrients to the aquatic environment (IJC, 2018). Agricultural practises contribute excessive P and N loadings to surface waters from over usage of fertilizers and manure, which commonly reach surface and groundwaters after precipitation events (Schoumans, 2014). Inorganic P and N are the main components in fertilizers, which have been identified as large nonpoint sources of nutrients to natural waters (Conley et al., 2009; Helm et al., 2012; IJC, 2018; Lin et al., 2019). Leaching of NO_3^- to groundwater increased by 24% from 1981 to 2001 in the Great Lakes Basin due to an increase in both livestock and fertilizer application, yet P input slightly declined as the amount of agricultural activity continued to grow (Grannemann & Van Stempvoort, 2016). Comparatively, another study characterized loadings from agricultural practices at 10 – 150 kg^{-1} ha^{-1} yr^{-1} of SRP compared to 5 – 11 kg^{-1} ha^{-1} yr^{-1} from septic systems in the US (Lombardo, 2006).

1.3 Tracers for determining sources of contamination

Characterizing sources of contaminants in the environment is challenging as there can be multiple input origins (Hogan et al., 2023). The use of tracers, both naturally occurring and from wastewater, have been used extensively to track and predict the fate of emerging contaminants (Hoque et al., 2014; Lee et al., 2019; Li et al., 2010). An ideal tracer is present at concentrations above the analytical detection limit and is conservative, meaning it is transported by water in the dissolved phase and is not lost to chemical or biological processes (Van Stempvoort et al., 2013).

Stable isotopes have also been used alongside chemical and biological tracers for nutrient source identification (Lapointe et al., 2015; Tyre et al., 2023).

Artificial sweeteners, acesulfame potassium (ACE-K) and sucralose (SUC), are considered ideal human-specific tracers. These tracers are found in abundance in wastewater, minimally biodegrade, and are persistent through wastewater treatment (Buerge et al., 2009; Fu et al., 2020; Metcalfe et al., 2014; Robertson et al., 2013; Snider et al., 2017). Pharmaceuticals, including caffeine (CAF), carbamazepine (CBZ), gemfibrozil (GEM), ibuprofen (IBU), naproxen (NAP), and sulfamethoxazole (SMX) have also been used as tracers to delineate sources of human wastewater in multiple studies (Carrara et al., 2008; Digaletos et al., 2023; Liu et al., 2014; Richards et al., 2017). Fecal indicator bacteria (FIB) such as *Escherichia coli* (*E. coli*) have been used to identify wastewater sources but have limited effectiveness in rural areas with multiple sources of fecal contamination from humans and animals (Edge et al., 2020; Richards et al., 2017). Host specific-FIB, such as human and bovine *Bacteroides*, can be used to distinguish human from livestock fecal contamination sources (Lee et al., 2014). Uncertainty related to predictions of the origin of contaminants decreases as multiple tracers are used simultaneously (Digaletos et al., 2023; Richards et al., 2017).

Countries worldwide commonly use the herbicide glyphosate (N-[phosphonomethyl] glycine; commercial name of Roundup®) on transgenic crops including soybean, corn, and cotton in agricultural practices to control herbaceous plants and weeds (Aparicio et al., 2013). The movement of glyphosate can be through soil particles, which carry adsorbed glyphosate and are transported with surface run-off. This allows the glyphosate to be introduced into surface waters where it desorbs from the soil particles and biodegrades to AMPA, which accumulates on the bottom sediment (Aparicio et al., 2013). Glyphosate is bonded through phosphate groups to

soil particle surfaces that contain Fe-OH and Al-OH binding sites (Duke & Powles, 2008). The main degradation product of glyphosate is aminomethylphosphonic acid (AMPA) which forms through microbiologically mediated reactions. Degradation of glyphosate to AMPA makes the compound moderately persistent, as the degradation time varies from 13.8 to 300 days (Van Bruggen et al., 2018). AMPA is often found in higher concentrations in catchments than glyphosate as it is also the degradation product of other phosphonate compounds; the presence of AMPA in water does not always indicate the presence of glyphosate (Poiger et al., 2020).

The main pathway for glyphosate transport into surface water is either directly from surface runoff or through the subsurface in shallow groundwater (Van Stempvoort et al., 2014). The presence of glyphosate and AMPA in the Nottawasaga River in Ontario, Canada, indicated that groundwater can transmit these compounds from a catchment dominated by agricultural practises to surface waters (Van Stempvoort et al., 2016). In jurisdictions, such as Ontario, that limit the cosmetic use of glyphosate (e.g., banned use on lawns at homes, parks and schools) this pesticide is likely more of an agricultural origin in rural areas (Cosmetic Pesticides Ban Act, 2008).

1.4 Development and evaluation of passive samplers

Continued evaluation of passive samplers is vital for their expanding use in environmental monitoring. Many recent studies have aimed to further develop the original DGT passive sampler (Zhang & Davison, 1995) to expand the diversity of compounds captured with different sorbents (Challis et al., 2016; Huang et al., 2017; Wang et al., 2022). Currently, there is limited information on the use of passive samplers for the uptake of artificial sweeteners. HLB reversed phase sorbent has been used in past studies in POCIS (Alvarez et al., 2004; Li et al., 2011; Metcalfe et al., 2016) with varying success to accumulate the artificial sweetener ACE-K, as

uptake of ACE-K is likely low on HLB (Digaletos, 2019; Liu et al., 2023). ACE-K is of interest for tracking wastewater as it is an excellent anthropogenic tracer. ACE-K is recalcitrant, as it is consistently found in WWTP influent and effluent (Van Stempvoort et al., 2020). While many compounds in wastewater are biodegraded by chemical, physical, or biological processes, recalcitrant compounds are not readily transformed. ACE-K has a removal typically <2% at WWTPs (Castronovo et al., 2017). Based on this low removal rate, similar conditions are likely to be observed with wastewater output from septic systems where ACE-K is found in rural communities (Digaletos et al., 2023; Robertson et al., 2013).

HLB sorbent has been the dominant binding phase used in POCIS and DGT samplers for uptake of pharmaceuticals and personal care products. The reversed phase sorbent allows uptake of a wide range of acidic, basic, and neutral compounds that have multiple functional groups (Alvarez et al., 2007). Reversed phase sorbent typically has poor recovery for artificial sweeteners, so investigations into a new sorbent have been explored. Sultana & Metcalfe (2022) evaluated a weak anion exchange (WAX) sorbent (Strata X-AW) loaded into a POCIS for ACE-K uptake, as ACE-K is in the anionic form ($pK_a = 2$) at the pH of their study (pH = 8). ACE-K was underestimated on the WAX sorbent compared to POCIS loaded with HLB sorbent from their field study. Another WAX sorbent (OASIS^{TM}, Waters Corporation) showed high recoveries of ACE-K when this sorbent was used in solid phase extraction (SPE) to remove ACE-K from water samples (Ordóñez et al., 2012).

Uptake of phosphate, glyphosate, and AMPA has been evaluated and optimized on the Metsorb®-DGT sampler in past studies (Fauvelle et al., 2015; Panther et al., 2010). Metsorb®, made from TiO_2, is the optimal binding phase for phosphonates. Evaluation of competing ions has been studied extensively for most established DGT samplers (Huang, Bennett, Teasdale, et

al., 2016; Price et al., 2013; Wang et al., 2016), yet the Metsorb®-DGT sampler has not been evaluated for potential competition impacts between only phosphate-bearing compounds.

1.5 Research objectives

The objective of this study was to develop and implement passive sampling technology deployed for uptake of nutrients and multiple anthropogenic- and agricultural-specific tracers to compare their effectiveness in estimating surface water concentrations to that of discrete samples, and to distinguish contamination sources. In this study, passive samplers were used to elucidate dominant nonpoint septic-system contamination from agricultural sources in rural headwater streams. Passive samplers can assist in determining contaminant origins from nonpoint sources in rural watersheds, and reduce sampling frequency and variability often associated with discrete sampling in surface water bodies (Criquet et al., 2017; Hawker et al., 2022; Huang, Bennett, Teasdale, et al., 2016). Species included those found predominantly in wastewater (pharmaceuticals, artificial sweeteners), predominantly in agricultural settings (herbicides), and those derived from a range of sources, including anthropogenic, agricultural, and natural sources (nutrients). Passive and discrete samples were taken in a rural watershed, with one site downstream of a hamlet with known septic system contamination (Digaletos et al., 2023), an adjacent site that is predominantly agricultural land-use, and downstream of both sites (mixed land-use). A secondary objective of this study was to evaluate two types of passive samplers. The first was to develop and evaluate a passive sampler for the uptake of the artificial sweetener ACE-K. The second was the Metsorb®-DGT passive sampler to determine any possible competition between phosphate-bearing compounds, including pesticides and phosphate.

1.6 Thesis organization

This thesis is organized as three chapters representing one central study, and a smaller study structured as an appendix. Chapter 1, titled “Introduction”, provides a comprehensive background of the study, the research objectives, and the thesis organization. Chapter 2, “Array of passive surface-water samplers to assist in distinguishing nonpoint anthropogenic contamination from agricultural sources” is structured as a journal article and addresses the main research objective. The third Chapter titled “Conclusions” is a summary of the major findings, any limitations from an environmental sampling perspective, and future recommendations.

Chapter 2: Array of passive surface-water samplers to assist in distinguishing nonpoint anthropogenic contamination from agricultural sources

2.1 Summary

Passive samplers are increasingly utilized in environmental monitoring due to their ease of use, low cost, and provision of long-term time-weighted average (TWA) concentrations. The continued use and validation of passive samplers is crucial to understanding limitations and advantages associated with environmental sampling. Diffusive gradient in thin-films (DGT) and polar organic chemical integrative samplers (POCIS) were used alongside discrete sampling to characterize nutrient (P, N) sources in rural catchments using a suite of anthropogenic- (pharmaceuticals, artificial sweeteners) and agricultural-specific (herbicides) tracers. Passive samplers were deployed between 6 to 14 days at three distinct locations (*Hamlet, Agricultural,* and *Mixed-land Sites*) where discrete samples were collected every 3 days over 14 days during two sampling periods in the fall and spring. DGT passive samplers provided concentrations that were in good agreement with discrete sample concentrations when diffusive boundary layer (DBL) impacts, which are typically associated with environmental sampling, were considered. DGT concentrations were higher than POCIS for 24 of 30 paired observations and estimates were on average 2.84 times greater across all analytes. Anthropogenic tracers were routinely detected on average 63 times higher in concentration at the *Hamlet Site,* downstream of a community serviced solely by on-site septic systems, than at the *Agriculture Site.* Agricultural tracers glyphosate and AMPA had highest occurrences and mean concentrations at the *Agricultural Site* (0.86 ± 1.66 µg L^{-1} and 1.41 ± 0.85 µg L^{-1}, respectively). At the *Hamlet Site,* P concentrations were correlated to all anthropogenic tracers from both discrete and passive

samples. The presence of anthropogenic-specific tracers and elevated nutrient concentrations at the *Hamlet Site* suggest septic systems may be an underappreciated source of nutrient loading in small headwater streams in rural areas. The results also suggest that the selected array of passive samplers may be a powerful tool to distinguish nonpoint sources of nutrients and contaminants in small headwater streams.

2.2 Introduction

The successful use of passive sampling devices for environmental monitoring has been reported in many recent studies (Challis et al., 2020; Fang et al., 2019; Fauvelle et al., 2015; Huang et al., 2017; Metcalfe et al., 2019; Renaud et al., 2022), and continued evaluation of their performance in surface waters remains an important aspect of technique validation. Passive samplers, an alternative to discrete sampling, provide a time-weighted average (TWA) concentration by accumulating target compounds *in situ* over a period of a few days or weeks. Discrete sampling generally requires the collection of large volumes of water at a pre-established time, potentially missing variability in stream water concentrations.

A range of passive samplers has been used to detect a variety of compounds in past studies such as diffusive gradient in-thin films (DGT) (e.g., Zhang & Davison, 1995), polar organic chemical integrative sampler (POCIS) (e.g., Alvarez et al., 2004), semipermeable membrane device (SPMD) (e.g., Huckins et al., 1993), P-Traps (Müller et al., 2008), and Chemcatcher® (e.g., Kingston et al., 2000). POCIS are well-established passive samplers used to detect and quantify a range of polar to moderately hydrophilic compounds in water (Alvarez et al., 2004; H. Li et al., 2010; Sultana & Metcalfe, 2022; Liu et al., 2023). Similarly, DGT samplers are used to detect a suite of compounds ranging from metals, to nutrients, to a variety of anthropogenic organic compounds (Vrana et al., 2005) and help to fill in gaps where POCIS

are not applicable (Panther et al., 2010; Wu et al., 2023; Zhuo et al., 2023). Each type of passive sampler varies in its application in environmental conditions, target contaminants, and ease of compound extraction.

Excessive nutrient loading by phosphorus (P) and nitrogen (N) contribute to the growing problem of eutrophication in lakes and rivers around the world (Jarvie et al., 2017; Lapointe et al., 2015; Schindler et al., 2016). Phosphate is the most bioavailable form of P, meaning it is the most readily used form of P by aquatic organisms. A considerable amount of P enters surface water bodies following runoff from the surrounding landscape, with most P losses occurring after these events (Ross et al., 2022). P concentrations are highly variable and can change rapidly over different flow conditions, particularly in small streams, and can be important for periphyton growth in rivers and export of P among watersheds (Pearce et al., 2023; Ross et al., 2022). Determining the origin of nutrients in the environment becomes challenging when there are multiple nonpoint input sources such as septic systems, fertilizer, and manure run-off from fields and livestock grazing areas (Carey & Migliaccio, 2009; Carpenter et al., 1998; Taebi & Droste, 2004). P has been shown to sorb onto organic matter and soil particles where it enters the aquatic environment primarily from runoff following precipitation events (Ross et al., 2022). Dissolved forms of P, including SRP, have been shown to transport through subsurface tiles in agricultural watersheds. NO_3^- is highly soluble in water and does not adsorb onto particulate matter or form inorganic solids and is mainly transformed through biological processes. The primary pathway for NO_3^- entry into surface waters is from runoff of fertilizers containing NO_3^-, typically from agricultural practises in rural watersheds (Carpenter et al., 1998; Grannemann & Van Stempvoort, 2016).

Agricultural practises can contribute to nutrient loading in rural watersheds from extensive application of fertilizers and manure that is released to surface and ground waters most commonly after precipitation events (Schoumans, 2014). Agricultural activities are considered one of the largest contributions of nutrient loading to the Laurentian Great Lakes and other waterbodies globally (Carpenter et al., 1998; IJC, 2018). Fertilizers are rich in inorganic N and P and are main nonpoint sources of these compounds to natural waters (Conley et al., 2009; Helm et al., 2012; Lin et al., 2019). Manure consists of organic-bound N and P which contribute inputs to surface water bodies at varying concentrations depending on precipitation and flow conditions.

Septic systems are onsite wastewater treatment units that an estimated 14% of Canadian households (Statistics Canada, 2011) and 20% of US households (USEPA, 2023) use. Effluent from septic tanks flows into the drain field to induce infiltration to the unsaturated zone. The wastewater is treated through aerobic and partially oxidizing conditions while slowly filtering through the soil, until recharge into groundwater (USEPA, 2023). After effluent reaches the water table it is transported with groundwater flow and may discharge into nearby surface waters (Conn et al., 2006, 2010; Spoelstra et al., 2020). After the effluent leaves the drain field, substantial retention of P can occur through a combination of adsorption and precipitation reactions (Ptacek, 1998; Robertson et al., 2019; Zanini et al., 1998). If retention in the unsaturated zone is limited, elevated concentrations of soluble PO_4 can persist in the saturated zone, potentially reaching surface waters (Robertson & Harman, 1999). Septic systems can also output large quantities of N into the environment as typically less than 5% of total N is removed from wastewater in septic systems (Water Environment Research Foundation (WERF), 2008). Septic systems have been identified as a nonpoint anthropogenic source of nutrients into the

environment (Carpenter et al., 1998; Oldfield et al., 2020; Spoelstra et al., 2020; Withers et al., 2011) and input may be underappreciated, especially in smaller headwater streams (Digaletos et al., 2023; Hogan et al., 2023; Lapointe et al., 2015; Tyre et al., 2023).

Multiple sources of nutrient input become challenging to characterize in watersheds with both anthropogenic and agricultural land use. Using multiple tracers decreases the uncertainty of differentiating sources, can help to understand transport pathways of contaminants (Buerge et al., 2009; Digaletos et al., 2023; Richards et al., 2017), and can lead to targeted mitigation measures to reduce impacts to the aquatic environment. Several artificial sweeteners, including acesulfame-K (ACE-K) and sucralose (SUC), have been identified as optimal tracers in many studies for characterizing human wastewater due to their persistence and minimal biodegradation in the environment (Buerge et al., 2009; Fu et al., 2020; Metcalfe et al., 2014; Robertson et al., 2013; Snider et al., 2017; Spoelstra et al., 2017; Van Stempvoort et al., 2011). Pharmaceuticals including caffeine (CAF), carbamazepine (CBZ), gemfibrozil (GEM), ibuprofen (IBU), naproxen (NAP), and sulfamethoxazole (SMX), and bacteriological human-specific tracers, such as *Bacteroides*, have also been successfully used to track and predict the fate and transport of wastewater contaminants from human-specific sources (Buerge et al., 2009; Carrara et al., 2008; Digaletos et al., 2023; Liu et al., 2014; Robertson et al., 2016).

Agricultural-specific tracers can help to distinguish between agricultural and anthropogenic nonpoint sources, including pesticides and livestock-associated bacteriological markers. The herbicide glyphosate is used on transgenic crops such as corn and soybeans. Along with its degradation product aminomethylphosphonic acid (AMPA), these compounds can be used as tracers to characterize groundwater from areas dominated by agricultural practises (Struger et al., 2015; Van Stempvoort et al., 2014, 2016). The main pathway for glyphosate

transport is either directly from surface runoff, or through soils in the subsurface where it has been detected in shallow groundwater. Glyphosate is an ideal tracer of agricultural impacts on surface water quality in rural areas due to its moderate persistence in the environment and large input from agricultural practises, compared to its smaller-scale use by households (Van Bruggen et al., 2018). In Ontario (Canada) and other jurisdictions, glyphosate has been banned or restricted for cosmetic use by homeowners, with sources from rural areas likely tied to agricultural practises (Cosmetic Pesticides Ban Act, 2008; Todd & Struger, 2014).

Development and implementation of passive sampling technology for uptake of a range of anthropogenic- and agricultural-specific tracers was performed in this study to compare the effectiveness of passive samplers to discrete samples to delineate nonpoint sources of contamination to small rural headwater streams. Passive samplers reduce sampling frequency and variability often associated with discrete sampling. Discrete and passive samples were collected in surface waters at three sampling locations in small rural headwater streams every 3 days for 14 days in Fall 2021 and Spring 2022. A range of anthropogenic and agricultural tracers targeting N, P, glyphosate, AMPA, pharmaceuticals and artificial sweeteners, were collected to determine nonpoint sources of nutrients in these surface water bodies. Human and bovine specific biomarkers were collected at discrete times to further elucidate sources of nutrients.

2.3 Methods

2.3.1 DGT and POCIS specifications

Three types of DGT passive samplers were purchased pre-assembled from DGT Research (Lancaster, UK). Metsorb®-DGT samplers were loaded with Metsorb® binding layer (TiO_2, 0.8 mm) and used for the uptake of phosphate, glyphosate, and AMPA. A520E-DGT samplers were loaded with a A520E binding layer (0.78 mm) which is selective for nitrate. HLB-DGT samplers

were loaded with a HLB binding layer (0.5 mm) and used for uptake of pharmaceuticals and artificial sweeteners. The sampling units were stored in the refrigerator at 4°C until deployment.

Two laboratory-assembled DGT samplers were developed and prepared for uptake of ammonium (PrCH-DGT) and ACE-K (Strata-DGT), as preloaded samplers for these compounds were not available. PrCH and Strata X-AW binding layers were prepared by adding 6.25 g of PrCH or 1.00 g of Strata X-AW sorbent to 15 mL of a 1.5% agarose solution. The solution was cast between two glass plates separated by a 0.75 mm spacer and was set for 45 min at room temperature. Once set, the layers were cut into 2.54 cm diameter circles and stored in ultrapure water (MilliQ A10 water system 18.2 MΩ cm @ 25 °C). Each gel binding disc had an area of 4.91 cm^2 and contained 156 mg of PrCH sorbent or 25 mg of Strata X-AW sorbent (Huang et al., 2016a; Challis et al., 2016). POCIS were purchased pre-assembled from Environmental Sampling Technologies (St. Joseph, MO, USA) and contained 200 mg of Oasis HLB sorbent between two PES membranes.

Table 2-1. Properties and diffusion coefficients/sampling rates of compounds.

Compound	Passive Sampler	Diffusion coefficient (D) (25°C, 10^{-6} cm^2s^{-1})	Sampling rate (R_s) (25°C, L day^{-1})	Reference (D/R_s)
PO_4	Metsorb®-DGT	6.05	-	Panther et al. 2010
NO_3	A520E-DGT	14.2	-	Huang et al. 2016b
NH_4	PrCH-DGT	17.1	-	Huang et al. 2016a
GLY	Metsorb®-DGT	3.28	-	Fauvelle et al. 2015
AMPA	Metsorb®-DGT	4.01	-	Fauvelle et al. 2015
CAF	HLB-DGT	6.42		Fang et al. 2019
	HLB-POCIS		0.151	Li et al. 2010
CBZ	HLB-DGT	5.01		Challis et al. 2016
	HLB-POCIS		0.397	Li et al. 2010
GEM	HLB-DGT	3.58		Challis et al. 2016
	HLB-POCIS		0.306	Li et al. 2010

IBU	HLB-DGT	4.07		Challis et al. 2016
	HLB-POCIS		0.348	Li et al. 2010
NAP	HLB-DGT	4.37		Challis et al. 2016
	HLB-POCIS		0.298	Li et al. 2010
SMX	HLB-DGT	5.1		Chen et al. 2017
	HLB-POCIS		0.348	Li et al. 2010
ACE-K	Strata-DGT	4.85		*This study
	HLB-POCIS		0.0014[a]	Liu et al. 2023
SUC	Strata-DGT	3.86		*This study
	HLB-POCIS		0.114[b]	Sultana & Metcalfe 2022

Table 2-1 continued

Compound	pK$_a$	logK_{OW}	logD_{OW}[1]
H_3PO_4, $H_2PO_4^-$, HPO_4^{2-}, PO_4^{3-}	2.16, 7.21, 12.32	-	-
NO_3	-9.90	-	-
NH_4	9.25	-	-
GLY	5.90	-3.40	-5.50
AMPA	5.60	-	-
CAF	-1.16	-0.55	-0.55
CBZ	-3.80	2.77	2.77
GEM	4.42	4.39	1.14
IBU	4.85	3.84	0.85
NAP	4.19	2.98	-0.36
SMX	1.97 (acid) 6.16 (base)	0.79	-0.11
ACE-K	3.00	-0.69	-3.06
SUC	11.9	-0.47	-0.47

*No diffusion coefficient available in the literature and was developed for this study based on Davison (2016; *see* Appendix A).
[a]R_s at 20°C.
[b]R_s at 15°C.
[1]logD_{OW} (pH dependent logK_{OW}) values reported using a pH of 8, which is the mean value of pH at all three sampling sites.

2.3.2 Field site characterization and study design

Three sampling locations were chosen in a small rural headwater stream in the Grand River watershed (GRW, ON, Canada) based on differences in land-use (Fig. 2-2). The *Hamlet Site* was

downstream of a rural hamlet that is serviced exclusively by septic systems. The *Agriculture Site* was downstream of agricultural activities, dominated by crop land and small farms, while the *Mixed-land Site* was further downstream after the convergence of the *Hamlet* and *Agricultural Site* catchments, but also had cattle farms immediately upstream. A nearby flow gauge in an adjacent stream (Water Survey of Canada 02GA005) was monitored, to observe hydrometric data before and during deployment. Precipitation data were collected from the closest weather station approximately 14 km away (Environment Canada, station ID: 6142402). Annual precipitation totalled 953 mm for all sites. This watershed was characterized by overburden material that is primarily composed of a low permeability diamicton (silty clay till) (Digaletos et al., 2023).

Two field deployments were conducted over a two-week period in Fall 2021 (5 Oct. 2021 – 19 Oct. 2021) and Spring 2022 (31 May 2022 – 14 June 2022). The passive samplers for NO_3-N (A520E-DGT) and PO_4-P (Metsorb®-DGT) were deployed in triplicate for three days and in duplicate for 6 days to gauge the appropriate deployment time based on manufacturer's recommendations (DGT Research Ltd). Samplers for NH_4-N (PrCH-DGT) were deployed in triplicate for 6 days and in duplicate for 14 days, while samplers (HLB-DGT, POCIS) for a suite of pharmaceuticals (CAF, CBZ, IBU, GEM, NAP, SMX) and sweeteners (ACE-K and SUC) were deployed in triplicate for 14 days. Wired cages were used to secure the passive samplers in place in the streams, as well as protect them from environmental debris (Fig. F-5). All passive sampler membranes were placed parallel to the streamflow and deployed in the middle of the stream to ensure adequate contact with flowing water. Upon retrieval, all samplers were rinsed with ultrapure water onsite, covered and transported on ice to the laboratory.

Discrete stream water samples were collected on days 0, 3, 6, 9, 12, and 14 during each sampling period concurrent with deployment and retrieval of passive samplers. In some instances, discrete samples were collected at a lower frequency for general water quality characterization. Discrete samples were collected using a grab pole or by wading into the middle of the stream. Samples analyzed at University of Waterloo (general chemistry, nutrients, and tracers) were collected using 2x 1-L amber glass bottles. Samples were filtered with 0.45 µm PES membranes upon return to the University, then preserved and stored at 4°C or frozen until analysis. Samples analysed at the Ontario Ministry of the Environment, Conservations and Parks (MECP) laboratory (Toronto, ON) were collected in 500 mL polyethylene terephthalate (PET) bottles (general chemistry), 250 mL PET bottles (microbiological analysis), and field filtered with a syringe through 0.45 µm membranes into glass vials (dissolved nutrient analyses). All discrete samples were transported on ice to the respective laboratories.

Determinations of pH were made in the field using a pH electrode (Ross combination, Orion 815600) calibrated with pH 4.0, pH 7.0, and pH 10.0 buffers prior to each measurement. Water temperature was measured using a thermistor during each site visit. Alkalinity was analyzed on filtered samples using a standardized acid titrant (0.16 N H_2SO_4) and a HACH digital titrator following method 8203 (AHPA, 1992).

Table 2-2. Land use characteristics for each sampling site.

Characteristic	*Hamlet*	*Agriculture*	*Mixed-land*
Drainage area (km^2)[a]	1.21	4.57	12.35
Wetland (%)[a]	0.00	2.97	3.58
Agricultural (%)[a]	60.0	94.2	88.0
Domestic/infrastructure (%)[a]	39.7	2.73	7.72
Homes/buildings[b]	166	15	181

[a]Ontario Watershed Information Tool (OWIT); [b]Google Earth Imagery

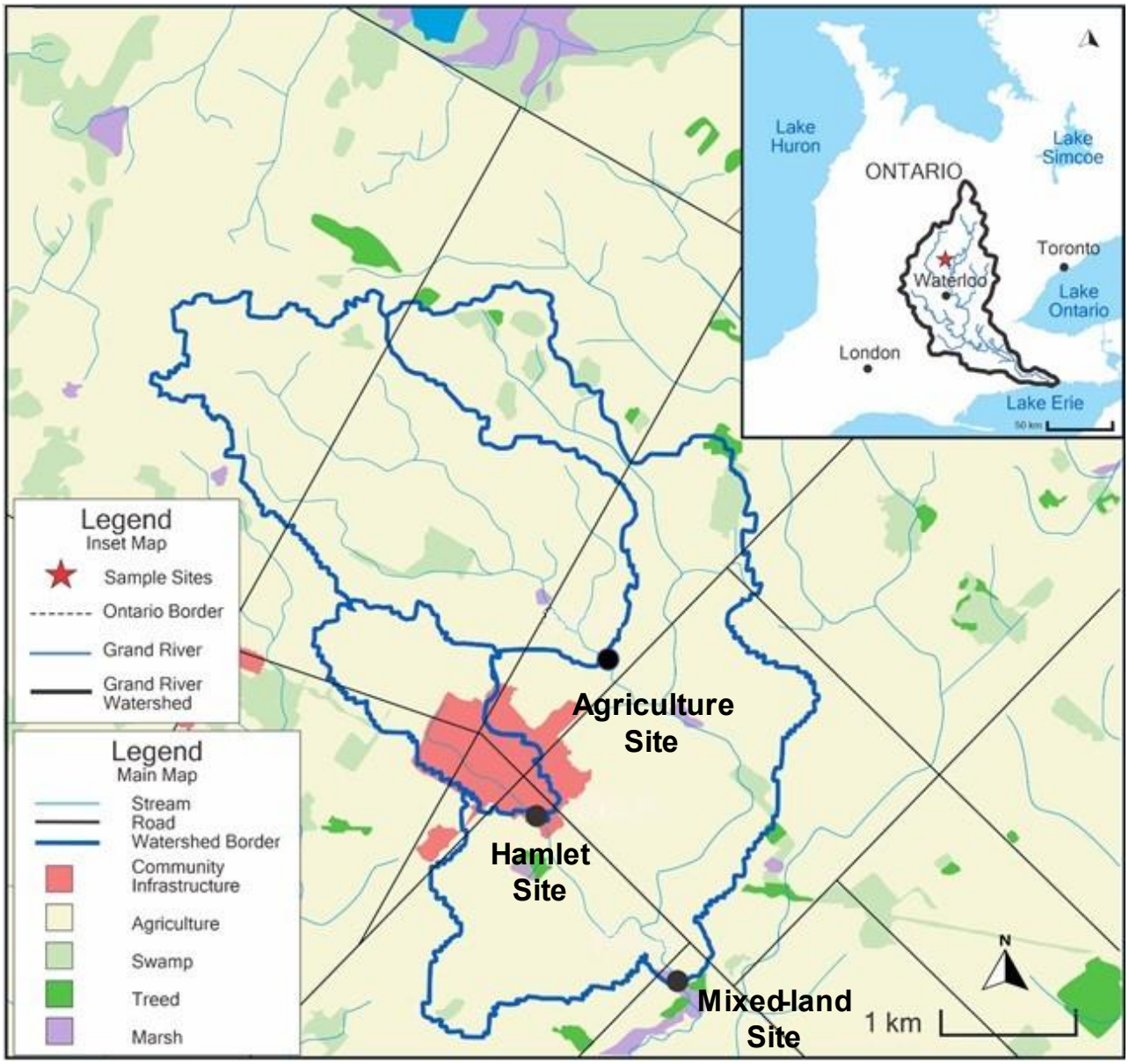


Figure 2-1. Locations of sampling sites (black dots), watershed boundaries, and regional land use for *Hamlet Site*, *Agriculture Site*, and *Mixed-land Site*. Watershed boundaries were delineated using the Ontario Watershed Information Tool (OWIT). Inset includes the location of the study area (red star) within the Grand River Watershed, Ontario, Canada.

2.3.3 Sample analysis

2.3.3.1 Water quality analysis

Orthophosphate (PO_4-P) and ammonia (NH_3-N) concentrations were determined using a HACH spectrometer DR/8400 following the ascorbic acid method (4500 P: E) and the salicylate method (4500-NH3), respectively (APHA, 2005). Anion (Cl^-, F^-, NO_3^-, SO_4^{2-}) concentrations were determined by ion chromatography (Dionex ICS-5000+, Mississauga, CA). Nutrients, dissolved organic carbon (DOC), dissolved inorganic carbon (DIC), and other water chemical properties were analyzed by the MECP LaSB using colourimetry (Tables F1 and F2).

Total (BacGen), human-specific (BacHum), and bovine-specific (BacBov) *Bacteroides* genetic markers were measured in discrete samples through quantitative polymerase chain reaction (qPCR) following an MECP accredited method (MECP, 2022), based on Lee et al. (2010, 2014), expressed as cells (C) $(100\ mL)^{-1}$ (calculated as 5.5 copies of PCR target per cell). *E. coli* were analyzed by *Colilert* substrate and incubated in *Quanti-trays* (35.0 ± 0.5°C for 24-28 h), with results expressed as most probable number (MPN) per 100 mL (MECP, 2017).

Target compounds were extracted from DGT passive samplers by placing the diffusive layer in either a 1.0 M solution of NaOH (phosphate, glyphosate, AMPA), a 2.0 M solution of NaCl (nitrate, ammonium), or 3x3 mL extractions of MeOH (pharmaceuticals, sweeteners) (Challis et al., 2016; Fauvelle et al., 2015; Huang et al., 2017; Huang, Bennett, Teasdale, et al., 2016; Huang, Bennett, Welsh, et al., 2016). POCIS were extracted with 40 mL of MeOH and passed through 3 cc Strata X cartridges (Li et al., 2010). Details of the extraction procedures are provided in Appendix B.

2.3.3.2 Tracer analysis

The analysis of target compounds involved isotope dilution of each compound to track analyte recovery, instrument variability, and matrix suppression during sample analysis. Native compounds for CAF, CBZ, GEM, IBU, NAP, SMX, ACE-K, SUC, glyphosate, and AMPA were purchased from Sigma-Aldrich (Oakville, Canada). Dry powder isotope-labelled compounds were purchased in the form of SMX-d4, ACE-K-d4, SUC-d6, glyphosate-c3-d2, and AMPA-15n (Toronto Research Chemicals, Canada) along with CAF-d3, CBZ-d10, IBU-d3, GEM-d6, and [13C]-NAP (Cambridge Isotope Laboratory Inc., USA).

Pharmaceutical compounds were extracted from discrete samples using solid phase extraction (SPE) following Liu et al. (2014). Briefly, 500 mL of sample was diluted with 500 mL of ultrapure water and passed through SPE cartridges (Oasis HLB 6 mL glass cartridges; Waters Corp., Mississauga, Canada). After extraction with MeOH from the cartridges, samples were evaporated to dryness under N_2 flow and reconstituted in 1 mL of MeOH. Further details are provided in Appendix C.

Pharmaceutical extracts from discrete and passive samples, as well as artificial sweetener extracts from passive samplers, were analyzed using a high-performance liquid chromatography (HPLC) (Agilent 1100, Agilent Technologies, Mississauga, Canada) coupled with tandem electrospray mass spectrometry (MS/MS; 4000 Q TRAP, Applied Biosystems, Foster City, USA). Discrete samples for artificial sweeteners (ACE-K, sucralose) were analyzed by direct injection using IC coupled with tandem MS (6460 QQQ, Agilent Technologies, Mississauga, ON, Canada) modifying a method from Van Stempvoort et al. (2011) reported by Liu et al. (2014). Glyphosate and AMPA discrete and passive samples were analyzed by HPLC (Agilent

1100, Agilent Technologies, Mississauga, Canada) coupled with tandem MS (6460 QQQ) using a method from Agilent (Agilent Technologies, 2019).

Further details on analytical procedures, including quality assurance/quality control (QA/QC), method detection limits of compounds, and calibration curve preparation are provided in Appendix D.

2.3.3.3 Determination of Time-Weighted Averages for C_{DGT} and C_{POCIS}

TWA concentrations for DGT (C_{DGT}) were determined using Eqn. 2-1 (Zhang & Davison, 1995):

$$C_{DGT} = \frac{M\Delta g}{DAt} \qquad (2\text{-}1)$$

Where M is the mass accumulated on the binding layer (ng), Δg is the thickness of the diffusive layer (cm), D is the diffusion coefficient ($cm^2\ s^{-1}$), A is the physical or effective area through which the compound diffuses (cm^2), and t is the deployment time (s). D was corrected using the mean stream temperature over the deployment time and diffusion coefficients (Table 2-1).

The diffusive boundary layer (DBL) can strongly impact concentrations calculated from DGT passive samplers, and the thickness of the DBL should be taken into consideration to ensure accuracy when calculating C_{DGT}. Any solid surface in flowing water will have a layer near the surface where there is effectively no flow, known as the DBL. In stronger flowing water, the DBL will become thinner but will never be completely eliminated. The most effective way to estimate the DBL in a flowing solution is to deploy DGTs with varying diffusive membrane thicknesses (Davison & Zhang, 2016) (additional information in Appendix E). To accommodate for the DBL, the effective area (A_E, 3.8 cm^2) is used instead of the physical area (A_P, 3.14 cm^2) in equation 2-1. If the DBL is taken into consideration equation 2-1 is modified to (Davison & Zhang, 2016):

$$C_{DGT} = \frac{M}{A_E t}\left(\frac{\delta^{DL}+\delta^{DBL}}{D}\right) \qquad (2\text{-}2)$$

Where δ^{DL} is the thickness of the diffusive layer (cm) and δ^{DBL} is the thickness of the DBL (cm). Multiple DGTs with different diffusive layer thicknesses were deployed during Spring 2022 for each type of sampler, so equation 2-2 and A_E were used to calculate C_{DGT}. Samplers deployed during Fall 2021 were not corrected for DBL impacts, so equation 2-1 and A_P were used to calculate C_{DGT}. All DGT concentrations were corrected for conductivity at each sampling location due to decreases in uptake of compounds in the presence of high conductivity over time (Huang et al., 2016a,b).

The TWA concentrations for POCIS (C_{POCIS}) were calculated using the Eqn. (2-3) (Alvarez et al., 2004):

$$C_{POCIS} = \frac{M}{R_s t} \qquad (2\text{-}3)$$

Where M is the mass of the target analyte found on the sampler (ng), R_s is the sampling rate (L day^{-1}) (Table 2-1) and t is the deployment time.

2.3.4 Competing compounds evaluation

The effect of potentially competing compounds (PO_4-P, glyphosate, AMPA) was evaluated for the Metsorb®-DGT sampler, as multiple phosphate-bearing compounds accumulate on the TiO_2 binding layer. Triplicate Metsorb®-DGT samplers were deployed in a continually mixed 2-L solution on a stir plate for 72- and 144-hours. The initial solution consisted of 1040 µg L^{-1} of PO_4-P, 0.372 µg L^{-1} of glyphosate, and 2.14 µg L^{-1} of AMPA in ultrapure water. Initial PO_4-P conditions are reflective of higher concentrations found in surface waters in Ontario (Provincial Water Quality Monitoring Network, Government of Ontario, 2020. Pesticide Concentrations in

Stream Water (Data accessed January 14, 2023)), while glyphosate and AMPA are reflective of median concentrations found in southern Ontario (Struger et al., 2015).

2.3.5 Statistical analysis and data visualization

Statistical analyses were conducted using a Kruskal-Wallis (KW) with Dunn's posthoc test for multiple comparisons, while a Mann Whitney U test was used for comparison of two groups. These tests were used to compare significant differences between (1) discrete and passive sample concentrations and (2) between sampling locations at a 95% confidence. Although the statistical power of a KW test is lower than an AVOVA, the data was assumed to be not normal as observed with multiple data sets in this study. Spearman rank order correlation was used to determine if relationships existed between nutrients and tracers, where positive correlation coefficients were divided into two categories: strong (>0.80) and moderate (0.50 – 0.80). Anything <-0.70 was considered a strong negative correlation. All statistical analyses were conducted using Sigma Plot (Version 11.0). Results below the MDL were reported as half the MDL when values were required for statistical analyses.

Overall, while statistics were conducted it should be noted that the sample size is commonly low due to the nature of this field of study, resulting in low statistical power. As a result, efforts are made to use descriptive statistics (e.g., means) where possible.

Principal component analysis (PCA) was performed in two-dimensions using results obtained from discrete and DGT samples to visualize relationships between nutrients and tracers. Variance Inflation Factor (VIF) was used to reduce multicollinearity in each dataset by removing variables with stepwise VIF > 5.

2.4 Results

Sampling events occurred in October 2021 (Fall 2021 sampling) and June 2022 (Spring 2022 sampling). Discrete samples (n = 36) were collected and DGT (n = 150) and POCIS (n = 18) were deployed/retrieved during the two sampling events.

2.4.1 General water quality parameters

Mean stream water temperature was 13.1°C (range: 9.5°C to 15°C) for Fall 2021 and 14.6°C (range: 12°C to 22°C) during Spring 2022. Mean pH was 8.1 and ranged between 7.65 to 8.40 during both sampling events. Alkalinity varied between 250 – 380 mg $CaCO_3$ L^{-1}, while mean water hardness was 320 ± 9.0 mg L^{-1} across all locations, classifying the streams as 'very hard' water. Mean concentrations of Ca^{2+} and Mg^{2+} were 100 ± 8.8 mg L^{-1} and 29 ± 0.43 mg L^{-1} respectively at all locations during both sampling events. Conductivity varied among the locations (700 – 1200 µS cm^{-1}) with the highest conductivity at the *Hamlet Site* and lowest at the *Agriculture Site* during both events. *E. coli* was highest at the *Hamlet Site* in Fall 2021 (mean 2920 ± 1683 MPN 100 mL^{-1}), followed by the *Mixed-land Site* (1522 ± 1270 MPN 100 mL^{-1}) and the *Agriculture Site* (176 ± 60 MPN 100 mL^{-1}). In Spring 2022, *E. coli* was highest at the *Mixed-land Site* (mean 3385 ± 1365 MPN 100 mL^{-1}) and lowest at the *Hamlet Site* (mean 991 ± 182 MPN 100 mL^{-1}). All water quality parameters including DOC, anions, cations, and turbidity are summarized in Table F-1.

2.4.2 Seasonal discrete vs. passive sampler results of nutrient and tracer concentrations

2.4.2.1 Nutrients

Concentrations of nutrients from discrete samples (C_{ACTIVE}) from the 2-week study period varied between the Fall 2021 and Spring 2022 sampling events across all three sites (Fig. 2-2). During

Fall 2021, PO_4-P and NO_3-N concentrations were above the LOD (6.5 and 23 µg L^{-1}, respectively) while NH_4-N was mainly below the MDL (<0.02 mg L^{-1}). Across all sites 62 ± 14% of total phosphorus (TP) was in the dissolved form. When examining the 2-week mean in Fall 2021, highest C_{ACTIVE} of PO_4-P (n = 6) were observed at the *Hamlet Site* (74 ± 8.2 µg L^{-1}), which was significantly different ($\rho < 0.05$) to mean C_{ACTIVE} at the *Agriculture* (35 ± 7.4 µg L^{-1}) and *Mixed-land* (34 ± 6.7 µg L^{-1}) *Sites*. NO_3-N (n = 6) and NH_4-N (n = 6) samples had mean C_{ACTIVE} of 6.8 ± 0.7 mg L^{-1} and 43 ± 24 µg L^{-1} respectively across all three sampling locations and were not significantly different across sites during Fall 2021. During Spring 2022 PO_4-P, NO_3-N, and NH_4-N had mean C_{ACTIVE} of 39 ± 21 µg L^{-1}, 5.2 ± 2.2 mg L^{-1}, and 65 ± 55 µg L^{-1} respectively across all sampling locations. None of the nutrient concentrations were significantly different between sampling locations in Spring 2022. When considering the 14-day variability between individual samples, large variability in C_{ACTIVE} was observed at all sites for each nutrient, with some parameters showing an order of magnitude difference over only a few days. These spikes in C_{ACTIVE} (at Days 9 and 12) correspond to increased run-off following rain events (Fig. F-3 and F-4).

DGT samplers for nutrients were deployed for 6 days during both sampling events. Additional results of the 3-day deployment of Metsorb®-DGT and A520E-DGT samplers, as well as 14-day deployment of PrCH samplers can be found in the Appendix F.

Mean P concentrations C_{DGT} (n = 2) during Fall 2021 were comparable or slightly lower than C_{ACTIVE} during the same time period (6-days). Metsorb®-DGT mean C_{DGT} for PO_4-P were highest at the *Hamlet Site* (49 ± 10 µg L^{-1}), followed by the *Mixed-land Site* (36 ± 24 µg L^{-1}) and the *Agriculture Site* (32 ± 0.1 µg L^{-1}), and were significantly lower in concentration at the *Hamlet Site* compared to C_{ACTIVE} (73 ± 6.8 µg L^{-1}) during the same time period (6-days). A520E-

DGT sampler concentrations for NO_3-N had a mean C_{DGT} of 3.6 ± 1.9 mg L^{-1} across all sites and were significantly different ($\rho < 0.05$) than C_{ACTIVE} at the *Hamlet* (6.4 ± 2.6 mg L^{-1}) and *Mixed-land* (7.9 ± 1.5 mg L^{-1}) *Sites* during the same time period (6-days). PrCH-DGT samplers for NH_4-N had a mean C_{DGT} of 12 ± 7.2 µg L^{-1} across all three sampling locations and were significantly different ($\rho < 0.05$) than C_{ACTIVE} (43 ± 24 µg L^{-1}) at all sites.

During Spring 2022, the mean PO_4-P C_{DGT} from Metsorb®-DGT samplers (n = 3) across all sites (n = 9) was 25 ± 8.2 µg L^{-1} and were not significantly different from C_{ACTIVE} ($\rho > 0.05$) during the same time period (6-days). NO_3-N C_{DGT} were significantly different ($\rho < 0.05$) at the *Hamlet* and *Agriculture Sites* compared to C_{ACTIVE}. PrCH-DGT samplers for NH_4-N C_{DGT} (n =3) were highest at the *Mixed-land Site* (9.3 ± 1.5 µg L^{-1}), followed by the *Hamlet Site* (4.6 ± 1.4 µg L^{-1}), and the *Agriculture Site* (2.4 ± 0.84 µg L^{-1}), and were <50% of discrete water sample concentrations. Details on the performance of the A520E-DGT and PrCH-DGT samplers in the presence of competing ions is summarized in Appendix E.

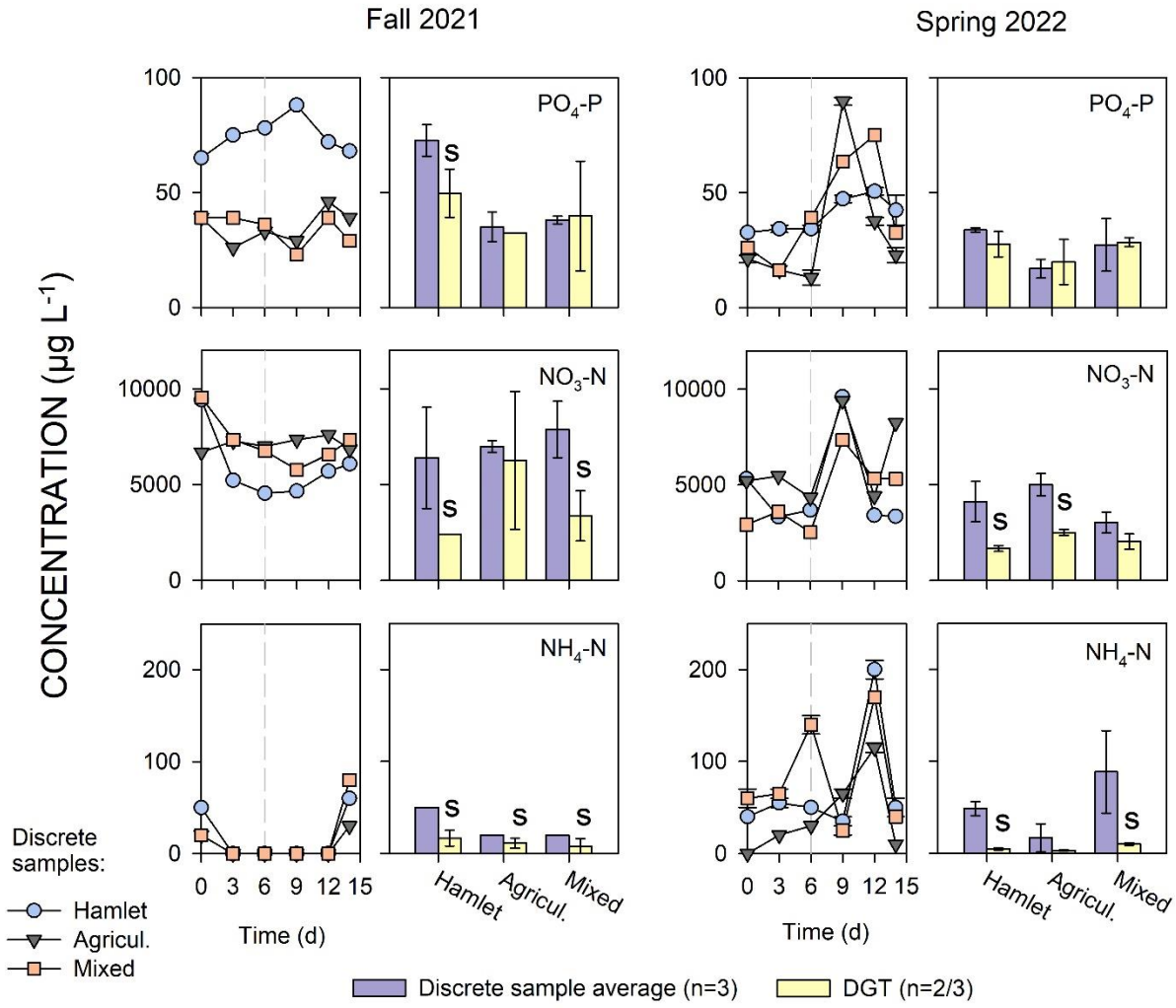


Figure 2-2. Line graphs showing concentrations of PO_4-P, NO_3-N, and NH_4-N for discrete samples collected every 3 days at each site during the 14-day Fall 2021 and Spring 2022 deployments. Bar graphs show the mean and standard deviation of concentrations for duplicate or triplicate DGT passive samplers deployed for 6 days, and discrete samples on days 0, 3, and 6. Values along the x-axis for line graphs indicate compounds were below detection limits. Dashed vertical lines represent the time comparison from discrete samples on the line graphs to that of the bar graphs. Letter 'S' represents significant differences between discrete and passive samplers.

2.4.2.2 Human tracers

For the discrete samples, the abundance of human-specific *Bacteroides* (BacHum) was highest at the *Hamlet Site* during both Fall 2021 and Spring 2022 (12,825 and 4,675 C 100 mL^{-1}, respectively), while the *Agricultural Site* showed the lowest concentration during Spring 2022 (811 C 100 mL^{-1}). Other target human-specific tracers, including sweeteners and pharmaceuticals, were detected in all discrete samples (n = 12) at the *Hamlet Site*. The *Agriculture Site* had the lowest concentration and detection frequency of samples above the detection limits in discrete samples for all human-specific chemical tracers (Fig. 2-4 and Table F-1) during both sampling events. During Fall 2021, SUC exhibited the highest concentration among the target compounds at the *Hamlet Site* (18.5 µg L^{-1}), followed by ACE-K (441.9 ng L^{-1}). Artificial sweetener concentrations were an order of magnitude higher than other tracers detected. At the *Agriculture Site* only CAF was detected in 100% of discrete samples (n = 6) while IBU, NAP, SMX, and SUC were detected in 16 to 83% of samples. Concentrations of ACE-K, CBZ, and GEM were below detection limits (100 ng L^{-1}, 0.4 ng L^{-1}, 0.04 ng L^{-1} MDL respectively) at the *Agriculture Site*, while ACE-K and GEM were undetected at *Mixed-land Site*. Seven of the eight human-specific tracers were higher in concentration at the *Hamlet Site* compared to the *Agriculture Site* ($\rho < 0.05$), while five tracers were higher at the *Hamlet Site* compared to the *Mixed-land Site* ($\rho < 0.05$).

During Spring 2022 the highest mean C_{ACTIVE} of all anthropogenic tracers were measured at the *Hamlet Site* and were consistently detected in discrete samples. Only CAF, IBU, and SUC were consistently detected at the *Agriculture Site* in discrete samples, while the *Mixed-land Site* had detections of all target compounds at considerably lower concentrations compared to the

Hamlet Site. All tracers had significantly different concentrations at the *Hamlet Site*, which were higher compared to the *Agriculture Site* ($\rho < 0.05$).

DGTs for artificial sweeteners were only deployed during the Spring 2022 sampling. Similar to discrete sample results, samples at the *Hamlet Site* had the highest concentration of all target human-specific tracers on DGT and POCIS, followed by the *Mixed-land Site* then the *Agriculture Site* during both sampling events. Of the pharmaceutical tracers, CAF had the highest C_{DGT} concentration. All tracers detected at the *Hamlet Site* had concentrations 3 to 106 times higher on DGT compared to the *Agriculture* and *Mixed-land Sites*. Measured CAF C_{DGT} was 33.3 ng L^{-1} at the *Hamlet Site*, 0.53 ng L^{-1} at the *Agriculture Site*, and 1.98 ng L^{-1} at the *Mixed-land Site* and was the only compound detected on both DGT and POCIS at the *Agriculture Site*, while IBU was only detected on POCIS and not on DGT at the *Agriculture Site*. Concentrations calculated for ACE-K and SUC were generally lower from HLB-DGT compared to concentrations observed in discrete samples collected during the same time period ($\rho < 0.05$), however in several instances ACE-K was detected on POCIS but not in corresponding discrete samples at the *Agriculture* (Fall and Spring) and *Mixed-land Site* (Fall) and detected on DGT but not the discrete sample at the *Agriculture Site* (Spring).

DGT and POCIS were both deployed for the uptake of pharmaceuticals and artificial sweeteners to compare the effectiveness of both samples to estimate concentrations of compounds compared to C_{ACTIVE}. HLB-DGT have only an eighth of the intrinsic binding capacity compared to POCIS, potentially becoming saturated much faster and restricting deployment times. POCIS overall had more reliable uptake of compounds across all samplers. From 216 individual analyte samples, 14% of analytes were undetected at a sampling site on

POCIS and 16% of analytes were undetected at a sampling site by DGT. Although POCIS have a larger binding capacity, DGTs demonstrated a similar level of detection in this study.

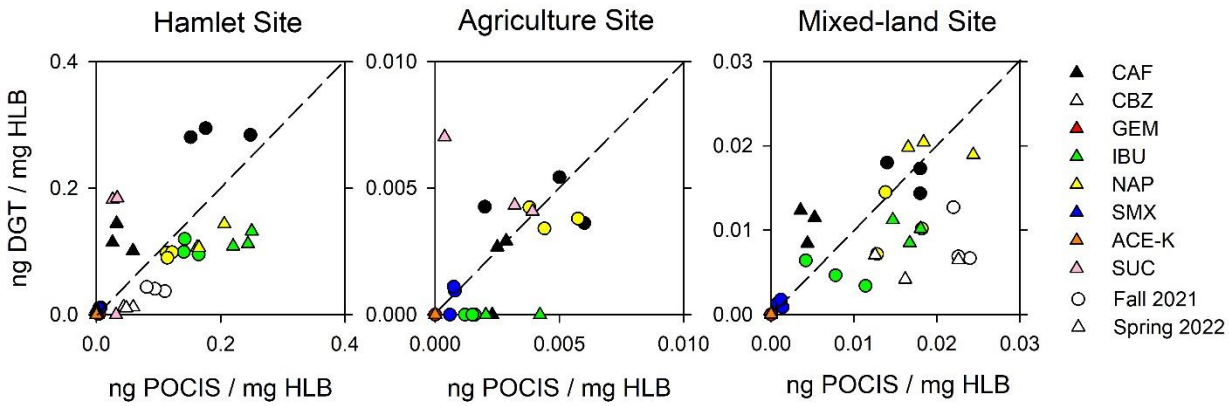


Figure 2-3. Mass of analytes (ng) recovered from POCIS versus DGT per mg of HLB. Samplers were deployed in triplicate and include compounds from both the Fall 2021 and Spring 2022 sampling events. Data points occurring only along the x- or y-axis indicate analytes were only found on POCIS or DGT samplers, respectively. The dotted line represents where DGT = POCIS in terms of mass of analyte recovered per mg of HLB.

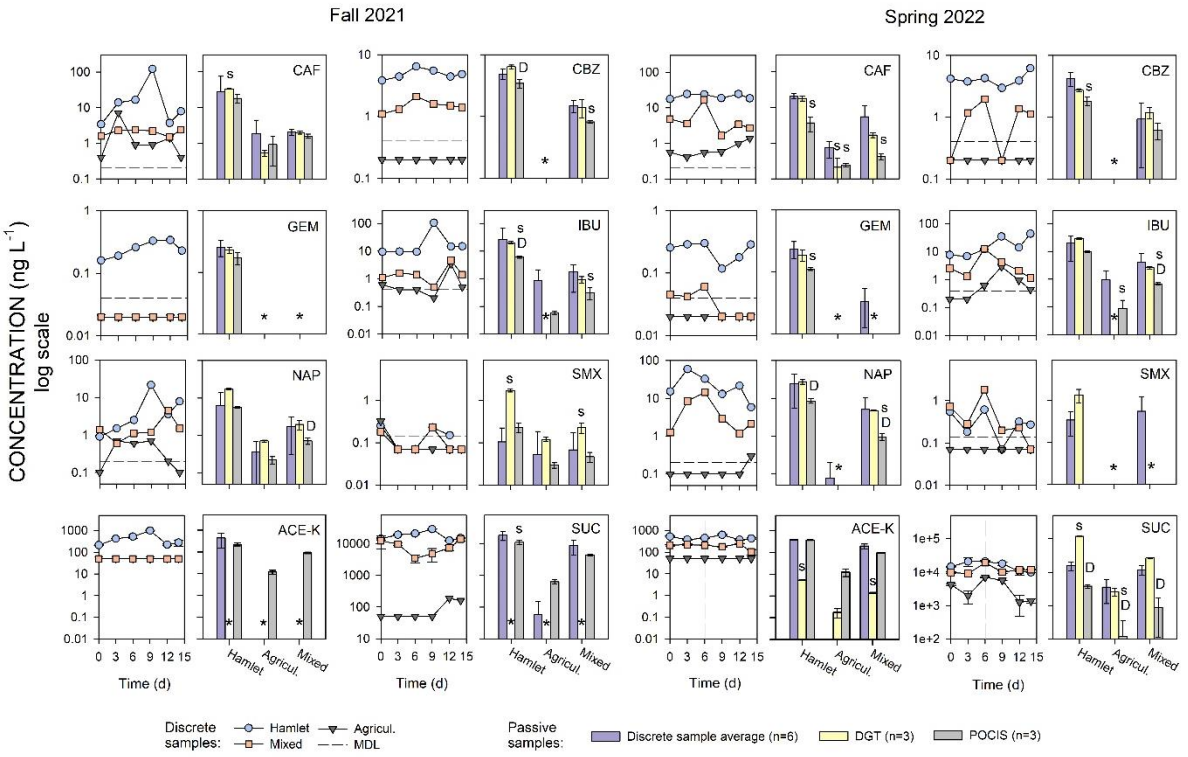


Figure 2-4. Line graphs showing concentrations of human-specific tracers CAF, CBZ, GEM, IBU, NAP, SMX, ACE-K, and SUC for discrete samples collected every 3 days at each site location during the 14-day Fall 2021 and Spring 2022 deployments. Bar graphs represent the mean and ± standard deviation of concentrations obtained from triplicate DGT and POCIS deployed for 14 days, and the mean concentration for discrete samples collected every 3 days for 14 days. Dashed vertical lines represent the time comparison from discrete samples on the line graphs to that of the DGT samplers on the bar graphs. Samples below the MDL on the line graphs are reported as half the MDL value. Letters represent statistical differences between discrete and passive samples (s) and between DGT and POCIS (D). * = Not detected.

2.4.2.3 Agricultural tracers

Agricultural-specific tracers included bovine-specific *Bacteroides* (BacBov) markers (Table F-1), as well as glyphosate and AMPA (Fig. 2-5). In discrete samples (n = 4 per site over two sampling periods), BacBov markers were undetected at the *Agriculture Site*, compared to being detected in 25% of samples at the *Hamlet Site* and 100% of samples at the *Mixed-land Site* over both sampling seasons. During the Fall 2021 sampling event BacBov markers were only detected

at the *Mixed-land Site*, which was directly downstream of a large cattle farm (13,865 ± 756 C 100 mL^{-1}, 60% of total *Bacteroides*), while glyphosate (0.12 ± 0.12 µg L^{-1}) and AMPA (1.41 ± 0.82 µg L^{-1}) were only detected above the MDL at the *Agriculture Site.* During the Spring 2022 sampling, low levels of BacBov (211 ± 299 C 100 mL^{-1}, 0.44% of the total *Bacteroides*) were observed at the *Hamlet Site*, while higher levels were observed at the *Mixed-land Site* (10,420 ± 6760 C 100 mL^{-1}, 43.5% of total *Bacteroides*).

Glyphosate (n = 12) and AMPA (n = 12) were below the MDL (<0.05 µg L^{-1} and <0.1 µg L^{-1} respectively) at the *Hamlet Site* while being detected in 100% of discrete samples from the *Agriculture Site* during both sampling events. Over the 14-day sampling period at the *Agriculture Site*, glyphosate ranged from <MDL – 0.31 µg L^{-1} in Fall 2021 (mean = 0.21 ± 0.12 µg L^{-1}) and 0.48 – 5.95 µg L^{-1} during Spring 2022 (mean = 1.60 ± 2.17 µg L^{-1}), with the largest peak in concentration occurring after a precipitation event.

Mean concentrations of agricultural tracers (glyphosate, AMPA) from DGT passive samplers (n = 2/3) were comparable to discrete samples over the 6-day deployment. At the *Agriculture Site* during both sampling events DGT concentrations for glyphosate/AMPA were not significantly different from discrete samples ($\rho > 0.05$). Glyphosate was undetected in discrete samples at the *Mixed-land Site* during both sampling events but detected on all passive samplers (0.14 ± 0.003 µg L^{-1}). Similarly, AMPA was undetected in discrete samples taken at the *Mixed-land Site* during the Fall 2021 sampling but detectable on passives (0.21 ± 0.012 µg L^{-1}).

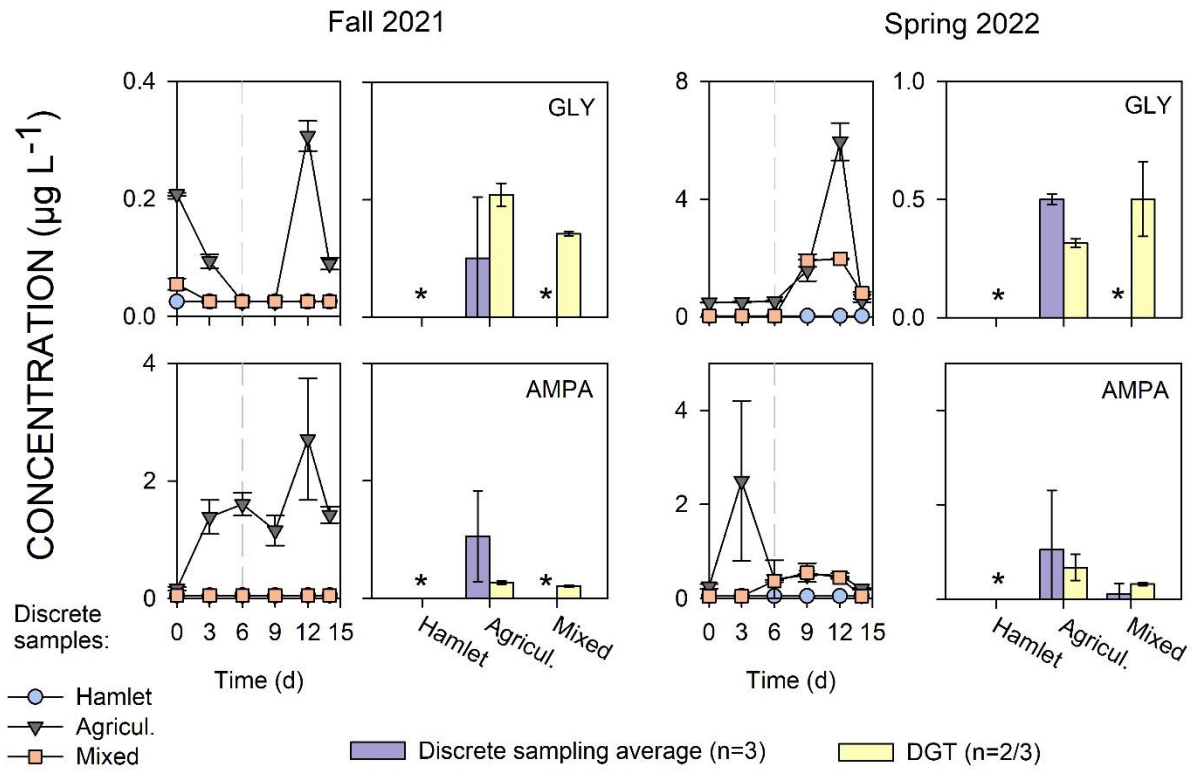


Figure 2-5. Line graphs represent concentrations of agricultural-specific tracers (glyphosate, AMPA) for discrete samples taken every 3 days at each site location during the 14-day Fall 2021 and Spring 2022 deployments. Bar graphs represent the mean and ± standard deviation of duplicate or triplicate DGT passive samplers deployed for 6 days, and discrete samples taken on days 0, 3, and 6. Dashed vertical lines represent the time comparison from discrete samples on the line graphs to that of the bar graphs. Samples below the MDL on the line graphs are reported as half the MDL value. * = Not detected.

2.4.3 Relationships among nutrients and tracers from discrete and passive samples

Spearman correlation coefficients between nutrients (PO_4-P, NO_3-N, NH_4-N) and tracers (CAF, CBZ, GEM, IBU, NAP, SMX, ACE-K, SUC, GLY, AMPA) were calculated using discrete and passive sample values (Tables F-3 and F-4). Positive correlations were observed between most anthropogenic-specific tracers at the *Hamlet Site* during Fall 2021 ($\rho > 0.52$) and Spring 2022 ($\rho > 0.51$), and at the *Mixed-land Site* only during Spring 2022 ($\rho > 0.51$). Few correlations were observed between anthropogenic-specific tracers at the *Agriculture Site* during either sampling

event. There was a strong negative correlation between agricultural tracers, glyphosate and AMPA, and CAF and CBZ at the *Mixed-land Site* during Fall 2021 ($\rho < -0.92$), and a moderate positive correlation ($\rho > 0.66$) between glyphosate and AMPA at the *Mixed-land Site* during both sampling events.

Strong to moderate positive correlations between P species and all human-specific tracers (excluding SMX) were observed at the *Hamlet Site* during Fall 2021 ($\rho > 0.62$), while 50% of human tracers had a moderate positive correlation ($\rho > 0.61$) to PO_4-P during Spring 2022. There was a strong positive correlation at the *Mixed-land Site* between PO_4-P and glyphosate ($\rho = 0.91$) and a moderate correlation of PO_4-P to AMPA ($\rho = 0.77$) in Spring 2022, but not in the Fall 2021. There were few significant correlations between P and any anthropogenic tracers at the *Agricultural Site* during either sampling season.

Significant relationships between N species and tracers were less pronounced than for P. No strong significant correlations existed between NO_3-N and any tracers at the *Hamlet Site*, although some moderate relationships were observed. Strong negative correlations ($\rho < -0.76$) between NO_3-N and agricultural-specific tracers were observed at the *Mixed-land Site* during Fall 2021. There was a moderate positive correlation between NO_3-N and 50% of human-specific tracers at the *Hamlet Site* during Spring 2022. NH_4-N was not positively correlated to any tracer at any of the three sites during Fall 2021. A moderate positive correlation ($\rho > 0.52$) existed between NH_4-N and all anthropogenic tracers (excluding CBZ) at the *Mixed-land Site* only in Spring 2022.

PC1 and PC2 axes for both PCA plots were significant and captured 55.03% of the variation for discrete samples and 74.29% of variation for DGT samplers in the environmental data (Fig. 2-6). PC1 showed a negative correlation to all anthropogenic tracers, PO_4-P and NH_4-

N and positively correlated to agricultural tracers. Site specific clustering is evident in both the discrete and DGT datasets while loadings are similar in direction and magnitude (excluding NH_4-N). Clustering at the *Hamlet Site* is similar across both plots, while the *Mixed-land Site* clusters were closer to the center of the PCA plot for discrete samples (Fig. 2-6a) and spread across PC1 for the DGT samples (Fig. 2-6b). Anthropogenic- and agricultural-specific tracer loadings correlate well to their predicted sites (Table F-5). The *Hamlet Site* clustered to anthropogenic tracers, whereas the *Agriculture Site*, and to a lesser extent the *Mixed-land Site*, clustered to agricultural tracers. Correlation between PO_4-P and the *Hamlet Site* exists for Fall 2021 sampling data from both PCA plots, while NO_3-N loading is mostly in the same direction from both PCA plots but is lower in magnitude for DGT samples compared to discrete samples. NO_3-N may be related to either the *Agricultural* or *Mixed-land Site* during the Fall 2021 sampling.

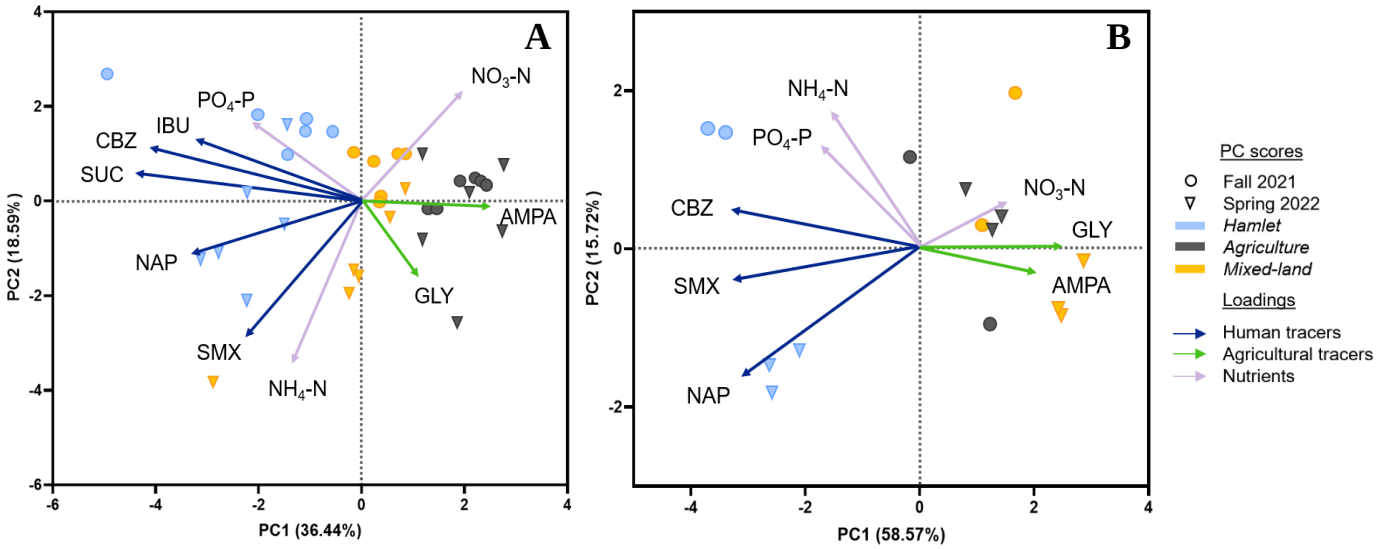


Figure 2-6. Nutrients, anthropogenic-, and agricultural-tracer site correlation visualized by PCA in two dimensions for (A) discrete samples and (B) DGT passive samplers.

2.4.4 Competition study between phosphate-bearing compounds

The PO_4-P concentration decreased in the solution from 1040 µg L^{-1} at the beginning of the experiment to 913 µg L^{-1} after 144 hours, while glyphosate decreased from 0.372 µg L^{-1} to 0.354 µg L^{-1} after 144 hours. Concentrations of PO_4-P and glyphosate from triplicate Metsorb®-DGT were in good agreement between samplers (mean relative standard deviation ≤ 8.8%). The ratio of the water concentration calculated from DGT (C_{DGT}) to the solution concentration (C_{SOLN}) is represented by C_{DGT}/C_{SOLN} as a ratio. Glyphosate showed mostly linear uptake up to 144 hours, with a C_{DGT}/C_{SOLN} ratio of 0.95 after 72 hours and a C_{DGT}/C_{SOLN} ratio of 0.84 at 144 hours. PO_4-P uptake linearity tapered off after ~120 hours, as the C_{DGT}/C_{SOLN} ratio decreased to 0.62 at 144 hours of deployment in solution (Fig. 2-7). AMPA was not successfully evaluated for this experiment (results not shown).

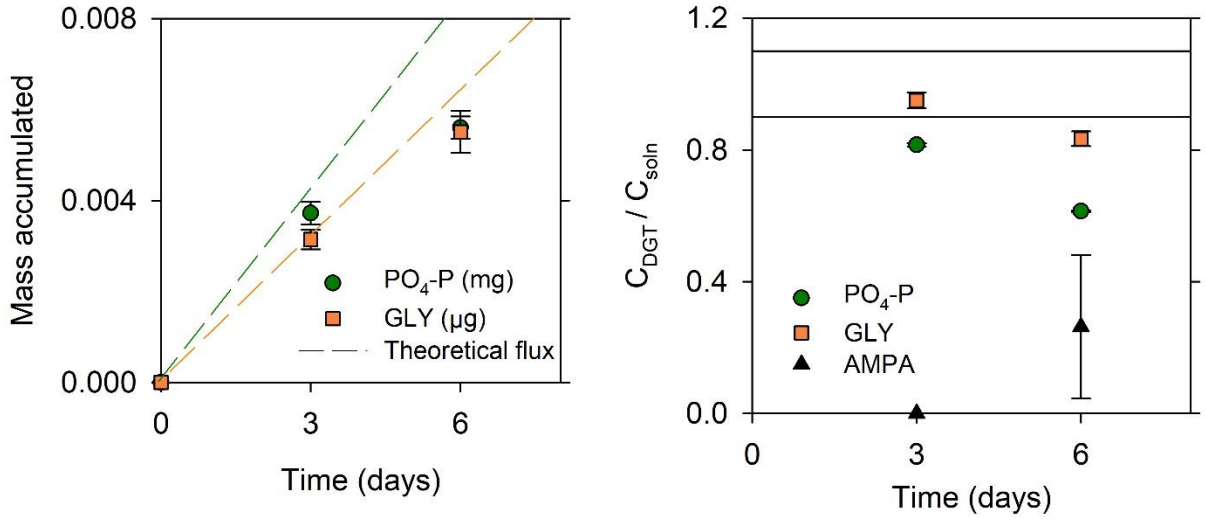


Figure 2-7. Effect of competing compounds on Metsorb® sorbent visualized by (A) mean mass of compound accumulated on triplicate DGT-Metsorb® samplers and (B) ratio of C_{DGT}/C_{SOLN}. Experimental conditions: initial PO_4-P = 1040 µg L^{-1}; glyphosate = 0.372 µg L^{-1}; AMPA = 2.14 µg L^{-1}.

2.5 Discussion

Passive samplers were deployed for uptake of nutrients and multiple anthropogenic- and agricultural-specific tracers to compare their effectiveness in estimating surface water concentrations to that of discrete samples, and to distinguish contamination sources. Large variabilities often associated with discrete sampling can be overcome through the use of passive samplers by providing a TWA concentration (Vrana et al., 2005).

2.5.1 Comparison of passive to discrete samples

Comparing concentrations of DGT (C_{DGT}) and POCIS (C_{POCIS}) to discrete samples (C_{ACTIVE}) across all sites during both sampling seasons indicated consistently lower C_{DGT} and C_{POCIS} values relative to $C_{ACTIVE;}$ the ratios of mean concentrations were 0.92 (C_{DGT}/C_{ACTIVE}) and 0.52 (C_{POCIS}/C_{ACTIVE}) for all compounds This observation is consistent with similar studies showing a higher ratio of C_{DGT} to C_{ACTIVE} compared to C_{POCIS} and C_{ACTIVE} (Challis et al., 2020).

Passive samplers provide a TWA that has a lower variability than observed in discrete sampling. Variability in nutrient concentrations was especially evident in discrete samples in the second week of Spring 2022 (Fig. 2-2), which was likely a result of increased runoff following a large precipitation event. In general, across all seasons, mean values for nutrient passive samplers were lower compared to discrete samples, even when the DBL was considered. However, C_{DGT} of PO_4-P showed better agreement between passives and discrete samples than both nitrogen species. Low uptake of nitrogen species onto similar samplers has been observed in the presence of competing ions (Huang et al., 2016a,b). “Hard” water and high conductivity at all three sampling locations likely resulted in the underestimation of C_{DGT} compared to C_{ACTIVE} for N species (more details provided in Appendix E). NH_4-N had especially low uptake onto PrCH sorbent. Ionized-ammonia (NH_4^+-N) and free-ammonia (NH_3-N) represent two forms of

inorganic nitrogen present in water, with the amount of each specie dependent on pH and temperature. The mean pH (8.1) and temperature (13.9°) across all sampling sites during both deployment seasons indicate approximately 2.47% of NH_{3+4}-N was present in the form of free-ammonia, indicating the majority was present in an ionic form. This suggests the overall uptake of NH_4-N onto PrCH-DGT was not affected substantially by hydrolysis, indicating the chemical properties of the water (elevated concentrations of major ions) were likely not suitable for deployment of this sampler.

Glyphosate and AMPA were more consistently detected on passive samplers than in discrete samples. When considering the *Agriculture* and *Mixed-land Sites*, glyphosate was detected in 100% of DGT samples (n = 10) and 54% of discrete samples (n = 24) while AMPA was detected in 100% of DGT samples (n = 10) and 63% discrete samples (n = 24). No glyphosate or AMPA was detected in passives or discrete samples at the *Hamlet Site.* Variability in C_{ACTIVE} for glyphosate and AMPA as well as frequent non-detects from discrete samples were both reduced using passive samplers. Over the 2-week sampling period, glyphosate and AMPA had a mean C_{ACTIVE} of 0.86 ± 1.7 µg L^{-1} and 1.1 ± 0.88 µg L^{-1} respectively at the *Agriculture Site* over both sampling seasons, with a notably large spike in C_{ACTIVE} on days 9 and 12. These concentrations are within the range reported in previous studies that observed glyphosate ranging between 0.010 – 40 µg L^{-1} and AMPA in the range of 0.010 – 15 µg L^{-1} in 219 surface water samples around Southern Ontario (Struger et al., 2015). A recent study by Raby et al. (2022) characterized pesticides in agriculturally dominated streams in southern Ontario and detected glyphosate and AMPA in <10% of discrete water samples, although higher detection limits could have resulted in a lower frequency of detection. The lower frequency of detection and variation

in glyphosate and AMPA concentrations in streams in this and other studies, suggest that passive samplers might be a more reliable way to detect these contaminants.

C_{ACTIVE} and C_{DGT} of pharmaceuticals and artificial sweeteners were in good agreement for most compounds measured, while C_{POCIS} was typically underestimated (Fig. 2-4). Discrete samples for some pharmaceuticals/sweeteners varied in concentration over both 2-week sampling periods at the *Hamlet Site*, potentially due to varied flow conditions following precipitation events, as well as varied usage of these compounds in the population (Table 2-2). Variability between triplicate HLB-DGT samplers was low compared to discrete samples; the mean relative standard deviation (RSD) for all compounds accumulated on HLB-DGT and POCIS during both deployment events across all sampling locations was 21.36% (n = 31) and 25.13% (n = 38) respectively, compared to 87.52% RSD for discrete samples (n = 40). Similar RSD values for pharmaceutical uptake by HLB-DGTs (n = 297) and POCIS (n = 38) were observed by Challis et al. (2018).

Installation of multiple DGT samplers with different membrane thicknesses, in Spring 2022, provided corrections for differences in *in situ* conditions to estimate the DBL in flowing water. The mean absolute ratio for Spring 2022 DGT samples compared to discrete samples (C_{DGT}/C_{ACTIVE}) increased from 0.66 when no DBL corrections were applied to 0.92 when the DBL was accounted for (Fig. F-2). C_{DGT} at the *Mixed-land Site* had the largest deviation from discrete samples when DBL corrections were not applied. Stream flow was considerably slower at the *Hamlet Site* compared to the *Agriculture* and *Mixed-land Sites* during both sampling events, which can contribute to a larger DBL impact. From the calculated DBLs, the *Hamlet* and *Mixed-land Site*s were most impacted due to a thicker DBL, while the *Agriculture Site* had minimal DBL interference. C_{DGT} increased by an average of 37% at the *Hamlet Site*, 6% at the

Agriculture Site, and 51% at the *Mixed-land Site* when DBL corrections were applied to the Spring 2022 sampling data. The *Mixed-land Site* had on average the lowest flow rate and visibly more fouling on passive samplers after deployment, likely contributing to a larger correction in C_{DGT}. Through discrete samples, artificial sweetener ACE-K has been shown to be a good tracer for wastewater contamination from municipal WWTPs (Liu et al., 2014; Tanna et al., 2020) and septic systems on streams (Digaletos et al., 2023; Oldfield et al., 2020; Spoelstra et al., 2020). Recent advancements have improved the estimation of C_{POCIS} by deriving R_s values from field deployments (Liu et al., 2023; Sultana & Metcalfe 2022) rather than from lab-derived R_s values (Li et al., 2010; 2018). In previous studies ACE-K has been underestimated on HLB sorbent, likely from the use of a lab-derived R_s value. An R_s value for ACE-K of 0.097 L day^{-1} at 20°C (Li et al., 2018) was previously reported for C_{POCIS} calculations. More recent research has produced updated values of R_s calculated *in situ* for ACE-K to correct for temperature impacts to sampling rates, which have been shown to reduce the underestimation of compounds from POCIS compared to discrete samples, at 0.001 L day^{-1} at 15°C (Sultana and Metcalfe, 2022) and 0.0014 L day^{-1} at 10°C (Liu et al., 2023). The use of the updated *in situ* R_s value (Liu et al., 2023) increased C_{POCIS} concentrations by two orders of magnitude and resulted in comparable mean C_{ACTIVE} and C_{POCIS} over the same timeframe.

HLB sorbent was used in both DGTs and POCIS in this study, yet DGTs underestimated concentrations of ACE-K compared to discrete samples. A new DGT passive sampler (Strata-DGT) was developed in this study using Strata X-AW, a weak anion exchange (WAX) sorbent, to evaluate the uptake of artificial sweeteners as an alternate to HLB sorbent. WAX resin was anticipated to have higher uptake of ACE-K compared to a reverse phase sorbent as a study by Ordóñez et al. (2012) showed good recovery of ACE-K from SPE onto this type of sorbent.

However, Strata-DGT samplers had low uptake of artificial sweeteners, severely underestimating concentrations compared to discrete samples (Fig. 2-4). The underestimation of ACE-K on DGTs can potentially be explained by the diffusion coefficient used for the calculation of C_{DGT}, which was estimated using the molecular weight of ACE-K (equation A-1). Certain physiochemical properties of compounds, including the octanol-water partition coefficient [logK_{OW} or pH-dependent logK_{OW} (logD_{OW})] (Table 2-1), could also explain the limited uptake of ACE-K by Strata-DGT and HLB. A compound will have a greater hydrophobicity the greater its logK_{OW} value. Although DGTs underestimated artificial sweeteners concentrations compared to discrete samples, ACE-K was concentrated on the sorbent to achieve a higher rate of detection in some instances (Fig. 2-4) These passive samplers may be of value for characterizing rivers that are expected to have lower concentrations of sweeteners.

2.5.2 DGT vs POCIS

HLB-DGT and POCIS, both containing HLB sorbent, were deployed in triplicate for 14-days to compare the effectiveness of different passive samplers for the uptake of pharmaceuticals and artificial sweeteners.

C_{POCIS} was typically underestimated compared to discrete samples, with 45% of human-specific tracers showing a significant difference, compared to 15% of the same compounds from HLB-DGT samplers during Spring 2022. Although C_{POCIS} was underestimated compared to C_{ACTIVE}, variability among triplicate passive samplers was low.

Comparison of HLB-DGT to POCIS for pharmaceuticals/artificial sweeteners across all sites during both sampling seasons showed a mean absolute ratio of 2.84 (C_{DGT}/C_{POCIS}). The underestimation of concentrations by POCIS is likely due to boundary impacts caused by biofouling and flowrate (Digaletos et al., 2023; Sultana & Metcalfe, 2022; Vrana et al., 2021).

Like ACE-K, field-derived R_s values for pharmaceutical compounds are being explored and may address the underestimation of C_{POCIS} of several compounds compared to C_{ACTIVE}. DGT samplers have some advantages over POCIS due to the *in situ* method to correct for DBL impacts. New methods to limit the effect of flow rate on POCIS using performance reference compounds (PRC) has recently been used (Buzier et al., 2019). This new method efficiently limited flow effects on POCIS uptake of compounds under flowing conditions. Under quiescent conditions, PRC was unable to desorb. Due to lower flow conditions observed at the sampling sites in this study during Fall 2021 this method was not utilized.

Mass of analytes recovered from triplicate DGT and POCIS per mg of HLB sorbent used was evaluated for pharmaceutical compounds (Fig. 2-3). POCIS provided a higher sensitivity, allowing more consistent detection of compounds compared to DGT. Targeted screening of analytes may be suitable using POCIS or DGT, but POCIS may be a better option for nontargeted screening or expected low levels of compounds due to the greater amount of binding sorbent per sampler and higher sensitivity (Martins de Barros et al., 2023; Renaud et al., 2022).

2.5.3 Competition study between phosphate-bearing compounds

A sorbent selective for multiple compounds may have preferential binding for one compound over another, leaving some compounds underestimated on passive samplers. Competition was not observed among the three P-bearing compounds evaluated (PO_4-P, glyphosate, and AMPA) on Metsorb®-DGTs (Fig. 2-7). Uptake of glyphosate was linear throughout the 6-day experiment, showing that binding was not impacted for one analyte at significantly lower concentrations. However, even higher concentrations of PO_4-P should be evaluated with low concentrations of glyphosate and AMPA to see if this result remains true.

A drawback of the Metsorb®-DGT sampler is the limited binding capacity compared to other DGTs due to less sorbent added per binding layer. Although the capacity was not reached in this study, longer deployments may not be suitable. The linearity of PO_4-P uptake onto the Metsorb® sorbent decreased in the competition experiment after ~5 days. This decrease in uptake of compounds can be caused by slowing rates of sorption as the binding capacity is approached, or by being in the presence of a high concentration of the analyte (Davison & Zhang, 2016). However, if low enough concentrations of PO_4-P and other phosphate-bearing compounds are present at a potential sampling location, estimates from Metsorb®-DGT passive samplers should be accurate if the DBL is corrected for *in situ*.

2.5.4 Tracking nutrient input with tracers

2.5.4.1 Anthropogenic and agricultural tracers

The *Hamlet Site*, which was previously known for septic contamination to small headwater streams (Digaletos et al., 2023), showed the highest concentrations and prevalence of the sweeteners and pharmaceuticals, human-specific *Bacteroides*, as well as general fecal bacteria (*E. coli* and general *Bacteroides*). The highest concentrations detected at the *Hamlet Site* for pharmaceuticals were all higher than the same compounds found downstream of a WWTP located within the GRW (Liu et al., 2014), while concentrations of pharmaceuticals were comparable to others reported downgradient of septic systems in Ontario (Carrara et al., 2008) and similar to values previously reported at this site (Digaletos et al., 2023), indicating the consistent contamination of septic-systems in this area.

Septic systems are often overlooked as contributors of nutrients to surface waters in communities without centralized WWTPs (Lapointe et al., 2015; L. Oldfield et al., 2020), which may be more pronounced when located in areas of low permeability (Digaletos et al., 2023). In

Ontario, septic systems must currently be 15 m away from surface waters (O.Reg. 332/12, Building Code), yet septic plume monitoring studies across southern Ontario and the United States have noted elevated concentrations of P and N downgradient of septic beds beyond this distance. Inadequate nitrification and incomplete immobilization of P have contributed to elevated P levels in previous studies 20 m downgradient of the tile bed (Ptacek, 1998) as well as in a recent study where the PO_4-P plume extended over 90 m downgradient of the septic system (Rakhimbekova et al., 2021), and elevated N concentrations in several monitoring wells associated with septic system effluent (Nitka et al., 2019). Other studies have observed conditions that allow for soil bypasses or preferential flow paths of septic system contamination to streams, including low permeable soil conditions that allow for rapid transport via macro pores and direct discharge through tile drainage pipes (Digaletos et al., 2023; King et al., 2015)

The presence of ACE-K is strongly indicative of a septic contamination reaching the stream (Digaletos et al., 2023) and was routinely detected at much higher concentrations at the *Hamlet Site* compared to the *Agriculture* and *Mixed-land Site*s. In a review by Schaider et al. (2017) the removal of organic wastewater compounds, such as pharmaceuticals noted that CAF, IBU, and NAP, by septic systems was >50% efficiency from drain fields, while CBZ (8%) and SMX (40%) had much lower removal efficiencies. Poor removal efficiency by the drain field could explain elevated concentrations of CBZ and SMX detected in the samples, while CAF has been previously detected at elevated concentrations in this area (Digaletos et al., 2023). A properly working septic system removes a large percentage of these compounds, but the presence of these tracers suggests a percentage of septic systems in the surrounding area could be leaking, exposing surface waters to these contaminants. The simultaneous presence of ACE-K, a conservative tracer, and human-*Bacteroides* have been shown to be a strong indication that septic

system contamination (Lee et al., 2010; Richards et al., 2017) may be reaching surface waters through bypasses in soils with low permeability (Digaletos et al., 2023).

Agricultural-specific tracers including glyphosate and AMPA were elevated at the *Agriculture Site*, where land-use is primarily crops (e.g., cash crop including corn), as well as the *Mixed-land Site*, for which the *Agriculture Site* catchment is nested within. Glyphosate and AMPA were consistently detected (92%) at the *Agriculture Site*, detected in 25% of samples from the *Mixed-land Site*, and undetected at the *Hamlet Site*. Bovine-specific *Bacteroides* (BacBov) was elevated mostly at the *Mixed-land Site* where cattle farms were observed immediately upstream, with a small occurrence at the *Hamlet Site* in Spring 2022.

While agricultural practices are commonly associated with elevated nutrient loading to streams – from manure, fertilizer application, and grazing animals – the *Agriculture Site* and *Mixed-land Sites* did not always have elevated nutrients compared to the *Hamlet Site*. During Fall 2021 baseflow conditions, the *Hamlet Site* had consistently higher PO_4-P concentrations, whereas concentrations peaked at the agricultural-dominated sites in the Spring 2022 following a precipitation event, which is commonly associated with transport of nutrients to streams (Lusk et al., 2017; Robertson et al., 2016; Spoelstra et al., 2017).

2.5.4.2 Relationship among nutrients, tracers, and characterizing nonpoint source contamination

PCA plots from both discrete and DGT passive samples (Fig. 2-6) further support the observation of PO_4-P loading to surface waters from a human-specific source. PO_4-P site clustering with all anthropogenic-specific tracers oriented in the general direction of the *Hamlet Site* is evident. Spearman rank correlation coefficients between PO_4-P and all anthropogenic-specific tracers at the *Hamlet Site* were also > 0.62 (excluding SMX) during the Fall 2021

sampling event, with no other significant relationships between PO_4-P and agricultural tracers at the other sampling sites. PO_4-P is moderately correlated ($\rho > 0.61$) to 50% of human-specific tracers at the *Hamlet Site* during the Spring 2022 sampling period, with no significant correlations between PO_4-P and any tracers at the other sampling locations. The PCA plots and correlation coefficients further support that PO_4-P is more strongly associated with septic system contamination at this site, particularly during Fall 2021.

Glyphosate and AMPA loadings associated with PC scores from the *Agriculture Site* during both sampling events is evident from the PCA plots. NO_3-N is also associated with the *Agriculture Site* for the DGT PCA plot, mainly during the Fall 2021 sampling event, and has a moderate positive correlation to AMPA ($\rho = 0.63$). There are many outputs of NO_3-N from agricultural practises, but in the Great Lakes region NO_3-N is not considered a limiting nutrient for algal bloom growth like PO_4-P (Heathwaite et al., 2005; Matlock et al., 1998; Søndergaard & Jeppesen, 2007), and the contribution of NO_3-N from the *Agriculture Site* likely has less of an impact on overall surface water quality compared to PO_4-P loading from the *Hamlet Site*.

2.6 Conclusions

The uptake of nutrients and tracers by passive samplers (DGT, POCIS) can be used to characterize nonpoint septic-system and agricultural sources in rurally impacted surface waters. Combined tracers associated with different land-use activities obtained by both discrete and passive sampling assisted to distinguish septic-system *versus* agricultural impacts to streams. Compared to discrete samples, passive samples resulted in similar to better detection, yet lower concentration, for certain compounds. Reducing variability in stream water concentrations is a main advantage of passive samplers over discrete sampling, as infrequent discrete sampling may not be representative of mean stream concentrations. Even over a short period of time (6-12

days), large variability was observed in many compounds in this study from discrete samples. DGT samplers provided concentrations more consistent with mean discrete concentrations relative to POCIS for most target analytes. Research into the development of more field-derived R_s values for POCIS compounds may increase estimation of concentrations calculated from POCIS compared to DGT, as was observed with ACE-K in this study.

The overall impact of nutrient loading to surface waters from a septic-system and agricultural perspective was investigated. Higher nutrient concentrations and the presence of anthropogenic-specific tracers at the *Hamlet Site* imply that septic systems may be an unappreciated source of nutrient loading in small headwater streams in rural settings. The results also suggest that the selected array of passive samplers may be a powerful tool to distinguish nonpoint nutrient sources in small headwater streams.

Chapter 3: Conclusions and future recommendations

The use of passive samplers continues to grow as an alternative to discrete sampling for environmental monitoring (Hawker et al., 2022; Renaud et al., 2022; Wu et al., 2023). Variability associated with infrequent discrete sampling was reduced when using a passive sampler with a collecting medium. Even short timeframes of three days between discrete samples resulted in large standard deviation for certain compounds. DGT and POCIS are commonly used passive samplers for a large range of compounds. DGTs display a few distinct advantages over POCIS including a vast array of commercially available samplers for different compounds, ease of extraction and lower cost, and simple adaptability to surface waters by estimating the DBL. Newer methods to correct for flow effects on POCIS, including the use of PRCs (Buzier et al., 2019) and producing field-derived R_s values (Liu et al., 2023), have successfully modified C_{POCIS} values to be more representative of field conditions.

Characterizing nonpoint sources of nutrients to surface water bodies was achieved in this study by using a suite of anthropogenic- and agricultural-specific tracers. Densely situated septic systems in rural hamlets, in particular those installed on finer grained overburden material, may be an underappreciated source of contamination to streams (Digaletos et al., 2023). Elevated concentrations of ACE-K, SUC, and *BacHum* at the *Hamlet Site* suggest the use of multiple tracers as an effective tool to delineate anthropogenic sources of wastewater. A correlation analysis showed a significant relationship between P and anthropogenic tracers at the *Hamlet Site*, indicating continued contamination by septic systems in this area.

Prior to this study, development of a passive sampler to capture ACE-K was an objective as it has been shown to be an optimal anthropogenic tracer due to its persistence and minimal biodegradation in the environment. Strata X-AW, a weak anion exchange sorbent, was evaluated

in this study as a potential binding sorbent for ACE-K and SUC but was unsuccessful as it severely underestimated C_{DGT} compared to C_{ACTIVE}. Using PRC compounds in POCIS may have been an effective method to increase uptake of ACE-K onto HLB sorbent, however flow conditions at the sampling locations likely were too low for this method. Producing field-derived R_s values is likely a more suitable option for POCIS to reflect field conditions under which samplers are deployed.

Sorbents used in passive samplers are susceptible to competing compounds in environmental waters. Initial analysis of a body of water should be evaluated to determine if the sampler of choice is appropriate for deployment, depending on general water chemistry to implement an appropriate sampling plan. Finally, further evaluation of competition impacts on the Metsorb®-DGT sampler at higher PO_4-P concentrations should be explored to confirm there are no competition impacts associated with multiple phosphate-bearing compounds at various concentrations. Intrinsic binding capacity of the Metsorb® binding layer is also limited compared to others developed for DGT, and creating a binding layer with a larger capacity would be crucial for longer monitoring periods.

References

Agilent Technologies (2019). Direct Analysis of Glyphosate, AMPA, and Other Polar Pesticides in Food. *Ion exchange LC/MS/MS with the Agilent 1260 Infinity II bio-inert LC and the Agilent 6495A triple quadrupole LC/MS.*

Alvarez, D. A. (2013). Development of semipermeable membrane devices (SPMDs) and polar organic chemical integrative samplers (POCIS) for environmental monitoring. *Environmental Toxicology and Chemistry*, *32*(10), 2179–2181. https://doi.org/10.1002/etc.2339

Alvarez, D. A., Huckins, J. N., Petty, J. D., Jones-Lepp, T., Stuer-Lauridsen, F., Getting, D. T., Goddard, J. P., & Gravell, A. (2007). Chapter 8 Tool for monitoring hydrophilic contaminants in water: polar organic chemical integrative sampler (POCIS). *Comprehensive Analytical Chemistry*, *48*(06), 171–197. https://doi.org/10.1016/S0166-526X(06)48008-9

Alvarez, D. A., Petty, J. D., Huckins, J. N., Jones-Lepp, T. L., Getting, D. T., Goddard, J. P., & Manahan, S. E. (2004). Development of a passive, in situ, integrative sampler for hydrophilic organic contaminants in aquatic environments. *Environmental Toxicology and Chemistry*. https://doi.org/10.1897/03-603

American Public Health Association, American Water Works Association, and Water Environment Federation (2017). Standard Methods for the Examination of Water and Wastewater. 23rd edition. Section 9223 B: Enzyme Substrate Coliform Test.

Aparicio, V. C., De Gerónimo, E., Marino, D., Primost, J., Carriquiriborde, P., & Costa, J. L. (2013). Environmental fate of glyphosate and aminomethylphosphonic acid in surface waters and soil of agricultural basins. *Chemosphere*, *93*(9), 1866–1873. https://doi.org/10.1016/j.chemosphere.2013.06.041

APHA, in Method 2320 B: alkalinity, American Public Health Association, Washington, D.C., (1992).

APHA, in Method 4500-NH3, American Public Health Association, Washington, D.C., (2005).

APHA, in Method 4500-P: E, American Public Health Association, Washington, D.C., (2005)

Bennett, W. W., Teasdale, P. R., Panther, J. G., Welsh, D. T., & Jolley, D. F. (2010). New diffusive gradients in a thin film technique for measuring inorganic arsenic and selenium(IV) using a titanium dioxide based adsorbent. *Analytical Chemistry*, *82*(17), 7401–7407. https://doi.org/10.1021/ac101543p

Bernard, M., Boutry, S., Lissalde, S., Guibaud, G., Saüt, M., Rebillard, J. P., & Mazzella, N. (2019). Combination of passive and grab sampling strategies improves the assessment of pesticide occurrence and contamination levels in a large-scale watershed. *Science of the Total Environment*, *651*, 684–695. https://doi.org/10.1016/j.scitotenv.2018.09.202

Buerge, I. J., Buser, H. R., Kahle, M., Müller, M. D., & Poiger, T. (2009). Ubiquitous occurrence of the artificial sweetener acesulfame in the aquatic environment: An ideal chemical marker of domestic wastewater in groundwater. *Environmental Science and Technology*, *43*(12), 4381–4385. https://doi.org/10.1021/es900126x

Buzier, R., Guibal, R., Lissalde, S., & Guibaud, G. (2019). Limitation of flow effect on passive sampling accuracy using POCIS with the PRC approach or o-DGT: A pilot-scale evaluation for pharmaceutical compounds. *Chemosphere*, *222*, 628–636. https://doi.org/10.1016/j.chemosphere.2019.01.181

Carey, R. O., & Migliaccio, K. W. (2009). Contribution of wastewater treatment plant effluents

to nutrient dynamics in aquatic systems. *Environmental Management*, *44*(2), 205–217. https://doi.org/10.1007/s00267-009-9309-5

Carpenter, S. R., Caraco, N. F., Correll, D. L., Howarth, R. W., Sharpley, A. N., & Smith, V. H. (1998). Nonpoint pollution of surface waters with phosphorus and nitrogen. *Ecological Applications*, *8*(3), 559–568. https://doi.org/10.1890/1051-0761(1998)008[0559:NPOSWW]2.0.CO;2

Carrara, C., Ptacek, C. J., Robertson, W. D., Blowes, D. W., Moncur, M. C., Sverko, E., & Backus, S. (2008). Fate of pharmaceutical and trace organic compounds in three septic system plumes, Ontario, Canada. *Environmental Science and Technology*, *42*(8), 2805–2811. https://doi.org/10.1021/es070344q

Castronovo, S., Wick, A., Scheurer, M., Nödler, K., Schulz, M., & Ternes, T. A. (2017). Biodegradation of the artificial sweetener acesulfame in biological wastewater treatment and sandfilters. *Water Research*, *110*, 342–353. https://doi.org/10.1016/j.watres.2016.11.041

Challis, J. K., Almirall, X. O., Helm, P. A., & Wong, C. S. (2020). Performance of the organic-diffusive gradients in thin-films passive sampler for measurement of target and suspect wastewater contaminants. *Environmental Pollution*, *261*, 114092. https://doi.org/10.1016/j.envpol.2020.114092

Challis, J. K., Hanson, M. L., & Wong, C. S. (2016). Development and calibration of an organic-diffusive gradients in thin films aquatic passive sampler for a diverse suite of polar organic contaminants. *Analytical Chemistry*, *88*(21), 10583–10591. https://doi.org/10.1021/acs.analchem.6b02749

Challis, J. K., Stroski, K. M., Luong, K. H., Hanson, M. L., & Wong, C. S. (2018). Field evaluation and in situ stress testing of the organic-diffusive gradients in thin-films passive sampler. *Environmental Science and Technology*, *52*(21), 12573–12582. https://doi.org/10.1021/acs.est.8b03622

Chen, C.-E., Zhang, H., Ying, G.-G., & Jones, K. C. (2013). Use of novel passive water sampling apparatus to quantify antibiotics in wastewater. *Environmental Science & Technology*, *47*(23), 13587–13593.

Conley, D. J., Paerl, H. W., Howarth, R. W., Boesch, D. F., Seitzinger, S. P., Havens, K. E., Lancelot, C., & Likens, G. E. (2009). Ecology - Controlling eutrophication: Nitrogen and phosphorus. *Science*, *323*(5917), 1014–1015. https://doi.org/10.1126/science.1167755

Conn, K. E., Barber, L. B., Brown, G. K., & Siegrist, R. L. (2006). Occurrence and fate of organic contaminants during onsite wastewater treatment. *Environmental Science and Technology*, *40*(23), 7358–7366. https://doi.org/10.1021/es0605117

Conn, K. E., Siegrist, R. L., Barber, L. B., & Meyer, M. T. (2010). Fate of trace organic compounds during vadose zone soil treatment in an onsite wastewater system. *Environmental Toxicology and Chemistry*, *29*(2), 285–293. https://doi.org/10.1002/etc.40

Cosmetic Pesticides Ban Act (2008). S.O. 2008, c. 11 - Bill 64.

Criquet, J., Dumoulin, D., Howsam, M., Mondamert, L., Goossens, J. F., Prygiel, J., & Billon, G. (2017). Comparison of POCIS passive samplers vs. composite water sampling: A case study. *Science of the Total Environment*, *609*, 982–991. https://doi.org/10.1016/j.scitotenv.2017.07.227

Davison, W., & Zhang, H. (2016). Diffusive gradients in thin-films for environmental measurements. *Diffusive Gradients in Thin-Films for Environmental Measurements*, 10–31. https://doi.org/10.1017/cbo9781316442654.003

Digaletos, M. (2019). *Integration of Active and Passive Sampling Techniques for Characterization of Non-point Source Contamination from Septic Systems in Rural Ontario Hamlets by*.

Digaletos, M., Ptacek, C. J., Thomas, J., & Liu, Y. (2023). Chemical and biological tracers to identify source and transport pathways of septic system contamination to streams in areas with low permeability soils. *Science of the Total Environment*, *870*(January), 161866. https://doi.org/10.1016/j.scitotenv.2023.161866

Edge, T. A., Boyd, R. J., Shum, P., & Thomas, J. L. (2020). Microbial source tracking to identify fecal sources contaminating the Toronto Harbour and Don River watershed in wet and dry weather. *Journal of Great Lakes Research*, *xxxx*. https://doi.org/10.1016/j.jglr.2020.09.002

Fang, Z., Li, K., Li, Y., Zhang, H., Jones, K. C., Liu, X., Liu, S., Ma, L. Q., & Luo, J. (2019). Development and application of the diffusive gradients in thin-films technique for measuring psychiatric pharmaceuticals in natural waters. *Environmental Science and Technology*, *53*(19), 11223–11231. https://doi.org/10.1021/acs.est.9b03166

Fauvelle, V., Nhu-Trang, T. T., Feret, T., Madarassou, K., Randon, J., & Mazzella, N. (2015). Evaluation of titanium dioxide as a binding phase for the passive sampling of glyphosate and aminomethyl phosphonic acid in an aquatic environment. *Analytical Chemistry*, *87*(12), 6004–6009. https://doi.org/10.1021/acs.analchem.5b00194

Fu, K., Wang, L., Wei, C., Li, J., Zhang, J., Zhou, Z., & Liang, Y. (2020). Sucralose and acesulfame as an indicator of domestic wastewater contamination in Wuhan surface water. *Ecotoxicology and Environmental Safety*, *189*(September), 109980. https://doi.org/10.1016/j.ecoenv.2019.109980

Government of Canada (2016). Governments of Canada and the United States announce phosphorus reduction targets of 40 percent to improve Lake Erie water quality. https://www.canada.ca/en/environment-climate-change/news/2016/02/governments-ofcanada-and-the-united-states-announce-phosphorus-reduction-targets-of-40-percent-toimprove-lake-erie-water-quality.html

Grannemann, N., & Van Stempvoort, D. (2016). *Groundwater science relevant to the Great Lakes Water Quality agreement: A status report*.

Hawker, D. W., Clokey, J., Gorji, S. G., Verhagen, R., & Kaserzon, S. L. (2022). Monitoring techniques-grab and passive sampling. In *Emerging Freshwater Pollutants: Analysis, Fate and Regulations*. Elsevier Inc. https://doi.org/10.1016/B978-0-12-822850-0.00014-4

Heathwaite, A. L., Dils, R. M., Liu, S., Carvalho, L., Brazier, R. E., Pope, L., Hughes, M., Phillips, G., & May, L. (2005). A tiered risk-based approach for predicting diffuse and point source phosphorus losses in agricultural areas. *Science of the Total Environment*, *344*(1-3 SPEC. ISS.), 225–239. https://doi.org/10.1016/j.scitotenv.2005.02.034

Helm, P. A., Howell, E. T., Li, H., L. Metcalfe, T., M. Chomicki, K., & D. Metcalfe, C. (2012). Influence of nearshore dynamics on the distribution of organic wastewater-associated chemicals in Lake Ontario determined using passive samplers. *Journal of Great Lakes Research*, *38*(SUPPL.4), 105–115. https://doi.org/10.1016/j.jglr.2012.01.005

Hogan, S. C., O'Sullivan, J. J., Bruen, M., Jarvie, H. P., Cox, E. J., Bowes, M. J., & Kelly-Quinn, M. (2023). A review of the nature and source of nutrient impairment in small streams: a desk based characterisation for targeted mitigation measures. *Hydrobiologia*, *0123456789*. https://doi.org/10.1007/s10750-022-05114-1

Hoque, M. E., Cloutier, F., Arcieri, C., McInnes, M., Sultana, T., Murray, C., Vanrolleghem, P. A., & Metcalfe, C. D. (2014). Removal of selected pharmaceuticals, personal care products

and artificial sweetener in an aerated sewage lagoon. *Science of the Total Environment*, *487*(1), 801–812. https://doi.org/10.1016/j.scitotenv.2013.12.063

Huang, J., Bennett, W. W., Teasdale, P. R., Gardiner, S., & Welsh, D. T. (2016). Development and evaluation of the diffusive gradients in thin films technique for measuring nitrate in freshwaters. *Analytica Chimica Acta*, *923*(3), 74–81. https://doi.org/10.1016/j.aca.2016.04.006

Huang, J., Bennett, W. W., Teasdale, P. R., Kankanamge, N. R., & Welsh, D. T. (2017). A modified DGT technique for the simultaneous measurement of dissolved inorganic nitrogen and phosphorus in freshwaters. *Analytica Chimica Acta*, *988*, 17–26. https://doi.org/10.1016/j.aca.2017.08.024

Huang, J., Bennett, W. W., Welsh, D. T., Li, T., & Teasdale, P. R. (2016). Development and evaluation of a diffusive gradients in a thin film technique for measuring ammonium in freshwaters. *Analytica Chimica Acta*, *904*, 83–91. https://doi.org/10.1016/j.aca.2015.11.022

Huckins, J. N., Manuweera, G. K., Petty, J. D., Mackay, D., & Lebo, J. A. (1993). Lipid-containing semipermeable membrane devices for monitoring organic contaminants in water. *Environmental Science and Technology*, *27*(12), 2489–2496. https://doi.org/10.1021/es00048a028

Jarvie, H. P., Johnson, L. T., Sharpley, A. N., Smith, D. R., Baker, D. B., Bruulsema, T. W., & Confesor, R. (2017). Increased soluble phosphorus loads to Lake Erie: Unintended consequences of conservation practices? *Journal of Environmental Quality*, *46*(1), 123–132. https://doi.org/10.2134/jeq2016.07.0248

Jarvie, H. P., Withers, P. J. A., Bowes, M. J., Palmer-Felgate, E. J., Harper, D. M., Wasiak, K., Wasiak, P., Hodgkinson, R. A., Bates, A., Stoate, C., Neal, M., Wickham, H. D., Harman, S. A., & Armstrong, L. K. (2010). Streamwater phosphorus and nitrogen across a gradient in rural-agricultural land use intensity. *Agriculture, Ecosystems and Environment*, *135*(4), 238–252. https://doi.org/10.1016/j.agee.2009.10.002

King, K. W., Williams, M. R., Macrae, M. L., Fausey, N. R., Frankenberger, J., Smith, D. R., Kleinman, P. J. A., & Brown, L. C. (2015). Phosphorus transport in agricultural subsurface drainage: A review. *Journal of Environmental Quality*, *44*(2), 467–485. https://doi.org/10.2134/jeq2014.04.0163

Kingston, J. K., Greenwood, R., Mills, G. A., Morrison, G. M., & Persson, L. B. (2000). Development of a novel passive sampling system for the time-averaged measurement of a range of organic pollutants in aquatic environments. *Journal of Environmental Monitoring*. https://doi.org/10.1039/b003532g

Lapointe, B. E., Herren, L. W., Debortoli, D. D., & Vogel, M. A. (2015). Evidence of sewage-driven eutrophication and harmful algal blooms in Florida's Indian River Lagoon. *Harmful Algae*, *43*, 82–102. https://doi.org/10.1016/j.hal.2015.01.004

Lapointe, B. E., Herren, L. W., & Paule, A. L. (2017). Septic systems contribute to nutrient pollution and harmful algal blooms in the St. Lucie Estuary, Southeast Florida, USA. *Harmful Algae*, *70*, 1–22. https://doi.org/10.1016/j.hal.2017.09.005

Lee, D. Y., Lee, H., Trevors, J. T., Weir, S. C., Thomas, J. L., & Habash, M. (2014). Characterization of sources and loadings of fecal pollutants using microbial source tracking assays in urban and rural areas of the Grand River Watershed, Southwestern Ontario. *Water Research*, *53*, 123–131. https://doi.org/10.1016/j.watres.2014.01.003

Lee, D. Y., Weir, S. C., Lee, H., & Trevors, J. T. (2010). Quantitative identification of fecal water pollution sources by TaqMan real-time PCR assays using Bacteroidales 16S rRNA

genetic markers. *Applied Microbiology and Biotechnology*, *88*(6), 1373–1383. https://doi.org/10.1007/s00253-010-2880-0

Lee, H. J., Kim, K. Y., Hamm, S. Y., Kim, M. S., Kim, H. K., & Oh, J. E. (2019). Occurrence and distribution of pharmaceutical and personal care products, artificial sweeteners, and pesticides in groundwater from an agricultural area in Korea. *Science of the Total Environment*, *659*, 168–176. https://doi.org/10.1016/j.scitotenv.2018.12.258

Li, D., Xu, X., Li, Z., Wang, T., & Wang, C. (2020). Detection methods of ammonia nitrogen in water: A review. *TrAC - Trends in Analytical Chemistry*, *127*, 115890. https://doi.org/10.1016/j.trac.2020.115890

Li, H., Helm, P. A., & Metcalfe, C. D. (2010). Sampling in the great lakes for pharmaceuticals, personal care products, and endocrine-disrupting substances using the passive polar organic chemical integrative sampler. *Environmental Toxicology and Chemistry*, *29*(4), 751–762. https://doi.org/10.1002/etc.104

Li, H., Helm, P. A., Paterson, G., & Metcalfe, C. D. (2011). The effects of dissolved organic matter and pH on sampling rates for polar organic chemical integrative samplers (POCIS). *Chemosphere*, *83*(3), 271–280. https://doi.org/10.1016/j.chemosphere.2010.12.071

Lin, K., Zhu, Y., Zhang, Y., & Lin, H. (2019). Determination of ammonia nitrogen in natural waters: Recent advances and applications. *Trends in Environmental Analytical Chemistry*, *24*, e00073. https://doi.org/10.1016/j.teac.2019.e00073

Liu, Y. Y., Blowes, D. W., Groza, L., Sabourin, M. J., & Ptacek, C. J. (2014). Acesulfame-K and pharmaceuticals as co-tracers of municipal wastewater in a receiving river. *Environmental Sciences: Processes and Impacts*, *16*(12), 2789–2795. https://doi.org/10.1039/c4em00237g

Lombardo, P. (2006). Phosphorus geochemistry in septic tanks, soil absorption systems, and groundwater.

Lusk, M. G., Toor, G. S., Yang, Y. Y., Mechtensimer, S., De, M., & Obreza, T. A. (2017). A review of the fate and transport of nitrogen, phosphorus, pathogens, and trace organic chemicals in septic systems. *Critical Reviews in Environmental Science and Technology*. https://doi.org/10.1080/10643389.2017.1327787

Martins de Barros, R., Rougerie, J., Guibal, R., Lissalde, S., Buzier, R., Simon, S., & Guibaud, G. (2023). Interest of a new large diffusive gradients in thin films (L-DGT) for organic compounds monitoring: On-field comparison with conventional passive samplers. *Environmental Pollution*, *323*(January). https://doi.org/10.1016/j.envpol.2023.121257

Matlock, M. D., Matlock, M. E., Storm, D. E., Smolen, M. D., & Henley, W. J. (1998). Limiting nutrient determination in lotic ecosystems using a quantitative nutrient enrichment peripphytometer. *Journal of the American Water Resources Association*, *34*(5), 1141–1147. https://doi.org/10.1111/j.1752-1688.1998.tb04160.x

MECP, 2017. Ontario Ministry of Environment, Conservation and Parks (MECP). A membrane filtration method for the detection and enumeration of total coliform, Escherichia coli, Pseudomonas aeruginosa and Fecal Streptococci in environmental samples (method E3371). Laboratory Services Branch, Etobicoke, Ontario.

MECP, 2022. Ontario Ministry of Environment, Conservation and Parks (MECP). Identification of fecal water pollution sources by real-time polymerase chain reaction (PCR) using Bacteroidales 16S rRNA genetic markers (method E3499). Laboratory Services Branch, Etobicoke, Ontario.

Metcalfe, C. D., Helm, P., Paterson, G., Kaltenecker, G., Murray, C., Nowierski, M., & Sultana, T. (2019). Pesticides related to land use in watersheds of the Great Lakes basin. *Science of*

the Total Environment, *648*, 681–692. https://doi.org/10.1016/j.scitotenv.2018.08.169
Metcalfe, C. D., Sultana, T., Li, H., & Helm, P. A. (2016). Current-use pesticides in urban watersheds and receiving waters of western Lake Ontario measured using polar organic chemical integrative samplers (POCIS). *Journal of Great Lakes Research*, *42*(6), 1432–1442. https://doi.org/10.1016/j.jglr.2016.08.004
Metcalfe, C., Hoque, M. E., Sultana, T., Murray, C., Helm, P., & Kleywegt, S. (2014). Monitoring for contaminants of emerging concern in drinking water using POCIS passive samplers. *Environmental Sciences: Processes and Impacts*, *16*(3), 473–481. https://doi.org/10.1039/c3em00508a
Mitrovic, S. M., Chessman, B. C., Davie, A., Avery, E. L., & Ryan, N. (2008). Development of blooms of Cyclotella meneghiniana and Nitzschia spp. (Bacillariophyceae) in a shallow river and estimation of effective suppression flows. *Hydrobiologia*, *596*(1), 173–185. https://doi.org/10.1007/s10750-007-9094-1
Mohamed, M. N., Wellen, C., Parsons, C. T., Taylor, W. D., Arhonditsis, G., Chomicki, K. M., Boyd, D., Weidman, P., Mundle, S. O. C., Van Cappellen, P., Sharpley, A. N., & Haffner, D. G. (2019). Understanding and managing the re-eutrophication of lake erie: Knowledge gaps and research priorities. *Freshwater Science*, *38*(4), 675–691. https://doi.org/10.1086/705915
Müller, B., Stierli, R., & Gächter, R. (2008). A low-tech, low-cost passive sampler for the long-term monitoring of phosphate loads in rivers and streams. *Journal of Environmental Monitoring*, *10*(7), 817–820. https://doi.org/10.1039/b806465b
Nitka, A. L., DeVita, W. M., & McGinley, P. M. (2019). Evaluating a chemical source-tracing suite for septic system nitrate in household wells. *Water Research*, *148*, 438–445. https://doi.org/10.1016/j.watres.2018.10.019
O Duke, S., & B Powles, S. (2008). Glyphosate: a once-in-a-century herbicide. *Pest Management Science*, *63*(11), 1100–1106. https://doi.org/10.1002/ps
Oldfield, L. E., Roy, J. W., & Robinson, C. E. (2020). Investigating the use of the artificial sweetener acesulfame to evaluate septic system inputs and their nutrient loads to streams at the watershed scale. *Journal of Hydrology*, *587*(January), 124918. https://doi.org/10.1016/j.jhydrol.2020.124918
Oldfield, L., Rakhimbekova, S., Roy, J. W., & Robinson, C. E. (2020). Estimation of phosphorus loads from septic systems to tributaries in the Canadian Lake Erie Basin. *Journal of Great Lakes Research*, *xxxx*. https://doi.org/10.1016/j.jglr.2020.08.021
Ordóñez, E. Y., Quintana, J. B., Rodil, R., & Cela, R. (2012). Determination of artificial sweeteners in water samples by solid-phase extraction and liquid chromatography-tandem mass spectrometry. *Journal of Chromatography A*, *1256*, 197–205. https://doi.org/10.1016/j.chroma.2012.07.073
Panther, J. G., Teasdale, P. R., Bennett, W. W., Welsh, D. T., & Zhao, H. (2010). Titanium dioxide-based DGT technique for in situ measurement of dissolved reactive phosphorus in fresh and marine waters. *Environmental Science and Technology*, *44*(24), 9419–9424. https://doi.org/10.1021/es1027713
Pearce, N. J. T., Parsons, C. T., Pomfret, S. M., & Yates, A. G. (2023). Periphyton phosphorus uptake in response to dynamic concentrations in streams: Assimilation and changes to intracellular speciation. *Environmental Science and Technology*. https://doi.org/10.1021/acs.est.2c06285
Poiger, T., Keller, M., Buerge, I. J., & Balmer, M. E. (2020). Behavior of glyphosate in

wastewater treatment plants. *Chimia*, *74*(3), 156–160. https://doi.org/10.2533/CHIMIA.2020.156

Price, H. L., Teasdale, P. R., & Jolley, D. F. (2013). An evaluation of ferrihydrite- and Metsorb^{TM}-DGT techniques for measuring oxyanion species (As, Se, V, P): Effective capacity, competition and diffusion coefficients. *Analytica Chimica Acta*, *803*, 56–65. https://doi.org/10.1016/j.aca.2013.07.001

Provincial (Stream) Water Quality Monitoring Network (PWQMN) (2020). Accessed January 14 2023.

Ptacek, C. J. (1998). Geochemistry of a septic-system plume in a coastal barrier bar, Point Pelee, Ontario, Canada. *Journal of Contaminant Hydrology*, *33*(3–4), 293–312. https://doi.org/10.1016/S0169-7722(98)00076-X

Raby, M., Lissemore, L., Kaltenecker, G., Beaton, D., & Prosser, R. (2022). Characterizing the exposure of streams in southern Ontario to agricultural pesticides. *Chemosphere*, *294*(November 2021), 133769. https://doi.org/10.1016/j.chemosphere.2022.133769

Rakhimbekova, S., O'Carroll, D. M., Oldfield, L. E., Ptacek, C. J., & Robinson, C. E. (2021). Spatiotemporal controls on septic system derived nutrients in a nearshore aquifer and their discharge to a large lake. *Science of the Total Environment*, *752*. https://doi.org/10.1016/j.scitotenv.2020.141262

Renaud, J. B., Sabourin, L., Hoogstra, S., Helm, P., Lapen, D. R., & Sumarah, M. W. (2022). Monitoring of environmental contaminants in mixed-use watersheds combining targeted and nontargeted analysis with passive sampling. *Environmental Toxicology and Chemistry*, *41*(5), 1131–1143. https://doi.org/10.1002/etc.5192

Richards, S., Withers, P. J. A., Paterson, E., McRoberts, C. W., & Stutter, M. (2017). Potential tracers for tracking septic tank effluent discharges in watercourses. *Environmental Pollution*, *228*, 245–255. https://doi.org/10.1016/j.envpol.2017.05.044

Robertson, W. D., & Harman, J. (1999). *Phosphate Plume Persistence at Two Decommissioned Septic System Sites*.

Robertson, W. D., Van Stempvoort, D. R., Roy, J. W., Brown, S. J., Spoelstra, J., Schiff, S. L., Rudolph, D. R., Danielescu, S., & Graham, G. (2016). Use of an artificial sweetener to identify sources of groundwater nitrate contamination. *Groundwater*, *54*(4), 579–587. https://doi.org/10.1111/gwat.12399

Robertson, W. D., Van Stempvoort, D. R., & Schiff, S. L. (2019). Review of phosphorus attenuation in groundwater plumes from 24 septic systems. *Science of the Total Environment*, *692*, 640–652. https://doi.org/10.1016/j.scitotenv.2019.07.198

Robertson, W. D., Van Stempvoort, D. R., Solomon, D. K., Homewood, J., Brown, S. J., Spoelstra, J., & Schiff, S. L. (2013). Persistence of artificial sweeteners in a 15-year-old septic system plume. *Journal of Hydrology*, *477*, 43–54. https://doi.org/10.1016/j.jhydrol.2012.10.048

Ross, C. A., Moslenko, L. L., Biagi, K. M., Oswald, C. J., Wellen, C. C., Thomas, J. L., Raby, M., & Sorichetti, R. J. (2022). Total and dissolved phosphorus losses from agricultural headwater streams during extreme runoff events. *Science of the Total Environment*, *848*(July), 157736. https://doi.org/10.1016/j.scitotenv.2022.157736

Schaider, L. A., Rodgers, K. M., & Rudel, R. A. (2017). Review of organic wastewater compound concentrations and removal in onsite wastewater treatment systems. *Environmental Science and Technology*, *51*(13), 7304–7317. https://doi.org/10.1021/acs.est.6b04778

Schindler, D. W. (1977). Evolution of phosphorus limitation in lakes. *Science*, *195*(4275), 260–262. https://doi.org/10.1126/science.195.4275.260

Schindler, D. W., Carpenter, S. R., Chapra, S. C., Hecky, R. E., & Orihel, D. M. (2016). Reducing phosphorus to curb lake eutrophication is a success. *Environmental Science and Technology*, *50*(17), 8923–8929. https://doi.org/10.1021/acs.est.6b02204

Schoumans, O. F. (2014). Description of the phosphorus sorption and desorption processes in coarse calcareous sandy soils. *Soil Science*, *179*(5), 221–229. https://doi.org/10.1097/SS.0000000000000065

Snider, D. M., Roy, J. W., Robertson, W. D., Garda, D. I., & Spoelstra, J. (2017). Concentrations of artificial sweeteners and their ratios with nutrients in septic system wastewater. *Groundwater Monitoring and Remediation*, *37*(3), 94–102. https://doi.org/10.1111/gwmr.12229

Søndergaard, M., & Jeppesen, E. (2007). Anthropogenic impacts on lake and stream ecosystems, and approaches to restoration. *Journal of Applied Ecology*, *44*(6), 1089–1094. https://doi.org/10.1111/j.1365-2664.2007.01426.x

Spoelstra, J., Schiff, S. L., & Brown, S. J. (2020). Septic systems contribute artificial sweeteners to streams through groundwater. *Journal of Hydrology X*, *7*(June 2019), 1–8. https://doi.org/10.1016/j.hydroa.2020.100050

Spoelstra, J., Senger, N. D., & Schiff, S. L. (2017). Artificial sweeteners reveal septic system effluent in rural groundwater. *Journal of Environmental Quality*, *46*(6), 1434–1443. https://doi.org/10.2134/jeq2017.06.0233

Struger, J., Van Stempvoort, D. R., & Brown, S. J. (2015). Sources of aminomethylphosphonic acid (AMPA) in urban and rural catchments in Ontario, Canada: Glyphosate or phosphonates in wastewater? *Environmental Pollution*, *204*, 289–297. https://doi.org/10.1016/j.envpol.2015.03.038

Sultana, T., & Metcalfe, C. D. (2022). Calibration and field validation of POCIS passive samplers for tracking artificial sweeteners as indicators of municipal wastewater contamination in surface waters. *Environmental Monitoring and Assessment*. https://doi.org/10.1007/s10661-022-10150-4

Supowit, S. D., Roll, I. B., Dang, V. D., Kroll, K. J., Denslow, N. D., & Halden, R. U. (2016). Active sampling device for determining pollutants in surface and pore water - The in situ sampler for biphasic water monitoring. *Scientific Reports*, *6*(February), 1–9. https://doi.org/10.1038/srep21886

Taebi, A., & Droste, R. L. (2004). Pollution loads in urban runoff and sanitary wastewater. *Science of the Total Environment*, *327*(1–3), 175–184. https://doi.org/10.1016/j.scitotenv.2003.11.015

Tanna, R. N., Moncur, M. C., Jean Birks, S., Gibson, J. J., Ptacek, C. J., Mayer, B., Wieser, M. E., Wrona, F. J., & Munkittrick, K. R. (2020). Utility of a multi-tracer approach as a component of adaptive monitoring for municipal wastewater impacts. *Water Quality Research Journal of Canada*, *55*(3), 327–341. https://doi.org/10.2166/wqrj.2020.004

Todd, A., & Struger, J. (2014). Changes in acid herbicide concentrations in urban streams after a cosmetic pesticides ban. *Challenges*, *5*(1), 138–151. https://doi.org/10.3390/challe5010138

Tyre, K., Brewton, R., Kreiger, L., & Lapointe, B. E. (2023). Widespread human waste pollution in surface waters observed throughout the urbanized, coastal communities of Lee County, Florida, USA. *Science of the Total Environment*, *Ii*, 109181. https://doi.org/10.1016/j.scitotenv.2023.162716

Van Bruggen, A. H. C., He, M. M., Shin, K., Mai, V., Jeong, K. C., Finckh, M. R., & Morris, J. G. (2018). Environmental and health effects of the herbicide glyphosate. *Science of the Total Environment*, *616–617*, 255–268. https://doi.org/10.1016/j.scitotenv.2017.10.309

Van Stempvoort, D. R., Brown, S. J., Spoelstra, J., Garda, D., Robertson, W. D., & Smyth, S. A. (2020). Variable persistence of artificial sweeteners during wastewater treatment: Implications for future use as tracers. *Water Research*, *184*, 116124. https://doi.org/10.1016/j.watres.2020.116124

Van Stempvoort, D. R., Roy, J. W., Brown, S. J., & Bickerton, G. (2011). Artificial sweeteners as potential tracers in groundwater in urban environments. *Journal of Hydrology*, *401*(1–2), 126–133. https://doi.org/10.1016/j.jhydrol.2011.02.013

Van Stempvoort, D. R., Roy, J. W., Brown, S. J., & Bickerton, G. (2014). Residues of the herbicide glyphosate in riparian groundwater in urban catchments. *Chemosphere*, *95*, 455–463. https://doi.org/10.1016/j.chemosphere.2013.09.095

Van Stempvoort, D. R., Roy, J. W., Grabuski, J., Brown, S. J., Bickerton, G., & Sverko, E. (2013). An artificial sweetener and pharmaceutical compounds as co-tracers of urban wastewater in groundwater. *Science of the Total Environment*, *461–462*, 348–3359. https://doi.org/10.1016/j.scitotenv.2013.05.001

Van Stempvoort, D. R., Spoelstra, J., Senger, N. D., Brown, S. J., Post, R., & Struger, J. (2016). Glyphosate residues in rural groundwater, Nottawasaga River Watershed, Ontario, Canada. *Pest Management Science*, *72*(10), 1862–1872. https://doi.org/10.1002/ps.4218

Vrana, B., Allan, I. J., Greenwood, R., Mills, G. A., Dominiak, E., Svensson, K., Knutsson, J., & Morrison, G. (2005). Passive sampling techniques for monitoring pollutants in water. *TrAC - Trends in Analytical Chemistry*, *24*(10), 845–868. https://doi.org/10.1016/j.trac.2005.06.006

Vrana, B., Urík, J., Fedorova, G., Švecová, H., Grabicová, K., Golovko, O., Randák, T., & Grabic, R. (2021). In situ calibration of polar organic chemical integrative sampler (POCIS) for monitoring of pharmaceuticals in surface waters. *Environmental Pollution*, *269*. https://doi.org/10.1016/j.envpol.2020.116121

Wang, P., Challis, J. K., He, Z.-X., Wong, C. S., & Zeng, E. Y. (2022). Effects of biofouling on the uptake of perfluorinated alkyl acids by organic-diffusive gradients in thin films passive samplers. *Environmental Science: Processes & Impacts*, *24*(2), 242–251. https://doi.org/10.1039/d1em00436k

Wang, Y., Ding, S., Xu, D., Wang, Y., Li, Y., Gong, M., & Zhang, C. (2016). Simultaneous measurements of eight oxyanions using high-capacity diffusive gradients in thin films (Zr-Oxide DGT) with a high-efficiency elution procedure. *Environmental Science and Technology*, *50*(14), 7572–7580. https://doi.org/10.1021/acs.est.6b00206

Withers, P. J. A., Jarvie, H. P., & Stoate, C. (2011). Quantifying the impact of septic tank systems on eutrophication risk in rural headwaters. *Environment International*, *37*(3), 644–653. https://doi.org/10.1016/j.envint.2011.01.002

Wu, Z., Jiang, X., Chen, J., & Wang, S. (2023). Diffusive gradients in thin films for transfer of phosphorus, nitrate and ammonium in lake sediments. *Journal of Geochemical Exploration*, *247*(September 2022), 107175. https://doi.org/10.1016/j.gexplo.2023.107175

Xia, R., Wang, G., Zhang, Y., Yang, P., Yang, Z., Ding, S., Jia, X., Yang, C., Liu, C., Ma, S., Lin, J., Wang, X., Hou, X., Zhang, K., Gao, X., Duan, P., & Qian, C. (2020). River algal blooms are well predicted by antecedent environmental conditions. *Water Research*, *185*, 116221. https://doi.org/10.1016/j.watres.2020.116221

Zanini, L., Robertson, W. D., Ptacek, C. J., Schiff, S. L., & Mayer, T. (1998). Phosphorus characterization in sediments impacted by septic effluent at four sites in central Canada. *Journal of Contaminant Hydrology*, *33*(3–4), 405–429. https://doi.org/10.1016/S0169-7722(98)00082-5

Zhang, H., & Davison, W. (1995). Performance characteristics of diffusion gradients in thin films for the in situ measurement of trace metals in aqueous solution. *Analytical Chemistry*, *67*(19), 3391–3400. https://doi.org/10.1021/ac00115a005

Zhang, H., Davison, W., Gadi, R., & Kobayashi, T. (1998). In situ measurement of dissolved phosphorus in natural waters using DGT. *Analytica Chimica Acta*, *370*(1), 29–38. https://doi.org/10.1016/S0003-2670(98)00250-5

Zheng, J. L., Guan, D. X., Luo, J., Zhang, H., Davison, W., Cui, X. Y., Wang, L. H., & Ma, L. Q. (2015). Activated charcoal based diffusive gradients in thin films for in situ monitoring of bisphenols in waters. *Analytical Chemistry*, *87*(1), 801–807. https://doi.org/10.1021/ac503814j

Zhuo, T., Wan, Q., Chai, B., Lei, X., He, L., & Chen, B. (2023). Microbial pathways in the coupling of iron, sulfur, and phosphorus cycles at the sediment–water interface of a river system: An in situ study involving the DGT technique. *Science of the Total Environment*, *863*(September 2022), 160855. https://doi.org/10.1016/j.scitotenv.2022.160855

Appendix A:

Development and evaluation of DGT samplers

Estimation of ACE-K and SUC diffusion coefficients

Most diffusion coefficients used for DGT calculations were from previous literature values (Table 2-1). There is currently no published diffusion coefficient value for ACE-K and SUC. Estimation of diffusion coefficients without a diffusion cell experiment can be reasonably represented by the following equation A-1 (Davison & Zhang, 2016):

$$D = \frac{2.84.10^{-5}}{M_{wt}^{1/3}} \qquad \text{(A-1)}$$

Where M_{wt} is the molecular weight of a compound. Different protonated forms of inorganic ligands can be assumed to have the same diffusion coefficient, while diffusion coefficients of a ligand generally increase as the size increases. pH of 5 and above does not interfere with diffusion coefficient estimations. ACE-K and SUC diffusion coefficients were estimated using this equation (Table 2-1).

Strata-DGT

The concentrations of artificial sweeteners determined using the Strata-DGT samplers were much lower than by discrete samples and POCIS. At the *Hamlet Site,* with known wastewater contamination from septic systems, ACE-K concentrations from Strata-DGT were on average three times lower compared to discrete samples. Concentrations of SUC obtained using Strata-DGT samplers were closer to C_{ACTIVE} than ACE-K but were still over or underestimated.

Although underestimated, Strata-DGT samplers, like POCIS, were able to concentrate ACE-K to detectable levels at the *Agriculture Site* during the Spring 2022 sampling event as the discrete samples were below the MDL (<100 µg L^{-1}).

Appendix B:

Chemicals, passive sampler specifications

Solutes and solvents

HPLC-grade methanol and acetonitrile were purchased from Fisher Scientific™ (Toronto, ON), formic acid from Agilent Technologies (Mississauga, ON) and ammonium acetate from Sigma-Aldrich (Oakville, Canada).

Four sets of analyte and internal standards were prepared: one for ACE-K and SUC (HPLC), one for six pharmaceuticals, one for ACE-K and SUC (IC-MS), and one for glyphosate and AMAP (LC-MS).

DGT specifications

Metsorb®-DGT samplers were loaded with a PES membrane (0.14 mm thickness), 0.8 mm APA diffusion gel, and Metsorb® (TiO_2, 0.8 mm) binding layer. These samplers were used for the uptake of phosphate, glyphosate, and AMPA. A520E-DGT samplers were loaded with a PES membrane (0.14 mm thickness), 0.8 mm agarose diffusion gel, and a A520E binding layer (0.78 mm) which is selective for nitrate. HLB-DGT samplers were loaded with a PTFE membrane (0.14 mm thickness), 0.8 mm agarose diffusion gel, and HLB (0.5 mm) binding layer used for uptake of pharmaceuticals. The units were stored in the refrigerator at 4°C and were kept in their individually sealed bags until deployment. Samplers were used within 8 months for best results.

Metsorb®-DGT, A520E-DGT, and PrCH-DGT

The DGT sampler cap was removed, then the filter and diffusive gel layers were separated from the binding layer using sterilized tweezers and rinsed with ultrapure water. The binding layer

from Metsorb®-DGT (phosphate, glyphosate, AMPA) was placed in a 1.5 mL 1.0 M solution of NaOH while and A520E-DGT and PrCH-DGT (nitrate, ammonium) binding layers were placed in a 2.0 mL 2.0 M solution of NaCl to extract compounds. After 24 hours, the binding layer was removed, and the eluent was diluted as necessary and stored at 4°C or frozen until analysis.

HLB-DGT

Each gel binding layer was removed from the sampler and placed in 50-mL centrifuge tubes and spiked with 20 µL of a 100-ppb internal standard (IS) mixture. Then, 3x3 mL aliquots of HPLC-grade MeOH were added with 2 minutes of sonication in between each addition. The aliquots were combined in a separate 50-mL centrifuge tube and evaporated to dryness under N_2 flow. Dried samples were reconstituted in 1 mL of 50:50 H_2O:MeOH and vortexed for 1 minute before being passed through a 0.22 µm nylon filter (Thermo Fisher Scientific, New Hampshire, US) and stored at 4°C until analysis.

POCIS

Briefly, the bolts on the POCIS were removed and both membranes along with the HLB sorbent were transferred into 50 mL centrifuge tubes. 80 µL of 100-ppb IS mixture and 20 mL of HPLC-grade MeOH were added and sonicated for 30 minutes. Strata X 30 mL 3 cc cartridges (Phenomenex, California, USA) were washed with 2x3 mL MeOH then loaded with the extracts. The extraction was repeated (without addition of IS mixture) for a total final extract volume of 40 mL then loaded onto the cartridges. Samples were evaporated to dryness under N_2 flow then reconstituted in 4 mL of MeOH and stored at 4°C until analysis.

Appendix C:

Analytical methods

Pharmaceuticals

Pharmaceutical grab samples were analyzed using solid phase extraction and high-performance liquid chromatography (HPLC) closely following a method from Liu et al. (2014). Before analysis, 500 mL of sample and 500 mL of ultrapure water were mixed and spiked with 20 µL of a 100-ppb IS mixture. The samples were passed through SPE cartridges (Oasis HLB 6 mL glass cartridges; Waters Corp., Mississauga, Canada) and were preconditioned with 2x3 mL aliquots of MeOH followed by 2x3 mL aliquots of ultrapure water to equilibrate the cartridges. After loading the sample into the cartridges, they were washed with 2x3 mL 5% (vol.%) MeOH and eluted with 2x3 mL aliquots of MeOH. The extracts were evaporated to dryness under N_2 downflow. Dried samples were reconstituted in 1 mL of MeOH and vortexed for 1 minute before being transferred into LC vials and stored at 4°C until analysis.

The pharmaceutical extracts were analyzed using an Agilent 1100 HPLC (Agilent Technologies, Mississauga, Canada) coupled with tandem mass spectrometry (MS/MS; 4000 Q TRAP, Applied Biosystems, Foster City, USA). Samples were passed through a Zorbax Eclipse XDB C18 analytical column (4.6×150 mm) where CAF, SMX, and CBZ were analyzed in electrospray ionization positive (ESI+) mode, while IBU, GEM, and NAP were analyzed in ESI negative (ESI-) mode. The gradient and mobile phases for + mode consisted of 0.1% formic acid and 5 mM ammonium acetate in ultrapure water (phase A) and 0.1% formic acid and 99.9% MeOH (phase B) with an eluent gradient of phase B of 10% for three minutes, followed by 90% to 10 minutes, and held for 10 minutes. For analysis of ESI in - mode the mobile phases consisted of 6.9 mM acetic acid in 300 mL acetonitrile and 700 mL ultrapure water (phase A)

and 100% acetonitrile (phase B). The elution gradient for phase B started at 12%, increased to 40% to 10 minutes, and was held for 10 minutes. Sample injection volume was 15 µL for + mode and 10 µL for – mode and were injected at a flow rate of 1000 µL min^{-1}. The MDLs are reported for each compound as follows, considering the concentration factor applied and dilution (ng L^{-1}): 0.162 for CAF; 0.438 for CBZ; 0.032 for GEM; 0.228 for IBU; 0.254 for NAP; 0.394 for SMX.

Artificial sweeteners

Artificial sweetener analysis from POCIS and Strata-DGT samplers were analyzed the same way as for pharmaceutical samples using an Agilent 1100 HPLC (Agilent Technologies, Mississauga, Canada) coupled with tandem mass spectrometry (MS/MS; 4000 Q TRAP, Applied Biosystems, Foster City, USA) in ESI (-) (Liu et al., 2014). The mobile phases consisted of 20 mM ammonium acetate in water (phase A) and 20 mM ammonium acetate in methanol (phase B).

Artificial sweetener analysis from discrete samples were analyzed using a direct injection ion chromatography (IC) method coupled with tandem mass spectrometry modifying a technique by Van Stempvoort et al. (2011a) as reported by Liu et al. (2014). Each sample was prepared by adding 900 µL of sample filtered through 0.22 µm polyvinylidene difluoride (PVDF) membranes (Chromatographic Specialties Inc.) spiked with 100 µL of an artificial sweetener IS mixture; each sample contained 200 µg L^{-1} of SUC, and 50 µg L^{-1} of ACE-K IS in 1 mL of sample. Samples were injected into a Dionex ICS-5000 (Sunnyvale, CA, USA) where it was passed through a guard column (Dionex IonPac™ AG20 RFIC™, 2×50 mm) and an analytical column (Dionex RFIC™ IonPac® A520, 2×250 mm). The samples then passed into an Agilent 6460 QQQ (Mississauga, ON, CA) operating in ESI- mode with multiple reaction monitoring (MRM).

Glyphosate and AMPA

For a final volume of 1 mL, 979 µL of filtered sample (0.45 µm) was added into a 1.5 mL polypropylene tube and spiked with 20 µL of a 100-ppb of an IS mixture. Samples were passed through a 0.2 µm PES syringe filter (Agilent Technologies, Mississauga, ON) with a 10-mL HDPE disposable syringe. Samples were then acidified with 1 µL of concentrated formic acid, for a final concentration of 0.1% formic acid. Samples were capped and vortexed for 20 seconds, then 25 µL of each sample was injected into a Dionex ICS-500 (Sunnyvale, CA, USA) at a flow rate of 0.35 mL min^{-1} where it was passed through an analytical column (Agilent InfinityLab Poroshell 120 CS-C18, 2.1 × 150 mm, 2.7 µm). Injection of the sample into an Agilent 6470A Triple Quadrupole LC/MS (Mississauga, ON, CA) operating in ESI- mode followed by mass spectrometry (6460 QQQ, Agilent Technologies, Mississauga, ON, Canada). The mobile phases consisted of 0.1% formic acid + 5 µM Agilent InfinityLab deactivator additive in ultrapure water (phase A) and 0.1% formic acid in MeOH (phase B). The MDLs for glyphosate and AMPA were 0.1 µg L^{-1}.

Appendix D:

Quality assurance/quality control (QA/QC)

Pharmaceuticals

A low and high range calibration curve for pharmaceuticals analyzed from discrete samples and DGT/POCIS had standards ranging from 0.1 – 10 µg L^{-1} and 0.1 – 50 µg L^{-1}, respectively, with eight to 12-points each. The mean accuracy and RSD for all pharmaceutical compounds were 102 ± 7% for CAF, 101 ± 11% for CBZ, 100 ± 4% for GEM, 95 ± 7% for IBU, 99 ± 7% for NAP, and 99 ± 10% for SMX. All data points were fitted to a calibration curve with mean R^2 values of 0.9983 for CAF, 0.9986 for CBZ, 0.9990 for GEM, 0.9952 for IBU, 0.9966 for NAP, and 0.9988 for SMX (n = 5). Continuing calibration verification (CCV) samples were run between every 10 unknown samples. Mean accuracy and RSD for CCV samples were 96 ± 4% for CAF, 97 ± 7% for CBZ, 100 ± 4% for GEM, 88 ± 8% for IBU, 100 ± 5% for NAP, and 97 ± 8% for SMX. The mean absolute internal standard (IS) recovery for the CCV samples were 83 ± 7% for CAF, 86 ± 5% for CBZ, 85 ± 3% for GEM, 95 ± 4% for IBU, 91 ± 4% for NAP, and 85 ± 8% for SMX. Quality control (QC) samples were extracted in the same manner as pharmaceutical samples and added to the analytical batch. Mean accuracy and RSD for QC samples (n = 24) were 94 ± 3% for CAF, 100 ± 4% for CBZ, 94 ± 5% for GEM, 69 ± 9% for IBU, 101 ± 12% for NAP, and 90 ± 2% for SMX which were similar to those from standard and CCV samples. The mean absolute IS recovery for the QC samples were 58 ± 4% for CAF, 48 ± 5% for CBZ, 83 ± 5% for GEM, 95 ± 9% for IBU, 92 ± 5% for NAP, and 37 ± 17% for SMX.

Artificial sweeteners

Calibration standards for ACE-K and SUC from discrete samples ranged from 0.1 – 200 µg L^{-1} and a seven- to nine-point calibration curve was used to analyze each sample batch. The mean accuracy and RSD for ACE-K calibration standards was 103 ± 4% and 101 ± 10% for SUC calibration standards. A linear curve was fitted to the data with a mean R^2 value of 0.9991 for ACE-K and 0.9973 for SUC (n = 2). CCV samples (n = 10) were run between batches of samples from different sampling locations. The mean accuracy and RSD of the CCV samples was 104 ± 5% for ACE-K and 110 ± 21% for SUC. The mean absolute IS recovery for the CCV samples were 127 ± 23% for ACE-K and 158 ± 29% for SUC.

Calibration standards for ACE-K and SUC from passive samplers ranged from 0.1 – 5 µg L^{-1} and a 6-point calibration curve was used to analyze samples from POCIS and DGT passive samplers. The mean accuracy and RSD for ACE-K calibration standards was 100 ± 18% and 100 ± 15% for SUC. The data was fit to a linear curve with an R^2 of 0.9868 for ACE-K and 0.9801 for SUC (n = 1). CCV samples (n = 4) ranging in concentration between 0.1 – 0.5 µg L^{-1} were run every 10 samples and had a mean accuracy and RSD of 89 ± 14% for ACE-K and 112 ± 58% for SUC. The mean absolute IS recovery for the CCV samples were 80 ± 8% for ACE-K and 79 ± 10% for SUC.

Glyphosate and AMPA

Calibration standards for glyphosate and AMPA ranged from 0.1 to 10 µg L^{-1} and a seven-point curve was used to analyze each batch of samples. The mean accuracy and RSD of calibration standards was 99 ± 17% for glyphosate and 101 ± 13% for AMPA. A linear curve was used to fit the data with a mean R^2 value of 0.9976 for glyphosate and 0.9990 for AMPA (n = 5). CCV

samples (n = 15) were analyzed every 10 samples and ranged between 0.1 – 5 µg L^{-1}, with a mean accuracy and RSD of 109 ± 22% for glyphosate and 99 ± 22% for AMPA. The mean absolute IS recovery for the CCV samples was 94 ± 17% for glyphosate and AMPA. Spiked QC samples (n = 9) ranging from 0.2 – 2 µg L^{-1} were run every five samples. The mean accuracy and RSD were 87 ± 11% for glyphosate and 94 ± 18% for AMPA. The mean absolute IS recovery for the QC samples was 26 ± 3% for glyphosate and 32 ± 6% AMPA.

Appendix E:

Impacts to DGT sampling rates

Diffusive boundary layer

Passive samplers with varying diffusive layer thickness were only deployed during Spring 2022 after concentrations measured from passive samplers during Fall 2021 sampling event were underestimated compared to discrete samples. Calculated DBL thicknesses (δ) were applied to all compounds from the analyte at each sampling site with the highest linearity (R^2) (results not shown). At the *Hamlet Site* the DBL calculated from PO_4-P was used (δ = 0.0348 cm, R^2 = 0.9514), at the *Agriculture Site* ACE-K was used (δ = 0.00558 cm, R^2 = 0.8804), and at the *Mixed-land Site* NAP was used (δ = 0.0479 cm, R^2 = 0.9872).

Interfering species

Other parameters that have an impact on uptake of compounds onto passive samplers include competing ions. PrCH-DGT samplers strongly underperformed compared to discrete sample concentrations for NH_4-N during both deployment seasons. A study from Huang et al. (2016) showed how competing ions and high conductivities can strongly impact NH_4-N uptake onto the PrCH binding layers. The results from the study show that the diffusion coefficient (D) for NH_4-N decreases as water conductivity increases. Diffusion coefficients for NH_4-N can be corrected for conductivity using the regression model equation provided in Huang et al. (2016) up to 1000 µS cm^{-1}, after which there would be further changes in the diffusion coefficient up to 1200 µS cm^{-1}. In a follow up study by Huang et al. (2017), the impact of increasing conductivity on NH_4-N uptake onto the PrCH binding gel was investigated by comparing the C_{DGT}/C_{SOLN} ratio

observed. Without correction for water conductivity, the ratio between C_{DGT}/C_{SOLN} dropped to 0.5 at 783 µS cm^{-1} after only 12 hours of deployment. The uptake continued to drop off after longer deployments, with the ratio effectively becoming 0 after 72 hours of deployment in a 783 µS cm^{-1} solution. The water conductivity ranged from 700 – 1200 µS cm^{-1} at the locations where the samplers were deployed in this study, which would have severely impacted uptake of NH_4-N after only 12 hours of deployment.

The samplers in this study were deployed for 6 days at each sampling location for the Fall 2021 and Spring 2022 sampling events, explaining the low mass uptake of NH_4-N on each sampler (Fig. 2-2). The *Hamlet Site* showed the largest difference from C_{DGT} to C_{SOLN}, likely due to the highest conductivity observed. This site had the highest concentrations of Na^+ and Cl^-, as the site is downstream of a rural hamlet that is serviced exclusively on septic systems. In the same studies conducted by Huang et al. (2016, 2017) the impact of competing ions on NH_4-N uptake was also evaluated. The C_{DGT}/C_{SOLN} ratio was again used to compare how the DGTs performed under increasing ionic strength by major cations (Na^+, K^+, Mg^{2+}, and Ca^{2+}). The NH_4-N C_{DGT}/C_{SOLN} uptake ratio began to decrease below 1.0 at cation concentrations of 0.01 M and had dropped off to a ratio of 0.15 and 0.16 at an ionic strength of 0.01 M for Mg^{2+} and Ca^{2+}, respectively. Mg^{2+} and Ca^{2+} concentrations (Table F-1) were both elevated across all sampling locations due to hard groundwater that feeds into the streams. Mean concentrations of 30 mg L^{-1} and 100 mg L^{-1} for Mg^{2+} and Ca^{2+} respectively were observed at all locations. Heightened ionic strength, along with elevated water conductivities at all locations explain why PrCH-DGT samplers strongly underperformed at these sample locations compared to C_{ACTIVE}. Considering the PrCH binding layers performed well in laboratory trials in the absence of competing ions

(Huang et al., 2016a), the composition of the stream water at the chosen locations were not ideal for uptake of NH_4-N onto PrCH sorbent.

A520E-DGT samplers also underperformed for NO_3-N uptake compared to discrete samples. Alongside DBL impacts, high conductivity in surface waters has been shown to decrease NO_3-N uptake onto the A520E binding layers. In the same study conducted by Huang et al. (2017), the impact of different water conductivities on the ratio between C_{DGT}/C_{SOLN} for NO_3-N was determined. Results showed that A520E-DGT samplers deployed in a solution with conductivity > 700 µS cm^{-1} showed a decrease in uptake of NO_3-N onto the binding layer during longer deployments. Deployments longer than 48 hours in this solution showed a decrease in the ratio between C_{DGT}/C_{SOLN} to 0.6 after only 72 hours. A correction factor of 0.6 was used for all NO_3-N C_{DGT} calculations.

The results from the Fall 2021 and Spring 2022 deployment events also show a significant decrease in NO_3-N mass uptake onto the samplers after the 6-day deployment compared to the three-day deployment (Fig. F-1). Uptake was not inhibited by the binding capacity as the total mass on the samplers did not exceed the limit determined in previous literature (Huang et al., 2016b). Ion competition was likely the main source for a decrease in NO_3-N uptake over the sampling period. In the same study by Huang et al. (2016), the binding selectivity of the A520E absorbent is $NO_3^- > Cl^- > HCO_3^- > SO_4^{2-}$. The extracts from the A520E binding layers show SO_4^{2-} concentrations as 15 - 30% of NO_3-N values in the layers. Significant concentrations of Cl^- were also likely bound to the A520E binding layers, but as the layers were eluted in a 2 M NaCl solution, it is impossible to determine the contribution from the field deployment. Considering elevated Cl^- concentrations at the *Hamlet Site* (~100 mg L^{-1}) during

both deployment events, this could explain why the C_{DGT}/C_{SOLN} ratios were lower compared to the *Agriculture and Mixed-land Sites*.

pH and dissolved organic matter (DOM) can impact POCIS sampling rates (R_s) and DGT diffusion coefficients (Guibal et al., 2019). The simplest measurement of DOM is as dissolved organic carbon (DOC). DOC has typical concentrations of 2 – 10 mg L^{-1} in surface waters (Li et al., 2011) with the majority in the form of fulvic acid (~45 %) and humic acid (~5%). DOC concentrations were < 4.09 mg L^{-1} and pH values were < 8.35 at all sites from both sampling events. A study from Li et al. (2011) showed that pH in the range of 3 – 9 and DOM < 4 mg L^{-1} had little to no effect on R_s values for multiple organic contaminants onto POCIS, while pH ranges between 3 – 9 and DOM < 20 mg L^{-1} has negligible effects on uptake of compounds onto DGT binding layers (Huang et al., 2016a,b; Panther et al., 2010).

Appendix F:

Figures and tables

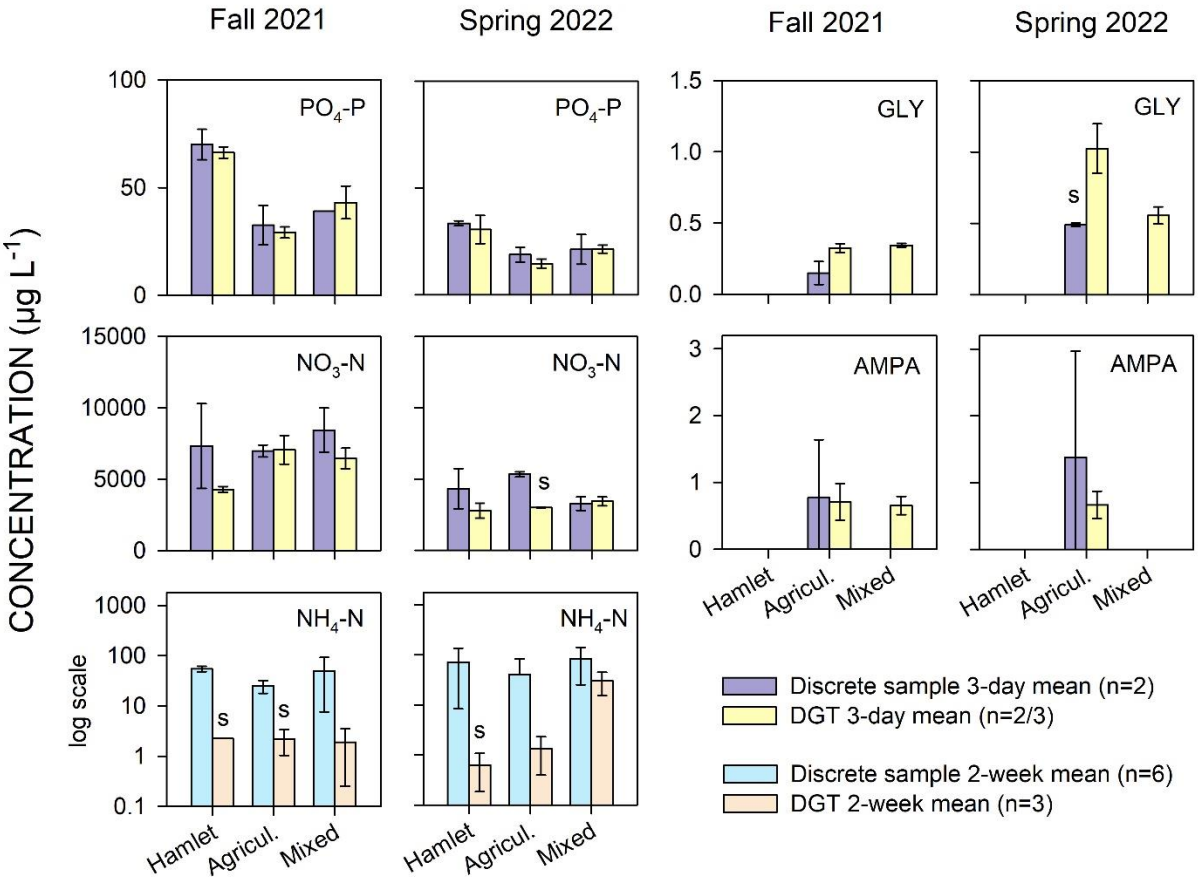


Figure F-1. Bar graphs showing mean and standard deviation of concentrations for duplicate or triplicate DGT passive samplers deployed for 3- or 14-days, and discrete samples on days 0 and 3, or days 0, 3, 6, 9, 12, 14. Letter 'S' represent significant differences between discrete and passive samplers.

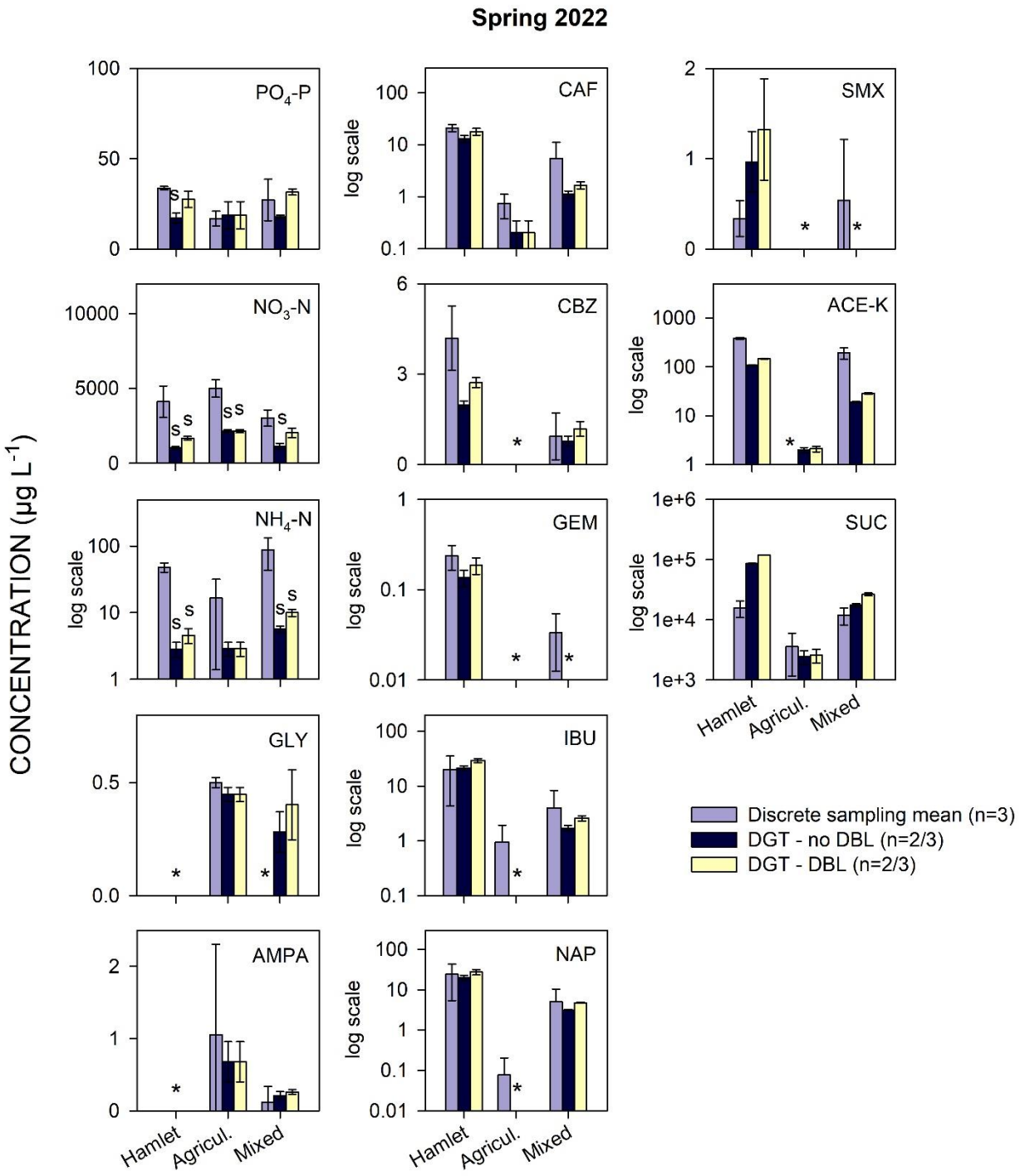


Figure F-2. Bar graphs showing mean and standard deviation of concentrations for duplicate or triplicate DGT passive samplers during Spring 2022 with and without DBL corrections. Samplers were deployed for 6- or 14-days, and discrete samples on days 0, 3, and 6 or days 0, 3, 6, 9, 12, 14. Letter 'S' represent significant differences between discrete and passive samplers.

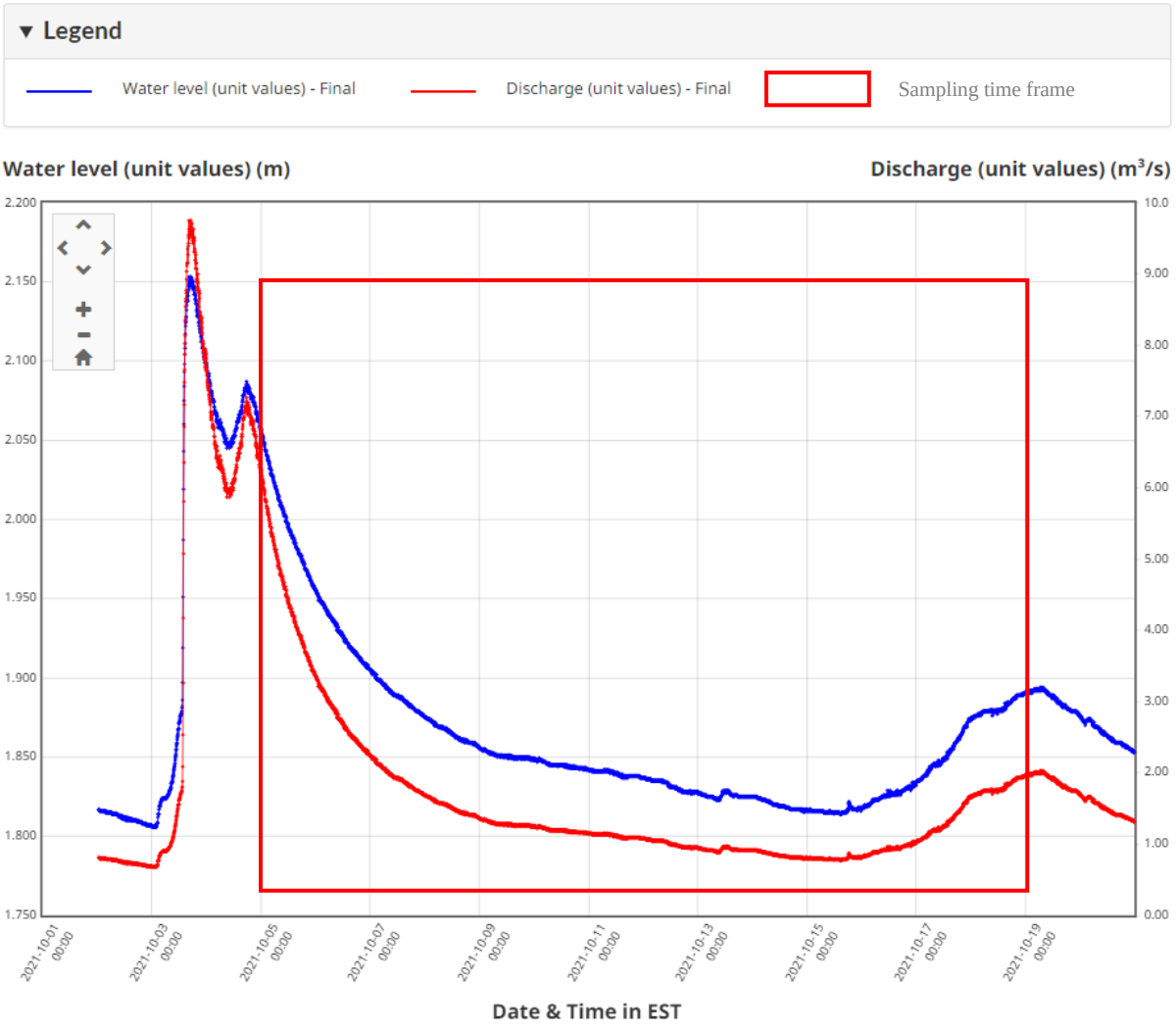


Figure F-3. Hydrograph for Irvine River near Salem (02GA005) from the Government of Canada (Water Office, data accessed: May 1st, 2023) from Oct. 1st 2021 – Oct. 20th 2021. Fall 2021 sampling event occured between Oct. 5th 2021 – Oct. 19th 2021.

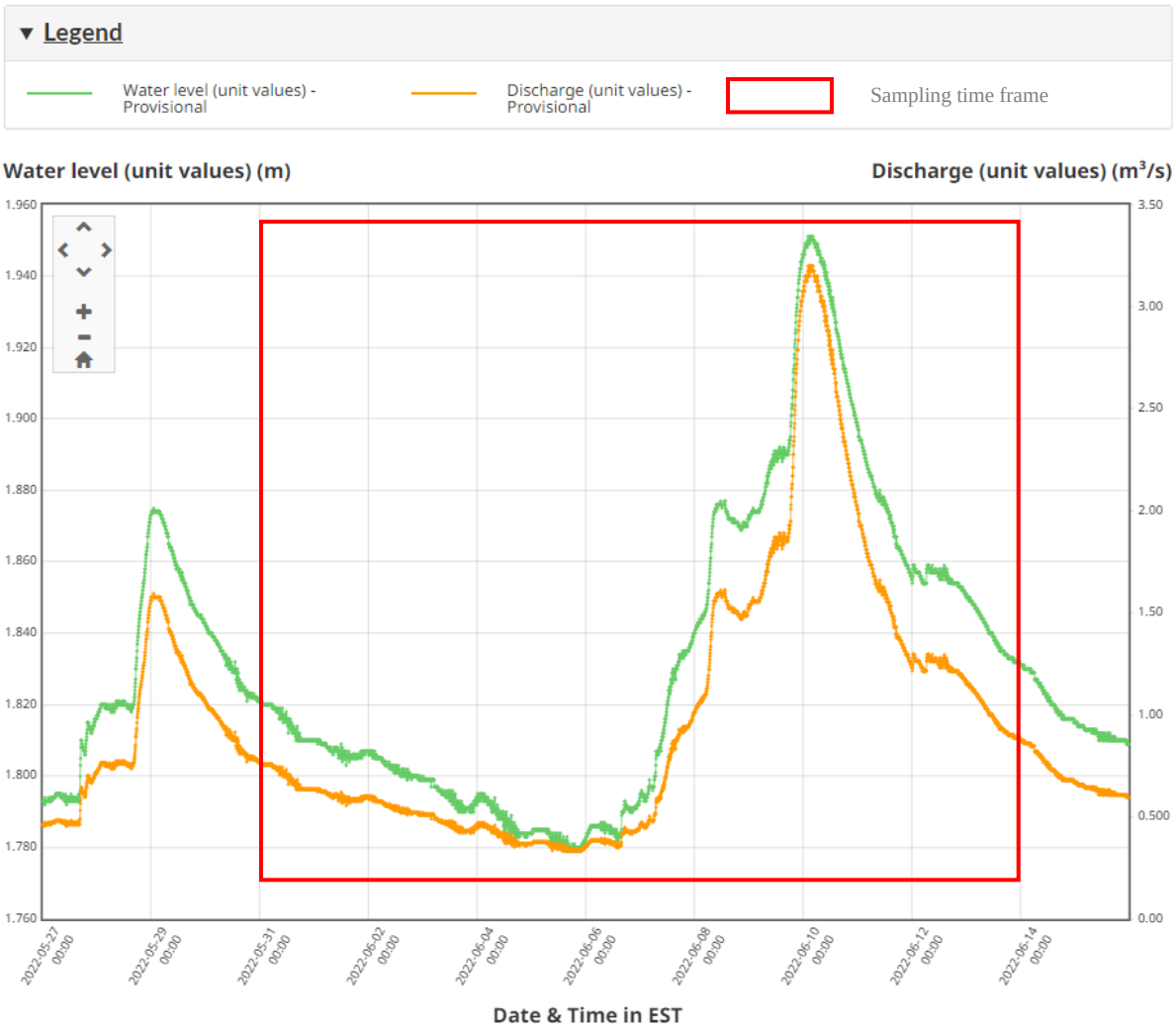


Figure F-4. Hydrograph for Irvine River near Salem (02GA005) from the Government of Canada (Water Office, data accessed: May 1st, 2023) from May 27th 2022 – June 15th 2022. Spring 2022 sampling event occurred between May 31st 2022 – June 14th 2022.

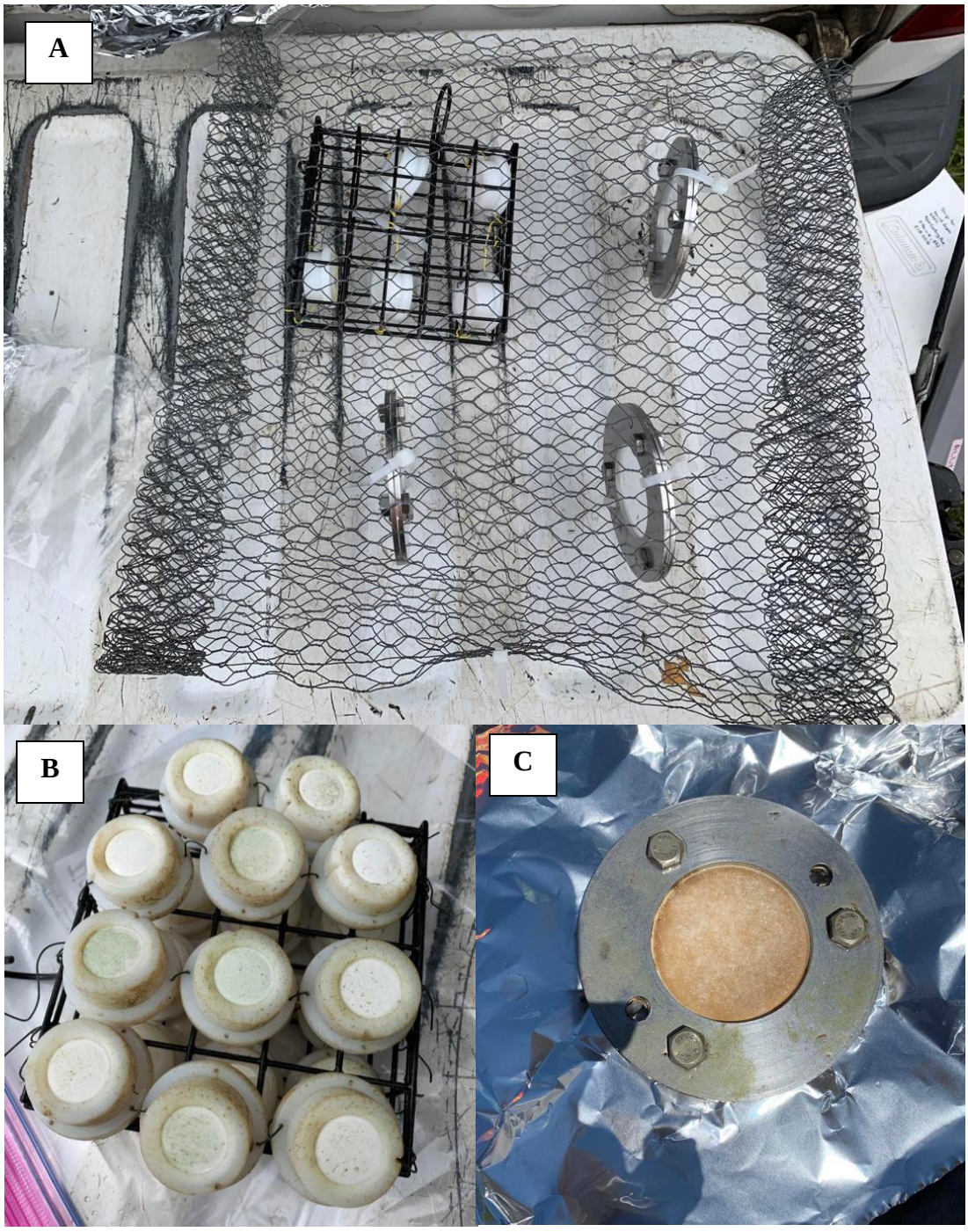


Figure F-5. (A) Wire cage used to protect passive samplers during deployment (B) Biofouling on DGT samplers after 6-days of deployment (C) Biofouling on POCIS after 2-weeks of deployment.

Table F-1. Mean measurements/concentrations for discrete samples collected on Day 0 and every 3rd day for 2-weeks (n = 6), unless noted below, at each sampling location during both seasonal studies.

Parameter	Units	FALL 2021			SPRING 2022		
		Hamlet Site	*Agri. Site*	*Mixed-land Site*	*Hamlet Site*	*Agri. Site*	*Mixed-land Site*
Water temp.	°C	13.5	12.8	13.0	14.0	14.0	15.9
pH	units	8.08	8.00	8.12	8.01	8.09	8.09
Alk.	mg $CaCO_3$ L^{-1}	357	335	333	310	300	307
Turbidity*	NTU	0.94	1.02	4.42	1.21	1.59	4.28
SPC*	µS cm^{-1}	1180	759	823	1320	673	846
Hardness*	mg L^{-1}	382	372.0	363	376	354	341
Cl^-	mg L^{-1}	178	22.2	64.8	207	17.7	83.2
SO_4^{2-}	mg L^{-1}	11.4	16.7	14.5	8.1	12.9	9.6
F^-	mg L^{-1}	<0.1	<0.1	<0.1	<0.1	<0.1	<0.1
Br^-	mg L^{-1}	<0.1	<0.1	<0.1	<0.1	<0.1	<0.1
Ca^{2+}*	mg L^{-1}	105.0	100.6	98.7	104.1	95.1	90.6
Mg^{2+}*	mg L^{-1}	29.0	29.4	28.4	28.1	28.4	27.9
K^+*	mg L^{-1}	3.20	3.01	3.02	2.46	2.64	2.67
Na^+*	mg L^{-1}	101	12.4	29.7	133	10.9	42.2
Sr*	mg L^{-1}	0.227	0.175	0.178	0.244	0.165	0.178
DOC*	mg L^{-1}	2.59	3.52	4.09	2.71	3.33	4.03
DIC*	mg L^{-1}	83.0	78.9	76.8	73.8	71.9	68.8
*E. coli**	MPN 100 mL^{-1}	2920	176	1520	991	132	3390
BacGen*	C 100 mL^{-1}	55000	16000	28000	42000	6700	25000
BacHum*	C 100 mL^{-1}	12800	580	950	4700	810	1300
BacBov*	C 100 mL^{-1}	0	0	14000	210	0	10000
ACE-K	ng L^{-1}	442	<100	<100	382	<100	194
SUC	ng L^{-1}	18500	70.0	8610	15700	3590	11900
CAF	ng L^{-1}	28.07	1.85	2.07	21.18	0.74	5.51
CBZ	ng L^{-1}	4.88	<0.02	1.50	4.20	<0.02	0.93
GEM	ng L^{-1}	0.25	<0.01	<0.01	0.24	<0.01	0.03
IBU	ng L^{-1}	27.32	0.88	1.77	19.88	0.93	3.98
NAP	ng L^{-1}	6.33	0.37	1.72	24.44	0.08	5.07
SMX	ng L^{-1}	0.11	0.05	0.07	0.34	<0.02	0.54
TP*	µg L^{-1}	68.0	37.0	36.0	57.3	34.8	57.4
PO_4-P	µg L^{-1}	74.3	35.3	34.2	40.2	33.4	42.1
NO_3-N	µg L^{-1}	5930	7120	7220	4780	6170	4510
NH_{3+4}-N	µg L^{-1}	55.0	25.0	50.0	71.7	40.0	83.3

*Based on samples taken on Day 0 and 14 (n = 2) in Fall 2021 and Days 0, 6 and 14 (n = 3) for Spring 2022. Analyzed by MECP.

Table F-2. Mean measurements/concentrations for discrete samples collected on Days 0 and 14 (n=2) during Fall 2021 and Spring 2022. All compounds analyzed by MECP.

Parameter	Units	FALL 2021			SPRING 2022		
		Hamlet Site	*Agri. Site*	*Mixed-land Site*	*Hamlet Site*	*Agri. Site*	*Mixed-land Site*
Aluminum	µg/L	1.16	<2	1.12	7.74	8.99	10.24
Barium	µg/L	70.40	67.25	62.65	63.50	53.70	63.05
Beryllium	µg/L	<0.1	<0.1	<0.1	<0.1	<0.1	<0.1
Bismuth	µg/L	<5	<5	<5	<5	<5	<5
Cadmium	µg/L	<0.9	<0.9	<0.9	0.53	1.43	1.49
Chromium	µg/L	0.54	<1	<1	<1	<1	<1
Cobalt	µg/L	1.26	0.55	<1	<1	<1	<1
Copper	µg/L	3.34	2.62	2.75	0.90	< MDL	0.29
Iron	µg/L	14.08	12.83	14.01	11.34	9.50	17.00
Lead	µg/L	<7	<7	<7	<7	<7	<7
Lithium	µg/L	<5	<5	<5	<5	<5	<5
Manganese	µg/L	13.05	4.67	9.38	22.65	5.52	19.90
Molybdenum	µg/L	<2	<2	<2	<2	<2	<2
Nickel	µg/L	<2	<2	<2	<2	<2	<2
Silver	µg/L	<9	<9	<9	<9	<9	<9
Tin	µg/L	<9	4.54	<9	<9	<9	<9
Uranium	µg/L	2.20	1.55	1.64	3.36	<3	<3
Vanadium	µg/L	0.44	0.70	11.30	<0.5	<0.5	0.35
Zinc	µg/L	19.00	24.20	9.90	19.90	18.20	19.60
Zirconium	µg/L	<1	<1	<1	<1	<1	<1

Table F-3. Spearman rank order results showing correlation coefficients (ρ) obtained for all sampling locations during the Fall 2021 sampling event between nutrient and tracer concentrations. Strong positive correlations (>0.80) are highlighted in green, moderate positive correlations (0.50 – 0.80) are highlighted in yellow, and strong negative correlations (<-0.72) are highlighted in red. Dashed line indicate that no test was conducted as the measurement was below MDL.

HAMLET SITE													
	CAF	*CBZ*	*GEM*	*IBU*	*NAP*	*SMX*	*ACE-K*	*SUC*	*GLY*	*AMPA*	*PO_4-P*	*NO_3-N*	*NH_4-N*
CAF	1.000												
CBZ	0.448	1.000											
GEM	0.522	0.923	1.000										
IBU	0.988	0.473	0.584	1.000									
NAP	0.943	0.524	0.629	0.970	1.000								
SMX	0.521	0.367	0.505	0.601	0.506	1.000							
ACE-K	0.951	0.613	0.468	0.894	0.837	0.206	1.000						
SUC	0.903	0.621	0.326	0.826	0.761	0.125	0.985	1.000					
GLY	-	-	-	-	-	-	-	-	1.000				
AMPA	-	-	-	-	-	-	-	-	-	1.000			
PO_4-P	0.617	0.896	0.874	0.628	0.631	0.398	0.953	0.924	-	-	1.000		
NO_3-N	0.014	0.616	0.538	0.094	0.104	0.612	-0.590	-0.569	-	-	0.491	1.000	
NH_4-N	-0.322	-0.089	-0.196	-0.251	-0.121	0.066	-0.507	-0.483	-	-	-0.377	0.377	1.000
AGRICULTURE SITE													
	CAF	*CBZ*	*GEM*	*IBU*	*NAP*	*SMX*	*ACE-K*	*SUC*	*GLY*	*AMPA*	*PO_4-P*	*NO_3-N*	*NH_4-N*
CAF	1.000												
CBZ	-	1.000											
GEM	-	-	1.000										
IBU	0.095	-	-	1.000									
NAP	0.635	-	-	-0.039	1.000								
SMX	-0.139	-	-	0.004	-0.304	1.000							
ACE-K	-	-	-	-	-	-	1.000						
SUC	-0.270	-	-	0.731	-0.554	-0.315	-	1.000					
GLY	-0.182	-	-	0.582	-0.737	0.249	-	0.580	1.000				
AMPA	0.299	-	-	0.764	0.431	-0.445	-	0.670	-0.026	1.000			
PO_4-P	-0.342	-	-	0.804	-0.404	0.307	-	0.777	0.491	0.510	1.000		
NO_3-N	0.370	-	-	0.401	0.543	0.091	-	0.285	-0.337	0.636	0.365	1.000	
NH_4-N	-0.421	-	-	-0.235	-0.663	0.367	-	0.315	0.166	-0.447	0.252	-0.173	1.000
MIXED-LAND SITE													
	CAF	*CBZ*	*GEM*	*IBU*	*NAP*	*SMX*	*ACE-K*	*SUC*	*GLY*	*AMPA*	*PO_4-P*	*NO_3-N*	*NH_4-N*
CAF	1.000												
CBZ	0.945	1.000											
GEM	-	-	1.000										
IBU	0.445	0.576	-	1.000									
NAP	0.417	0.571	-	0.948	1.000								
SMX	0.289	0.267	-	-0.162	0.057	1.000							
ACE-K	-	-	-	-	-	-	1.000						
SUC	0.356	0.880	-	0.023	-0.025	-0.415	-	1.000					
GLY	-0.955	-0.947	-	-0.588	-0.560	-0.173	-	-0.279	1.000				
AMPA	-0.938	-0.921	-	-0.556	-0.556	-0.328	-	-	0.955	1.000			
PO_4-P	-0.127	-0.090	-	0.157	0.063	-0.217	-	0.071	0.082	-0.002	1.000		
NO_3-N	0.800	0.738	-	0.452	0.443	0.348	-	-0.238	-0.758	-0.897	-0.056	1.000	
NH_4-N	0.241	0.066	-	-0.036	0.024	-0.106	-	-0.068	-0.202	-0.229	-0.087	0.303	1.000

Table F-4. Spearman rank order results showing correlation coefficients (ρ) obtained for all sampling locations during the Spring 2022 sampling event between nutrient and tracer concentrations. Strong positive correlations (>0.80) are highlighted in green, moderate positive correlations (0.50 – 0.80) are highlighted in yellow, and strong negative correlations (<-0.72) are highlighted in red. Dashed line indicate that no test was conducted as the measurement was below MDL.

HAMLET SITE													
	CAF	*CBZ*	*GEM*	*IBU*	*NAP*	*SMX*	*ACE-K*	*SUC*	*GLY*	*AMPA*	*PO_4-P*	*NO_3-N*	*NH_4-N*
CAF	1.000												
CBZ	0.878	1.000											
GEM	0.893	0.935	1.000										
IBU	0.506	0.709	0.466	1.000									
NAP	0.750	0.481	0.698	-0.012	1.000								
SMX	0.723	0.736	0.814	0.205	0.430	1.000							
ACE-K	0.972	0.902	0.882	0.590	0.655	0.720	1.000						
SUC	0.903	0.732	0.835	0.401	0.808	0.679	0.903	1.000					
GLY	-	-	-	-	-	-	-	-	1.000				
AMPA	-	-	-	-	-	-	-	-	-	1.000			
PO_4-P	0.676	0.613	0.402	0.707	0.201	0.260	0.688	0.447	-	-	1.000		
NO_3-N	0.503	0.406	0.294	0.601	0.165	0.258	0.641	0.628	-	-	0.587	1.000	
NH_4-N	0.649	0.488	0.391	0.214	0.348	0.382	0.561	0.308	-	-	0.723	0.106	1.000
AGRICULTURE SITE													
	CAF	*CBZ*	*GEM*	*IBU*	*NAP*	*SMX*	*ACE-K*	*SUC*	*GLY*	*AMPA*	*PO_4-P*	*NO_3-N*	*NH_4-N*
CAF	1.000												
CBZ	-	1.000											
GEM	-	-	1.000										
IBU	0.319	-	-	1.000									
NAP	0.044	-	-	-0.004	1.000								
SMX	-	-	-	-	-	1.000							
ACE-K	-0.777	-	-	-0.502	-0.247	-	1.000						
SUC	0.276	-	-	0.589	0.661	-	-0.672	1.000					
GLY	0.422	-	-	0.326	-0.143	-	-0.313	-0.059	1.000				
AMPA	-0.409	-	-	-0.235	-0.200	-	0.204	-0.305	-0.196	1.000			
PO_4-P	0.184	-	-	0.933	-0.244	-	-0.248	0.353	0.322	-0.164	1.000		
NO_3-N	0.698	-	-	0.756	-0.092	-	-0.723	0.513	0.066	-0.220	0.656	1.000	
NH_4-N	0.452	-	-	0.611	0.023	-	-0.473	0.224	0.926	-0.167	0.542	0.299	1.000
MIXED-LAND SITE													
	CAF	*CBZ*	*GEM*	*IBU*	*NAP*	*SMX*	*ACE-K*	*SUC*	*GLY*	*AMPA*	*PO_4-P*	*NO_3-N*	*NH_4-N*
CAF	1.000												
CBZ	0.851	1.000											
GEM	0.802	0.725	1.000										
IBU	0.949	0.782	0.748	1.000									
NAP	0.884	0.978	0.769	0.847	1.000								
SMX	0.974	0.808	0.836	0.941	0.830	1.000							
ACE-K	0.554	0.429	0.848	0.517	0.537	0.523	1.000						
SUC	0.825	0.614	0.770	0.800	0.740	0.742	0.827	1.000					
GLY	-0.291	-0.459	-0.197	-0.105	-0.335	-0.350	0.228	0.107	1.000				
AMPA	0.090	-0.020	0.007	0.338	0.027	0.111	0.036	0.061	0.665	1.000			
PO_4-P	0.066	-0.199	0.107	0.236	-0.082	0.025	0.415	0.351	0.905	0.774	1.000		
NO_3-N	-0.090	-0.215	0.073	0.068	-0.028	-0.173	0.509	0.436	0.794	0.319	0.696	1.000	
NH_4-N	0.676	0.491	0.696	0.588	0.525	0.603	0.772	0.750	0.217	0.229	0.520	0.197	1.000

Table F-5. Loadings table associated with the discrete and DGT PCA plots. Missing values were eliminated using VIF.

DGT		
Variable	PC1	PC2
CAF	-0.9520397	0.0838255
CBZ	-0.9239323	0.2453727
GEM	-0.9482226	-0.142389
IBU	-0.9076949	-0.3438122
NAP	-0.886263	-0.3710755
SMX	-0.9399866	-0.0805749
GLY	0.8507524	0.0072511
AMPA	0.6902784	-0.0860579
PO_4-P	-0.4544863	0.6137659
NO_3-N	0.5331702	0.26092
NH_4-N	-0.4403304	0.7996756

Discrete			
Variable	PC1	PC2	PC3
CBZ	-0.8469324	0.3040201	-0.0264399
IBU	-0.6621805	0.3480479	0.1255841
NAP	-0.6780463	-0.2331952	-0.2245423
SMX	-0.4631344	-0.5966804	-0.1688965
SUC	-0.904919	0.1597211	0.0046079
GLY	0.2844673	-0.3365679	0.769283
AMPA	0.6317518	-0.0177274	-0.0882525
PO_4-P	-0.4382262	0.4543841	0.6439185
NO_3-N	0.4963207	0.6200265	0.1600072
NH_4-N	-0.2761792	-0.7109958	0.4556847

Table F-6. Results of statistical analysis using a Kruskal-Wallis test to compare measured concentrations by discrete, DGT, and POCIS samples as well as between sites for both sampling events. For comparison of less than three groups a Mann Whitney U test was performed. Significant differences are highlighted in green and defined as $\rho < 0.05$ (95% confidence). Dashed lines indicate analyte was not sampled using that method. Compounds measuring below their respective MDLs were assigned a censored value of half the MDL. Discrete samples n = 3/6; DGT n = 2/3; POCIS n = 3.

	Hamlet Site						***Agriculture Site***						***Mixed-land Site***					
	FALL 2021			*SPRING 2022*			*FALL 2021*			*SPRING 2022*			*FALL 2021*			*SPRING 2022*		
p-value	Discrete vs. DGT	Discrete vs. POCIS	DGT vs. POCIS	Discrete vs. DGT	Discrete vs. POCIS	DGT vs. POCIS	Discrete vs. DGT	Discrete vs. POCIS	DGT vs. POCIS	Discrete vs. DGT	Discrete vs. POCIS	DGT vs. POCIS	Discrete vs. DGT	Discrete vs. POCIS	DGT vs. POCIS	Discrete vs. DGT	Discrete vs. POCIS	DGT vs. POCIS
CAF	0.0365	0.4328	0.2575	0.2393	0.0060	0.1742	0.4312	1.0000	0.4954	0.0310	0.0108	0.7341	0.7429	0.0765	0.2113	0.1698	0.0049	0.2129
CBZ	0.1232	0.0944	0.0054	0.0776	0.0033	0.3082	-	-	-	-	-	-	0.5563	0.0108	0.0894	0.4320	0.2947	0.1123
GEM	0.7678	0.0530	0.1555	0.4320	0.0088	0.1123	-	-	-	-	-	-	-	-	-	0.0288	0.0288	1.0000
IBU	0.2385	0.0495	0.0065	0.3268	0.3268	0.0894	0.0124	0.2713	0.2253	0.0052	0.0459	0.4892	0.3260	0.0073	0.1403	0.6949	0.0262	0.0235
NAP	0.0500	0.6949	0.1742	0.3268	0.1327	0.0315	0.0571	0.7429	0.0534	0.2278	0.2278	1.0000	0.3268	0.1327	0.0315	0.5339	0.0391	0.0201
SMX	0.0069	0.3225	0.1375	0.0755	0.0755	0.0021	0.1736	0.1736	0.9518	-	-	-	0.0357	0.6648	0.1489	0.0288	0.0288	1.0000
ACEK	-	0.0238	-	0.0097	0.0550	0.4090	-	0.0636	-	0.1724	0.0064	0.1724	-	0.0636	-	0.0070	0.1779	0.1779
SUC	-	0.0476	-	0.1396	0.0550	0.0050	-	0.0636	-	1.0000	0.0186	0.0415	-	0.7000	-	0.0776	0.0776	0.0022
GLY	-	-	-	-	-	-	0.4000	-	-	0.1212	-	-	0.1066	-	-	0.0636	-	-
AMPA	-	-	-	-	-	-	0.8000	-	-	0.7000	-	-	0.1066	-	-	0.6579	-	-
PO_4-P	0.2000	-	-	0.0765	-	-	0.7671	-	-	1.0000	-	-	0.7671	-	-	0.6579	-	-
NO_3-N	0.5000	-	-	0.1000	-	-	1.2000	-	-	0.1000	-	-	0.2000	-	-	0.1000	-	-
NH_4-N	0.1386	-	-	0.1000	-	-	0.1281	-	-	0.7000	-	-	0.0636	-	-	0.1000	-	-

Table F-7. Results of statistical analysis using a Kruskal-Wallis test to compare measured concentrations by discrete, DGT, and POCIS samples between study sites for both sampling events. For comparison of less than three groups a Mann Whitney U test was performed. Statistical differences are highlighted in green and defined as $\rho < 0.05$ (95% confidence). Dashed lines indicate analyte was not sampled using that method. Compounds measuring below their respective MDLs were assigned a censored value of half the MDL. For the *Hamlet/Agriculture/Mixed-land Sites* n = 2/3/6.

	DISCRETE SAMPLES						**DGT**						**POCIS**					
	FALL 2021			*SPRING 2022*			*FALL 2021*			*SPRING 2022*			*FALL 2021*			*SPRING 2022*		
p-value	Hamlet vs. Agri.	Hamlet vs. Mixed	Agri. vs. Mixed	Hamlet vs. Agri.	Hamlet vs. Mixed	Agri. vs. Mixed	Hamlet vs. Agri.	Hamlet vs. Mixed	Agri. vs. Mixed	Hamlet vs. Agri.	Hamlet vs. Mixed	Agri. vs. Mixed	Hamlet vs. Agri.	Hamlet vs. Mixed	Agri. vs. Mixed	Hamlet vs. Agri.	Hamlet vs. Mixed	Agri. vs. Mixed
CAF	0.0008	0.0329	0.2335	0.0000	0.0516	0.0516	0.0073	0.1797	0.1797	0.0073	0.1797	0.1797	0.0153	0.0954	0.4484	0.0073	0.1797	0.1797
CBZ	0.0001	0.0473	0.0427	0.0002	0.0174	0.1745	0.0064	0.1724	0.1724	0.0064	0.1724	0.1724	0.0064	0.1724	0.1724	0.0064	0.1724	0.1724
GEM	0.0168	0.0168	1.0000	0.0002	0.0222	0.1683	0.0168	0.0168	1.0000	0.0168	0.0168	1.0000	0.0168	0.0168	1.0000	0.0168	0.0168	1.0000
IBU	0.0004	0.0213	0.2127	0.0004	0.0660	0.0937	0.0064	0.1724	0.1724	0.0064	0.1724	0.1724	0.0073	0.1797	0.1797	0.0073	0.1797	0.1797
NAP	0.0009	0.2440	0.0323	0.0002	0.1030	0.0340	0.0073	0.1797	0.1797	0.0064	0.1724	0.1724	0.0073	0.1797	0.1797	0.0064	0.1724	0.1724
SMX	0.3500	0.5403	0.7472	0.0053	0.9556	0.0063	0.0171	0.1011	0.4561	0.0168	0.0168	1.0000	0.0166	0.0996	0.4542	-	-	-
ACEK	0.0168	0.0168	1.0000	0.0001	0.0474	0.0474	-	-	-	0.0139	0.2636	0.1336	0.0073	0.1797	0.1797	0.0070	0.1779	0.1779
SUC	0.0001	0.0646	0.0443	0.0007	0.3304	0.0150	-	-	-	0.0139	0.2636	0.1336	0.0073	0.1797	0.1797	0.0171	0.1011	0.4561
GLY	0.0168	1.0000	0.0168	0.0046	0.0645	0.3261	0.0301	0.2781	0.2781	0.0570	0.0272	0.7607	-	-	-	-	-	-
AMPA	0.0168	1.0000	0.0168	0.0022	0.1058	0.1487	0.0301	0.2781	0.2781	0.0064	0.1724	0.1724	-	-	-	-	-	-
PO_4-P	0.0041	0.0024	0.8697	0.1437	0.6846	0.2909	0.4386	0.7518	0.6056	0.3671	1.0000	0.3671	-	-	-	-	-	-
NO_3-N	0.0373	0.0699	0.7868	0.1764	0.9569	0.1597	0.1213	0.3017	0.5271	0.0171	0.4561	0.1011	-	-	-	-	-	-
NH_4-N	0.2224	0.6842	0.4159	0.2335	0.3226	0.0493	0.5493	0.0996	0.2947	0.2967	0.1360	0.0113	-	-	-	-	-	-